

University of Windsor

Scholarship at UWindor

Electronic Theses and Dissertations

Theses, Dissertations, and Major Papers

1984

Effect of unequal evaporator heating and charge distribution on the heat transfer performance of the evaporator of a multitube two phase thermosiphon heat exchanger.

Samar. Raza
University of Windsor

Follow this and additional works at: <https://scholar.uwindsor.ca/etd>

Recommended Citation

Raza, Samar., "Effect of unequal evaporator heating and charge distribution on the heat transfer performance of the evaporator of a multitube two phase thermosiphon heat exchanger." (1984). *Electronic Theses and Dissertations*. 1835.
<https://scholar.uwindsor.ca/etd/1835>

This online database contains the full-text of PhD dissertations and Masters' theses of University of Windsor students from 1954 forward. These documents are made available for personal study and research purposes only, in accordance with the Canadian Copyright Act and the Creative Commons license—CC BY-NC-ND (Attribution, Non-Commercial, No Derivative Works). Under this license, works must always be attributed to the copyright holder (original author), cannot be used for any commercial purposes, and may not be altered. Any other use would require the permission of the copyright holder. Students may inquire about withdrawing their dissertation and/or thesis from this database. For additional inquiries, please contact the repository administrator via email (scholarship@uwindsor.ca) or by telephone at 519-253-3000ext. 3208.



National Library
of Canada

Canadian Theses Service

Ottawa, Canada
K1A 0N4

Bibliothèque nationale
du Canada

Services des thèses canadiennes

CANADIAN THESES

THÈSES CANADIENNES

NOTICE

The quality of this microfiche is heavily dependent upon the quality of the original thesis submitted for microfilming. Every effort has been made to ensure the highest quality of reproduction possible.

If pages are missing, contact the university which granted the degree.

Some pages may have indistinct print especially if the original pages were typed with a poor typewriter ribbon or if the university sent us an inferior photocopy.

Previously copyrighted materials (journal articles, published tests, etc.) are not filmed.

Reproduction in full or in part of this film is governed by the Canadian Copyright Act, R.S.C. 1970, c. C-30. Please read the authorization forms which accompany this thesis.

**THIS DISSERTATION
HAS BEEN MICROFILMED
EXACTLY AS RECEIVED**

AVIS

La qualité de cette microfiche dépend grandement de la qualité de la thèse soumise au microfilmage. Nous avons tout fait pour assurer une qualité supérieure de reproduction.

S'il manque des pages, veuillez communiquer avec l'université qui a conféré le grade.

La qualité d'impression de certaines pages peut laisser à désirer, surtout si les pages originales ont été dactylographiées à l'aide d'un ruban usé ou si l'université nous a fait parvenir une photocopie de qualité inférieure.

Les documents qui font déjà l'objet d'un droit d'auteur (articles de revue, examens publiés, etc.) ne sont pas microfilmés.

La reproduction, même partielle, de ce microfilm est soumise à la Loi canadienne sur le droit d'auteur, SRC 1970, c. C-30. Veuillez prendre connaissance des formules d'autorisation qui accompagnent cette thèse.

**LA THÈSE A ÉTÉ
MICROFILMÉE TELLE QUE
NOUS L'AVONS REÇUE**

EFFECT OF UNEQUAL EVAPORATOR HEATING AND CHARGE DISTRIBUTION
ON THE HEAT TRANSFER PERFORMANCE OF THE EVAPORATOR OF A
MULTITUBE TWO PHASE THERMOSIPHON HEAT EXCHANGER

BY

SAMAR RAZA

A thesis
submitted to the
Faculty of Graduate Studies and Research
through the Department of
Mechanical Engineering in Partial Fulfillment
of the requirements for the Degree
of Master of Applied Science at
the University of Windsor

Windsor, Ontario, Canada

(c) SAMAR RAZA, 1983

IN THE NAME OF GOD, THE BENEFICIENT, THE MERCIFUL

Read: In the name of thy Lord who created
Created man from a clot

Read: And thy lord is the Most Bounteous
Who taught by the pen

Taught man that which he knew not (QURAN: XCVI :1-5)

To my parents

ABSTRACT

This thesis deals with an experimental study carried out on a unidirectional two phase thermosiphon heat exchanger using R-11 as the working fluid. The objective of this study was to investigate the effect of unequal heating of the evaporator tubes and of unequal charge distribution between adjacent tubes on the evaporator heat transfer performance. The evaporator unit consisted of three coplanar tubes, nominal 3/8" diameter, which were individually water jacketed and joined to a common vapour header. The condenser was similar to the evaporator in design except it was made of nominal 1/4" diameter tubes. The evaporator and the condenser units could be independently translated vertically, be rotated in the vertical plane about a horizontal axis normal to the tube plane and be inclined from the vertical while maintaining their vapour headers horizontal.

The heat transfer capabilities of the evaporator were found to be insensitive to static charge differences of as much as 3 to 13% between adjacent tubes for source-sink temperature differences of 20C and 10C.

Tests were carried out which showed that the total heat transfer rate for unequal evaporator heating was (4%-7%) better than that for the corresponding equal heating case. Most of the data for the average evaporator heat transfer coefficient were found to lie within 10% of the curve for the equally heated tubes. However, it was found that the tubes subjected to the highest and the lowest source fluid

temperature performed on average, 23%-54% better and 27%-87% worse respectively than would be expected from the tube if in each case all the tubes were subjected to the same elevated or reduced source fluid temperature.

ACKNOWLEDGEMENTS

The author wishes to express his profound gratitude to Prof. T. W. McDonald for his invaluable guidance, encouragement and patience at all stages of this project.

The author is extremely grateful to Dr. W.T. Kierkus and to Dr. N.W. Wilson for their suggestions and help throughout this study. The technical assistance extended by Mr. R. Tattersall and by Mr. W. Beck is highly appreciated. Special thanks to the Mechanical Engineering faculty in general, and to the graduate students in particular for having shared a very pleasant time with the author.

Acknowledgement is made to the NSERC Operating Grant A-877 for providing financial support.

The affectionate correspondence and constant encouragement from my parents was a source of great inspiration without which this study could not have been possible.

TABLE OF CONTENTS

ABSTRACT	iv
ACKNOWLEDGEMENTS	vi
LIST OF FIGURES	ix
LIST OF TABLES	xii
NOMENCLATURE	xiii
CHAPTER	
I. INTRODUCTION	1
1.1 General	1
1.2 Objective of the present study	3
1.3 Performance Rating	5
II. LITERATURE SURVEY	8
2.1 Previous work	8
2.2 Concurrent studies	16
III. APPARATUS AND INSTRUMENTATION	17
3.1 Loop assembly	17
3.2 Evaporator and condenser units	19
3.2.1 Header	20
3.2.2 Separator	24
3.3 Condenser liquid-header	24
3.4 Flexible tubing	26
3.5 Flowmeter assembly	27
3.6 Reservoir	28
3.7 Heat source and sink	31
3.8 Data acquisition system	31
3.9 Leakage Test	32
IV. EXPERIMENTAL PROCEDURE	34
4.1 Charging procedure	34
4.2 Testing procedure	35
4.3 Details of tests	37
4.3.1 Test sequence I	38
4.3.2 Test sequence II	38
4.3.3 Test sequence III	39
4.4 Data Analysis	40
4.5 Experimental uncertainty	41

V.	RESULTS AND DISCUSSION	42
	5.1 Comparison with earlier work	42
	5.2 The base system	45
	5.2.1 Comparison with theoretical predictions	51
	5.3 Effect of charge distribution	53
	5.4 Effect of unequal heating	60
VI.	CONCLUSIONS	75
	REFERENCES	78
	APPENDICES	
	A-Tabulated results of experiments	79
	B-Data Acquisition program	87
	C-Sample output	92
	D-Uncertainty analysis	93
	E-Equations used in the simulation program	96
	F-Flowmeter calibration curve for R11	104
	G-Least squares polynomial equations	105
	VITA AUCTORIS	106

LIST OF FIGURES

1. Schematic elevation of coil loop thermosiphon showing separator and liquid recirculation	2
2. Schematic elevation view of coil loop thermosiphon heat exchangers	4
3. Electrical analog of an idealized thermosiphon loop	6
4. Experimental loops of Hwang and Diciccio	9
5. Thermosiphon loop simulated by the computer	12
6. Schematic line diagram of the multitube two phase thermosiphon heat exchanger	18
7. Thermocouple junction on copper tubes	21
8. Side view of an evaporator tube	22
9. Side and front views of the evaporator header separator assembly	23
10. Front view of the condenser liquid header	25
11. Joint between flexible and copper tubing	25
12. Schematic of the plumbing arrangement to supply the flowmeters	29
13. Reservoir arrangement	30
14. Comparison between Sampath's data and current data	43
15. Heat transfer rate and overall conductance vs. evaporator static charge for $T(\text{source})=40\text{C}$ and $T(\text{sink})=20\text{C}$	47
16. Heat transfer rate and overall conductance vs. evaporator static charge for $T(\text{source})=35\text{C}$ and $T(\text{sink})=25\text{C}$	47
17. Average evaporator heat transfer coefficient vs. evaporator static charge for $T(\text{source})=40\text{C}$ and $T(\text{sink})=20\text{C}$	48
18. Average evaporator heat transfer coefficient vs. evaporator static charge for $T(\text{source})=35\text{C}$	48

19. Comparison of experimental and simulated results for $T(\text{source})=40\text{C}$ and $T(\text{sink})=20\text{C}$ 52
20. Comparison of the average evaporator heat transfer coefficient between experimental and simulated results for $T(\text{source})=40\text{C}$ and $T(\text{sink})=20\text{C}$ 52
21. Heat transfer rate and overall conductance vs. evaporator static charge for $T(\text{source})=40\text{C}$ and $T(\text{sink})=20\text{C}$ with the evap. tube bank inclined $0,30$ and 45 deg. 54
22. Heat transfer rate and overall conductance vs. evaporator static charge for $T(\text{source})=35\text{C}$ and $T(\text{sink})=25\text{C}$ with the evap. tube bank inclined $0,15$ and 30 deg. 54
23. Average evaporator heat transfer coefficient vs. evaporator static charge for $T(\text{source})=40\text{C}$ and $T(\text{sink})=20\text{C}$ with the evap. tube bank inclined $0,30$ and 45 deg. 55
24. Average evaporator heat transfer coefficient vs. evaporator static charge for $T(\text{source})=35\text{C}$ and $T(\text{sink})=25\text{C}$ with the evap. tube bank inclined $0,15$ and 30 deg. 55
25. Heat transfer rate and overall conductance vs. evaporator static charge for $T(\text{source})=40\text{C}$ and $T(\text{sink})=20\text{C}$ with the evap. tube bank rotated $0,30$ and 45 deg. 57
26. Heat transfer rate and overall conductance vs. evaporator static charge for $T(\text{source})=35\text{C}$ and $T(\text{sink})=25\text{C}$ with the evap. tube bank rotated $0,15$ and 30 deg. 57
27. Average evaporator heat transfer coefficient vs. evaporator static charge for $T(\text{source})=40\text{C}$ and $T(\text{sink})=20\text{C}$ with the evap. tube bank rotated $0,30$ and 45 deg. 59
28. Average evaporator heat transfer coefficient vs. evaporator static charge for $T(\text{source})=35\text{C}$ and $T(\text{sink})=25\text{C}$ with the evap. tube bank rotated $0,15$ and 30 deg. 59
29. Heat transfer rate and overall conductance vs. evaporator static charge for $T(\text{source})$ average $=40\text{C}$ and $T(\text{sink})=20\text{C}$ for $\Delta t=2\text{C}, 3\text{C} \ \& \ 4\text{C}$ 65

30. Average evaporator heat transfer coefficient vs. evaporator static charge for T(source) average =40C and T(sink)=20C for $\Delta t=2C, 3C$ and 4C	65
31. Heat transfer coefficients in individual tubes vs. static charge for $\Delta t=2$ deg. Celsius	68
32. Heat transfer coefficients in individual tubes vs. static charge for $\Delta t=3$ deg. Celsius	69
33. Heat transfer coefficients in individual tubes vs. static charge for $\Delta t=4$ deg Celsius	70
34. Heat transfer coefficients in individual tubes vs. static charge for a 42 C-42 C-40 C configuration	73
35. Heat transfer coefficients in individual tubes vs. static charge for a 42 C-40 C-40 C configuration	74

LIST OF TABLES

<u>TABLE</u>		<u>PAGE</u>
1	Performance data for $T(\text{source})=35\text{C}$, $T(\text{sink})=25\text{C}$ with different degrees of subcooling	50
2a	Performance data for $\Delta t=2\text{C}$. High source water flow rate	62
2b	Performance data for $\Delta t=2\text{C}$. Low source water flow rate	62
3	Performance data for $\Delta t=3\text{C}$	63
4	Performance data for $\Delta t=4\text{C}$	63
5	Performance data for source fluid temperatures of 42C , 42C and 40C	71
6	Performance data for source fluid temperatures of 42C , 40C and 40C	71

NOMENCLATURE

A_e	Evaporator inside surface area (sq.m)
H	Average evaporator heat transfer coefficient ($= Q/A (T_{ew} - T_{sat})$, W/sq.m K)
h	Heat transfer coefficient in an individual tube (W/sq.m K)
Q	Total heat transfer rate in the evaporator (Watts)
ΔT	Temperature difference between source and sink fluids (C)
Δt	Source temperature difference between adjacent evaporator tubes (C)
ΔT_{sub}	Temperature difference between the evaporator header temperature and refrigerant temperature measured upstream of the evaporator (C)
T_{ew}	Average evaporator wall temperature (C)
T_{sat}	Saturation temperature in the evaporator header (C)
U	Overall conductance based on the heat transfer in the evaporator and the evaporator area (W/sq.m K)
U_{ee}	Loop conductance based on the heat transfer rate in the evaporator and the evaporator area (W/sq.m K)

CHAPTER I

INTRODUCTION

1.1 GENERAL:

A two phase thermosiphon coil loop heat exchanger, with separator and liquid recirculation line, is shown schematically in Fig. 1. Such a system transports energy between a hot and a cold region through the flow of an intermediate working fluid between an evaporator and a condenser. The vapour flows from the evaporator to the condenser due to a saturation pressure difference which arises because of the fact that the liquid vapour interface temperature in the evaporator and hence the saturation pressure is always higher than that in the condenser. The geometric configuration must be such that the condensate can flow back to the evaporator by virtue of gravity. The presence of a separator and a liquid recirculation line allows a higher charge in the evaporator in order to suppress dryout without the penalties associated with liquid carryover into the condenser. For the system to operate, liquid must always be present in the evaporator coil. If the orientation of the system is such that liquid is present at all times in both coils then the loop can transfer heat in either direction. Such an installation is said to be bidirectional. However, if the liquid drains completely from one coil when the system is inoperative, as is the case in Fig. 1 then heat can only be transferred in one direction and the system is said to be unidirectional.

Two phase thermosiphon loop heat exchangers are currently being used as solar collectors for hot water systems. Another potential area

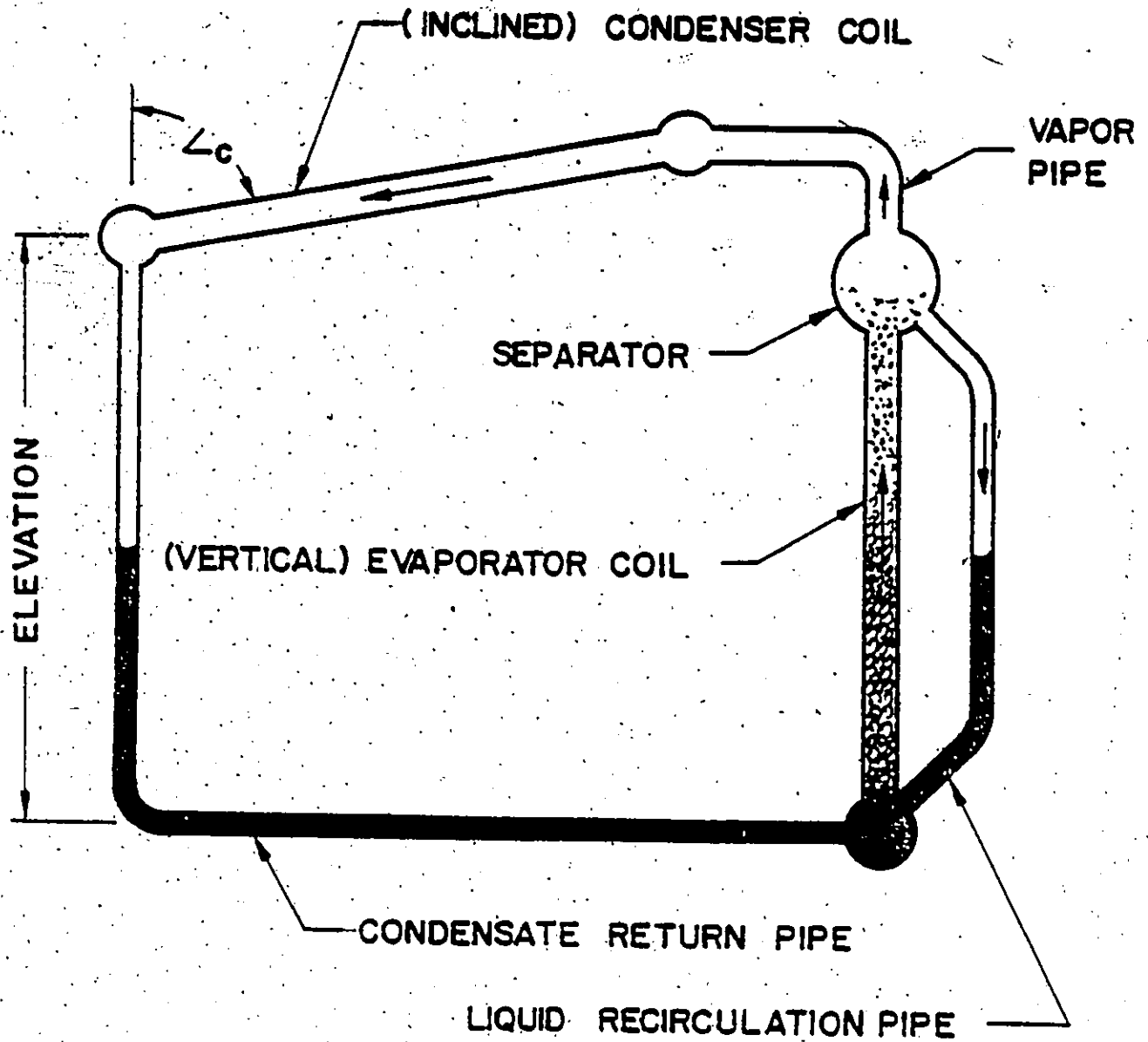


FIG. 1: Schematic elevation of a coil loop thermosiphon showing separator and liquid recirculation

of application is in the reclamation of waste energy. In their application as a typical air to air heat exchanger the evaporator and the condenser coils would be placed in the exhaust and supply air ducts interconnected by liquid and vapour headers as shown in Fig. 2.

Compared to forced circulation single phase coil loop systems, two phase coil loop thermosiphons may be the desired choice for reclaiming waste energy between inlet and exhaust air/gas ducts which are not adjacent to one another. For such systems there is no need for an external source of power since they do not require a pump and drive motor. In addition, being only partially filled with a working fluid such systems are lighter in weight than single phase coil loop heat exchangers.

The performance of two phase coil loop thermosiphons with evaporator tubes which are equally heated and which have the same charge of working fluid, has been previously reported (1,2).

1.2 OBJECTIVE OF THE PRESENT STUDY:

In a typical application for recovering waste energy, the evaporator of a two phase thermosiphon coil loop system may consist of several rows of tubes interconnecting common liquid and vapour headers. In such systems, as the source fluid passes through the evaporator coil it cools. Thus each successive row of tubes is subjected to a different source fluid temperature and hence a different heating condition. In addition, any temperature variations of the hot gas over the cross sectional area of the duct will also cause tubes in the same row to be

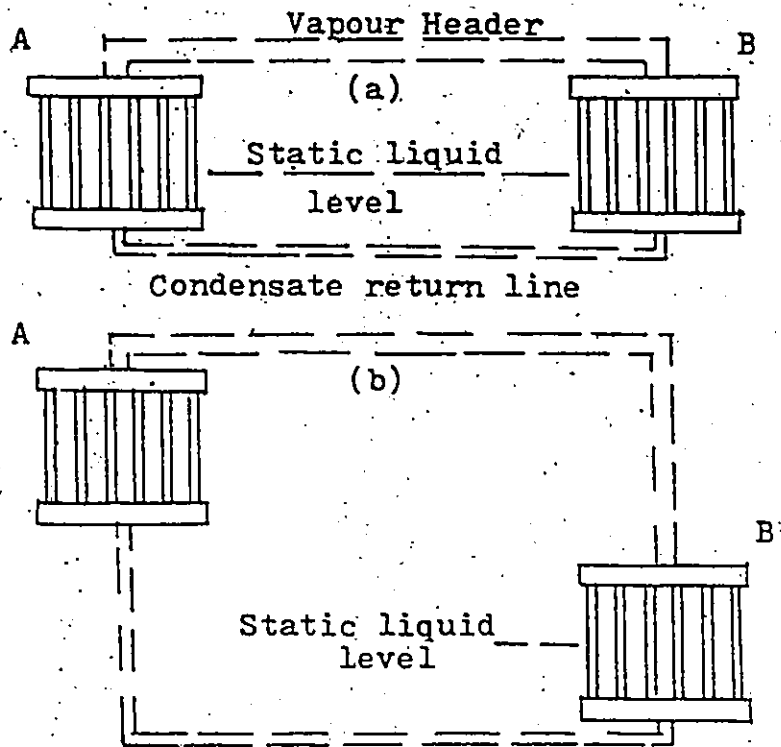


FIG. 2: Schematic elevation view of coil loop thermosiphon heat exchangers.

- (a) Bidirectional installation. Loop can transfer heat in either direction.
- (b) Unidirectional installation. Loop can transfer heat only from B to A.

subject to unequal heating. In certain applications, if the evaporator is installed with its header horizontal but with its tubes inclined from the vertical, then each row of tubes connected to a common header will have a different charge of working fluid. None of the previous experimental studies have explored the effect of these conditions.

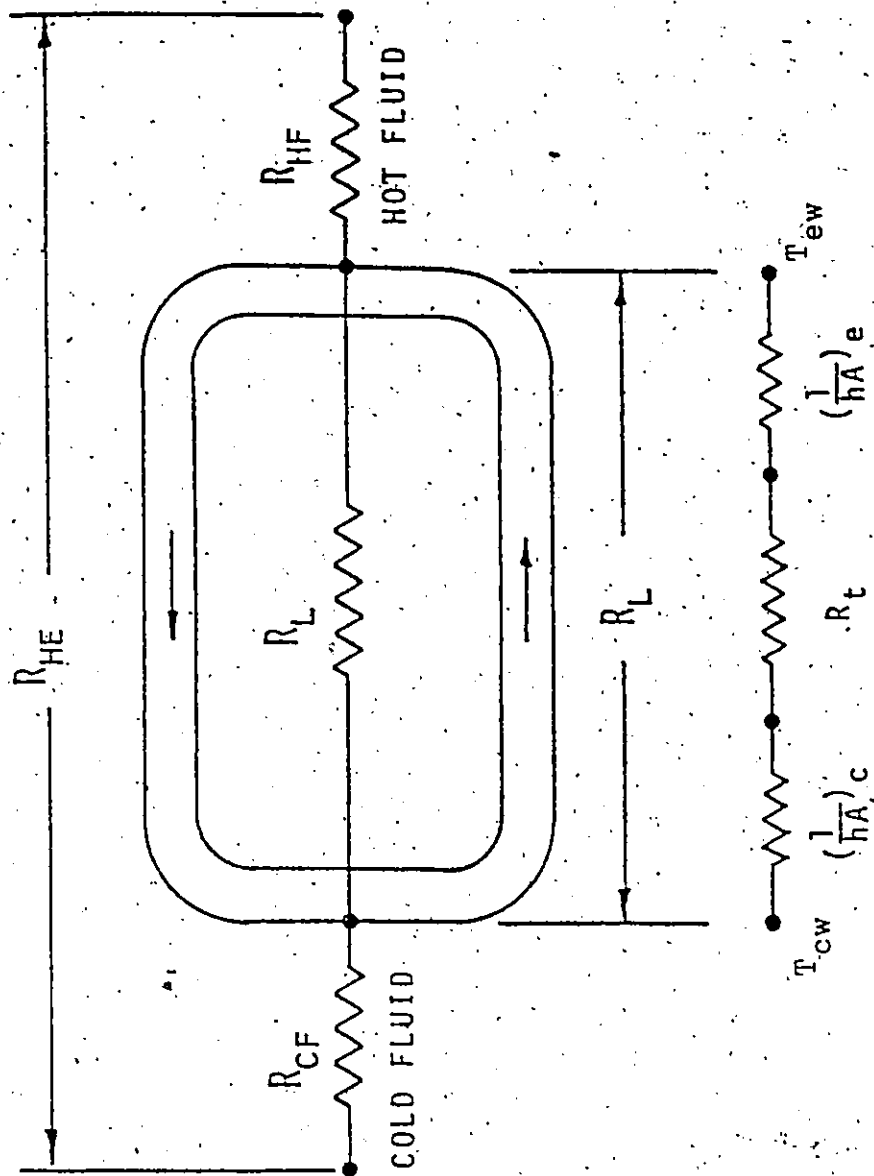
The objective of the present study is to investigate the behaviour of the evaporator of a two phase thermosiphon loop heat exchanger under the following conditions:

- i) Unequal proportion of the working fluid in each evaporator tube.
- ii) Unequal heating of the evaporator tubes.

1.3 PERFORMANCE RATING:

The overall conductance for a thermosiphon heat exchanger is defined as the amount of energy transferred per unit area per unit temperature difference between the source and the sink fluids. The external geometry of the system, the presence of fins, and the type and properties of the source/sink fluids all play an important role in the evaluation of this parameter since the external resistances are an integral component of the total resistance. Thus, no general tabulations are possible. Fig. 3 shows an electrical analog of an idealized two phase thermosiphon coil loop. It shows the hot and the cold side resistances and the loop resistance which may be divided into three parts namely:

- i) the boiling film resistance



HEAT EXCHANGER CONDUCTANCE $(UA)_{HE} = R_{HE}^{-1}$
 THERMOSIPHON LOOP CONDUCTANCE $(UA)_L = R_L^{-1}$

FIG. 3: Electrical analog of an idealized thermosiphon loop

ii) the transport resistance

iii) the condensing film resistance

For an indepth discussion of these resistances the reader is referred to reference (3).

Since the thermosiphon loop conductance is independent of the source and sink external resistances it has been used as a criterion to measure the performance of equally heated coil loops (1,2). The criterion used in this study to compare the performance of the evaporator under different operating conditions is the average evaporator heat transfer coefficient.

CHAPTER II

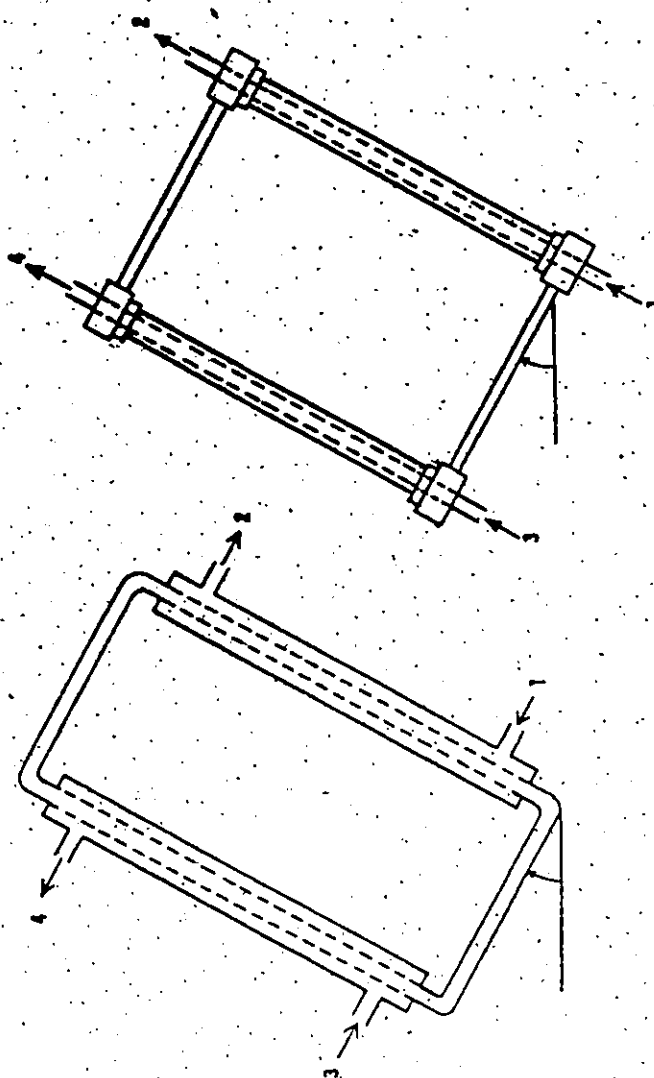
LITERATURE SURVEY

2.1 PREVIOUS WORK:

A literature survey of earlier research work on the performance characteristics of two phase thermosiphon heat exchangers subjected to a constant temperature boundary condition is presented in this chapter. To the author's best knowledge, work in this area has been carried out exclusively at the Department of Mechanical Engineering, University of Windsor. A major research project sponsored by ASHRAE titled "Development of performance characteristics for two phase thermosiphon loops" (4) was undertaken by the thermosiphon research group at the University of Windsor. Due to the complex nature of the variables which affect the performance of such loops, the major thrust of this research project was the development and validation of a computer program to simulate the behaviour of two phase thermosiphon heat exchangers. A flow visualization and an experimental study were carried out concurrently on two separate single tube, two phase, thermosiphon, heat exchangers to gain a better understanding of the boiling and condensation phenomenon and to gather data for the validation of the computer program.

Hwang and Diccio(5) initiated experimental work in this field. Their studies were on single tube two phase thermosiphon loops, shown schematically in Fig. 4 (a & b) respectively. The two loops could be charged to any desired percentage of full capacity. Each of the loops were mounted on a plane and could be oriented in any fashion in the gravity field.

1 and 2: Hot water (source) inlet and outlet, respectively.
3 and 4: Cold water (sink) inlet and outlet, respectively.



a) Large (1.12 x .61 m) loop
b) Small (.61 x .30 m) loop

FIG. 4: Experimental thermosiphon loops of Hwang and Dicicco

The loop designed by Diccio was primarily intended for flow visualization but was instrumented to measure wall temperatures and the energy transferred by both the evaporator and the condenser. The evaporator and the condenser were concentric tube heat exchangers with the inner surface consisting of 1/2" copper tubing containing the source and the sink fluids and the outer sheath being 5/8" inside diameter glass pipe. The evaporator and the condenser were 2 feet long and the interconnecting headers were 1 foot long.

The loop designed by Hwang(6), was primarily used to gather experimental data. The evaporator and condenser were 4 feet long concentric tube heat exchangers interconnected by 2 feet long vapour and condenser headers. The heat exchanger loop had 3/8" diameter copper tubes as the evaporator and the condenser. The source and the sink fluids were circulated through the annular jacket around the evaporator and the condenser. Three copper-constantan thermocouples, embedded in the outside surface of both the evaporator and the condenser, measured the wall temperatures. Two thermocouples measured the temperature of the working fluid at the top of the evaporator and at the bottom of the condenser. Also, water inlet and outlet temperatures in the evaporator and the condenser units were recorded to evaluate the amount of energy transferred. A refrigerant pressure gage measured the system pressure.

They studied the performance of their loops by varying the following parameters:

- i) the average temperature difference between the evaporator source and the condenser sink fluids
- ii) the inclination of the evaporator and the condenser

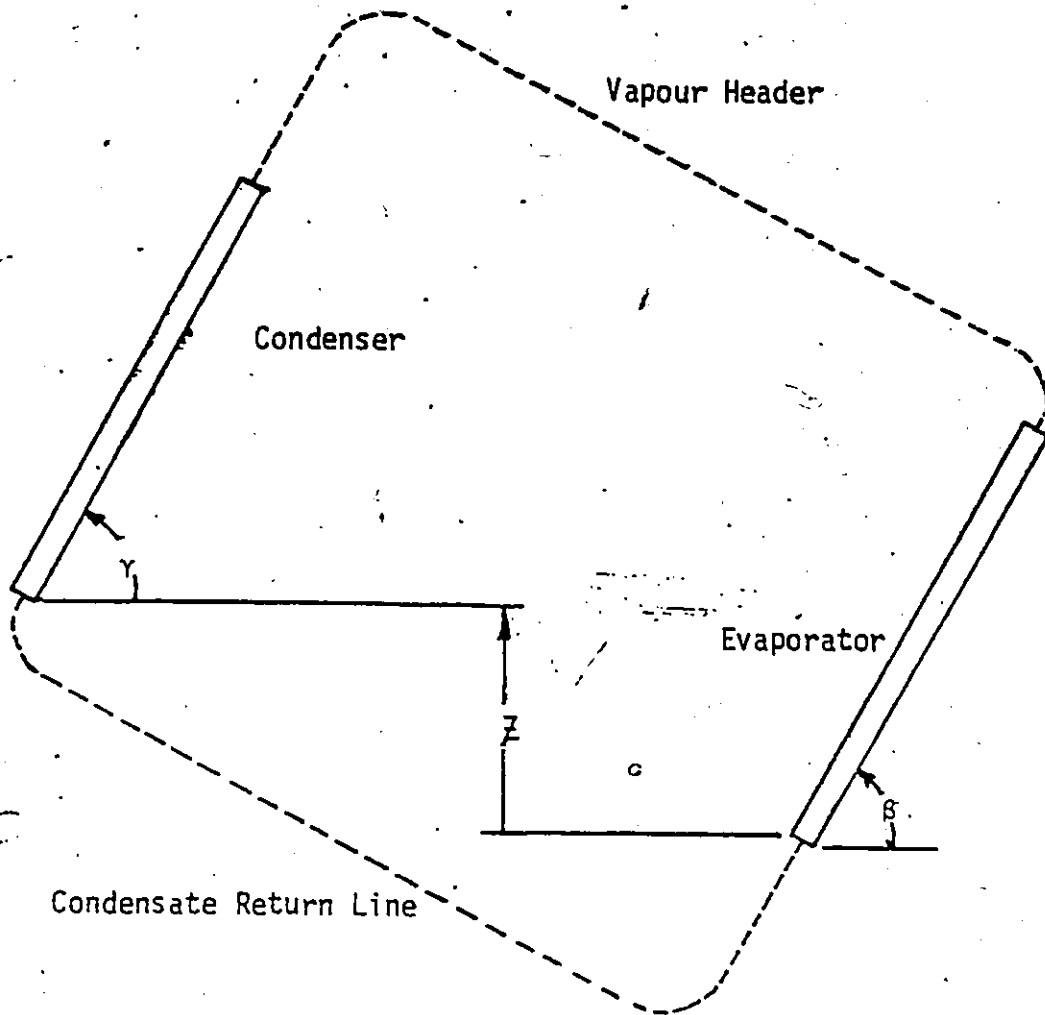
iii) the charge quantity and distribution

iv) the working fluid

The performance was found to depend strongly on each of the above factors. Their results showed that for a given geometry and source-sink fluid temperature an optimum charge exists which yields the maximum performance. It was found that the loops perform best when the condenser is nowhere flooded and no dryout occurs in the evaporator.

Ali(3) developed a computer simulation program for determining the performance characteristics of such loops. The computer program was capable of generating performance characteristics for loops of the type shown in Fig. 5. Ali tested the program by simulating the tests carried out by Hwang and Diccio and found the predictions of his program agreed with the experimental data within the limits of experimental error. The capability of the program to successfully predict performance characteristics pertaining to two different loop geometries and types of charges served as a severe test of its versatility. Ali also reported the predictions to be least reliable when dryout occurs over a significant portion of the evaporator.

The successful validation of the computer simulation program enabled Ali to study the effect of those parameters which would be very tedious to vary in an experimental study, e.g. the effect of the evaporator and condenser tube diameters and their lengths on the loop conductance. He reported that, for a given geometry and temperature difference between the source and sink fluids, the peak performance was a function of tube diameter and tube length. The peak performance, which was found to be most sensitive to changes in the tube length, decreased



The evaporator, condenser, vapour and condensate tube lengths and diameters must be specified as well as β , γ and Z , the angle of inclination of the evaporator and of the condenser from the horizontal and the elevation of the condenser base above the evaporator base respectively.

FIG. 5: Thermosiphon loop simulated by the computer program

with length.

Ali compared the loop performances for unidirectional and bidirectional cases. He found that the performance of the bidirectional loop was poorer than that for the unidirectional loop operating between the same set of conditions because the flooding of the condenser reduced the area available for condensation. The loop conductance versus static charge profiles for bidirectional loops were much flatter than the corresponding profiles for unidirectional loops due to their larger overall resistance. In bidirectional loops, due to condenser flooding, the condenser resistance is much larger than the boiling film and the transport resistances and changes in the latter two resistances have a negligible impact on the overall resistance. In unidirectional loops the liquid carried over to the condenser has to be thermally pumped to a higher elevation resulting in a substantial pressure drop and a significant increase in the transport resistance with increasing charge.

The interesting findings of RP-140 prompted ASHRAE to allocate additional funds for research in this area, as a result ASHRAE project RP-188, "Multiple tube evaporator and condenser loops" (7), was initiated by the thermosiphon research group at the University of Windsor. The major aspect of this study was to investigate the behaviour and stability of a two phase thermosiphon heat exchanger system with multiple evaporator tubes and liquid recirculation on the evaporator side, and also to compare the predictions of the computer simulation program against additional experimental data. A new multi-tube two phase thermosiphon heat exchanger with separator and liquid recirculation was designed and built and performance ratings for unidirectional and

bidirectional loops were investigated.

The multitube heat exchanger designed by Sampath has been reported in (8). However, since this draft is not readily available and since a few components were modified, details of the design can be found in the latter sections of this thesis. The major aspect of his design was the inclusion of a separator and a liquid recirculation line in the evaporator resulting in a significant decrease in the transport and condenser resistances. The presence of a separator and a liquid recirculation line suppresses the onset of dryout by permitting:

- i) a higher charge to be present in the evaporator without the penalties of liquid carryover;
- ii) a larger flow rate in the evaporator due to an additional flowpath because of the evaporator recirculation tube.

For a unidirectional loop Sampath found that a tilted condenser works better than a vertical because of the substantial reduction in the condenser resistance due to improved heat transfer coefficients for condensation. For a given set of conditions, he found the loop conductance to be relatively insensitive to condenser inclination angles between 15 and 75 degrees. However, a substantial improvement in performance was observed between 0 and 15 degrees measured from the vertical. He found that the presence of the separator resulted in the generation of much flatter curves of loop conductance versus evaporator static charge compared to the earlier findings of Hwang and Diciccio.

For a particular level of static charge he observed that the loop conductance was less sensitive to changes in the temperature

difference between the source and the sink for a constant mean temperature. Sampath reported that the use of a separator permits improved operation at low temperature differences due to the absence of liquid carryover, also dryout could be suppressed by increasing the charge in the evaporator.

Ali(1) modified his original computer simulation program so that the new test facility could be simulated. He also investigated the effect of evaporator tube diameter and length on the loop conductance for a given set of conditions. He found that as the evaporator tube diameter increases, the maximum loop conductance decreases and shifts to higher tube lengths.

Sampath(2) found that for bidirectional loops the variables which affect the loop conductance most are the charge and the angles of inclination. The greater sensitivity of the loop conductance to charge was due to the increased condenser resistance with increasing static charge due to condenser flooding. Inclination of the condenser tubes from the vertical with the vapour header remaining horizontal resulted in improved condensation coefficients and thus improved performance. The bidirectional configuration was found to be relatively insensitive to temperature differences between the evaporator and the condenser due to the absence of liquid carryover and less susceptibility to dryout, the two essential factors which can make the loop conductance very sensitive to imposed temperature differences.

The findings of ASHRAE RP-188 can be summarized as follows:

- i) The computer simulation program predicted the performance

within close agreement with the experimental results.

- ii) The recirculation two phase thermosiphon heat exchanger was found to have a higher loop conductance and significantly reduced sensitivity to operating conditions than the non recirculation loop.
- iii) Advisability of having an inclined condenser so as to have improved condensation coefficients.

2.2 CONCURRENT STUDIES:

Ali's original computer simulation program has been modified by Mathur(9) to study the effect of the parameters which were varied in this experimental study. Validation studies for the computer program, based on the experimental results, are currently underway.

Experimental studies on a full scale two phase thermosiphon air to air heat exchanger, a typical design for commercial applications, are currently underway. The test facility is capable of circulating approximately 1.0 cubic meter per second of air through the evaporator and the condenser while maintaining a 50C temperature difference. Eight rows of evaporator and condenser coils may be coupled to yield any combination of one to eight loops.

CHAPTER III

APPARATUS AND INSTRUMENTATION

3.1 LOOP ASSEMBLY:

An experimental test rig, originally designed by Sampath(8), was modified and used in this experimental work. Fig. 6 gives a schematic line diagram of the modified loop assembly. Since the primary purpose of Sampath's study was to provide data which could be used for the verification of a computer simulation program, it was designed and built so that the effect of as many variables as possible could be studied experimentally.

In order to simulate air flowing past a vertical tube in a cross flow configuration, a situation which would arise in a typical air to air thermosiphon heat exchanger, each of the evaporator and the condenser tubes were heated or cooled by water flowing in an annular jacket. The annulus was designed so that, for the heat transfer rates expected, a turbulent water flow rate could be maintained and still have a temperature change of approximately 1 degree Celsius in the source and the sink fluids. This was desirable in order to closely approximate a constant temperature and a reasonably constant source external resistance along the length of each tube as would be the case in typical applications.

The two heat exchangers were similar in design except different diameter tubing and annuli were used. Either unit could be used as the evaporator. Each unit could be inclined and/or rotated independently to study the effect of charge distribution. The relative elevation between

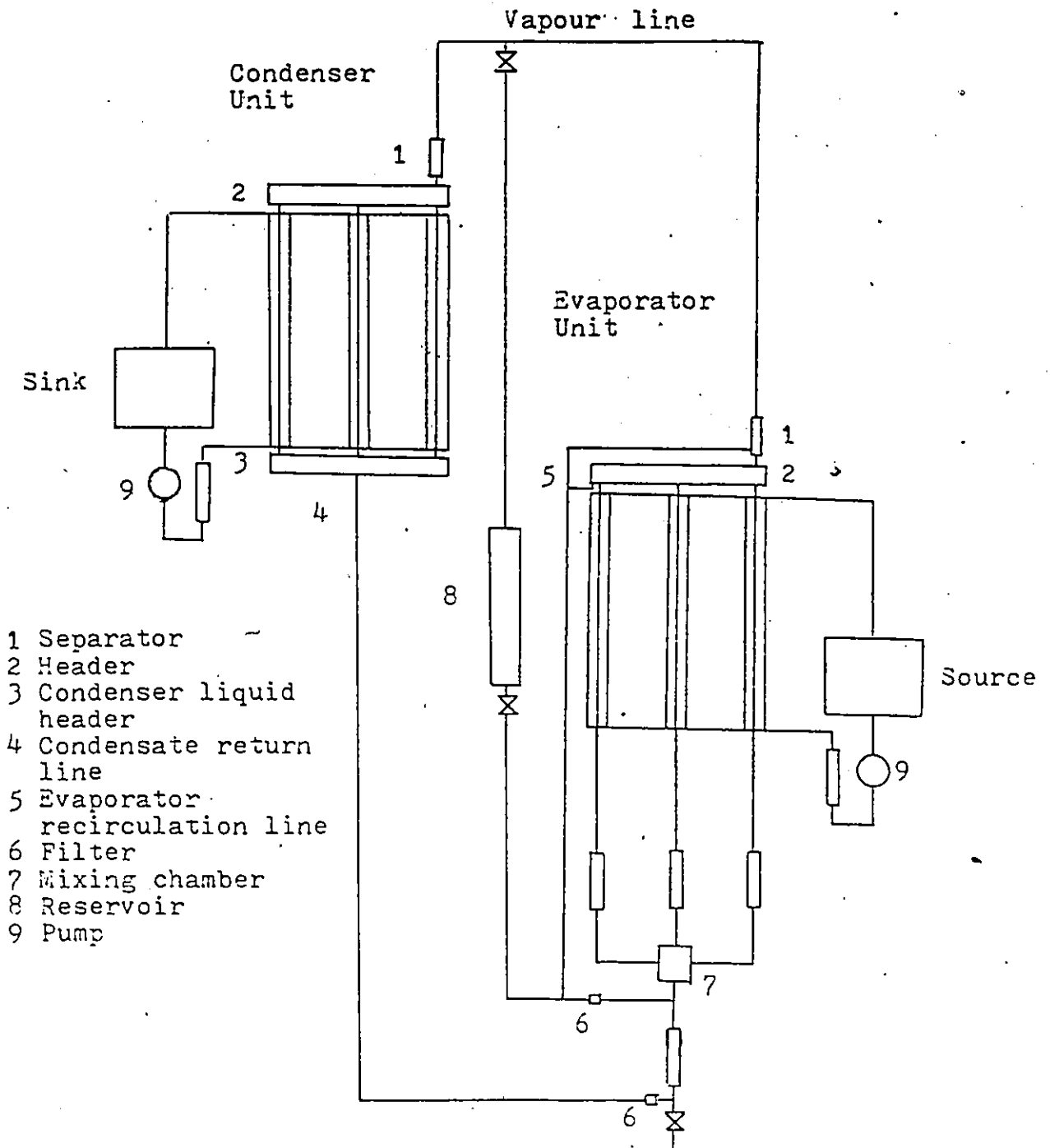


FIG. 6: Schematic line diagram of the multitube two phase thermosiphon heat exchanger

the two could be varied to a maximum of one meter for the loop to operate in a unidirectional mode. The condensate, before entering the mixing chamber, passed through a flowmeter. The condensate and the recirculation liquid came together in the mixing chamber. The liquid mix was supplied to three parallel evaporator tubes and the individual mass flowrate to each evaporator tube was measured.

The reservoir, installed between the liquid and the vapour headers, could be moved vertically to achieve any desired percentage static charge in the evaporator when the system was not in operation. During operation the reservoir was isolated from the main loop assembly by shutting the interconnecting valves.

3.2 EVAPORATOR AND CONDENSER UNITS:

The heat exchanger units are direct transfer double pipe heat exchangers. Both units consist of three coplanar tubes joined to a vapour header with 7.6 cm centre to centre spacing. Each tube has an effective heat transfer length of 0.61 m (2ft). One unit was constructed of nominal 3/8" copper tubing (7.9 mm ID, 9.53mm OD) and the other unit of nominal 1/4" tubing (4.83 mm ID, 6.35mm OD). The tubes of each unit were mounted concentrically within nominal 1/2" (13.84 mm ID, 15.88 mm OD) and nominal 3/8" (10.92 mm ID, 12.7 mm OD) copper pipes respectively to form six independent annular water jackets.

The tube wall temperatures at five locations; 10, 30, 50, 70 and 90% along the heated/cooled length of the tube, were measured by copper-constantan thermocouples. The thermocouple junction was formed

by making grooves circumferentially on the tube approximately 2mm apart, then silver soldering the wires in position, as shown in Fig. 7. A thermocouple placed in the vapour header measured the temperature of the working fluid. The working fluid temperature upstream of the evaporator was measured indirectly by measuring the well insulated tube wall temperature approximately 1 foot from the entrance to the evaporator.

Two thermocouples positioned at the entrance and exit of the annular jacket measured the source and the sink fluid temperatures flowing past the evaporator and the condenser respectively, Fig. 8 shows the arrangement of an evaporator tube.

The rightmost of the original nominal 1/4" tubes had to be replaced. The compression fitting at the inlet to the header was found to be leaking. In an effort to stop the leak the fitting was bent when overtightened. The evaporator header and the separator were also redesigned since they were found to be leaking. When these changes were being made it was decided that an additional 2" of evaporator tubing would be introduced between the evaporator tubes and the header by a coupling joint, so that, if desired, the effect of the length of evaporator tube protruding above the liquid surface in the evaporator header could be studied.

3.2.1 HEADER:

The three 3/8" dia evaporator tubes were connected to a common header, 26.7 cm in length and 5.7 cm in diameter, as shown in Fig. 9.

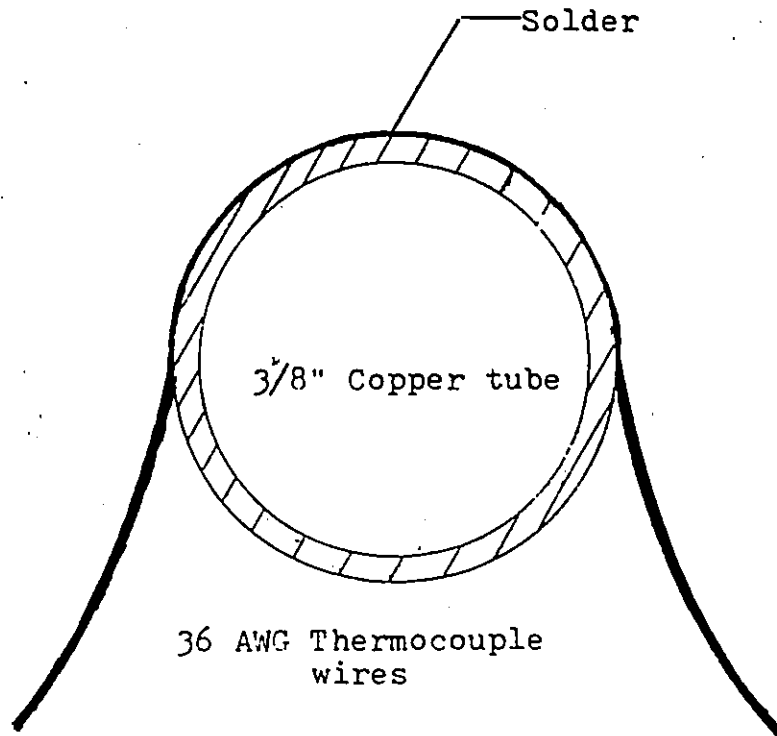


FIG. 7: Thermocouple junction on copper tubes

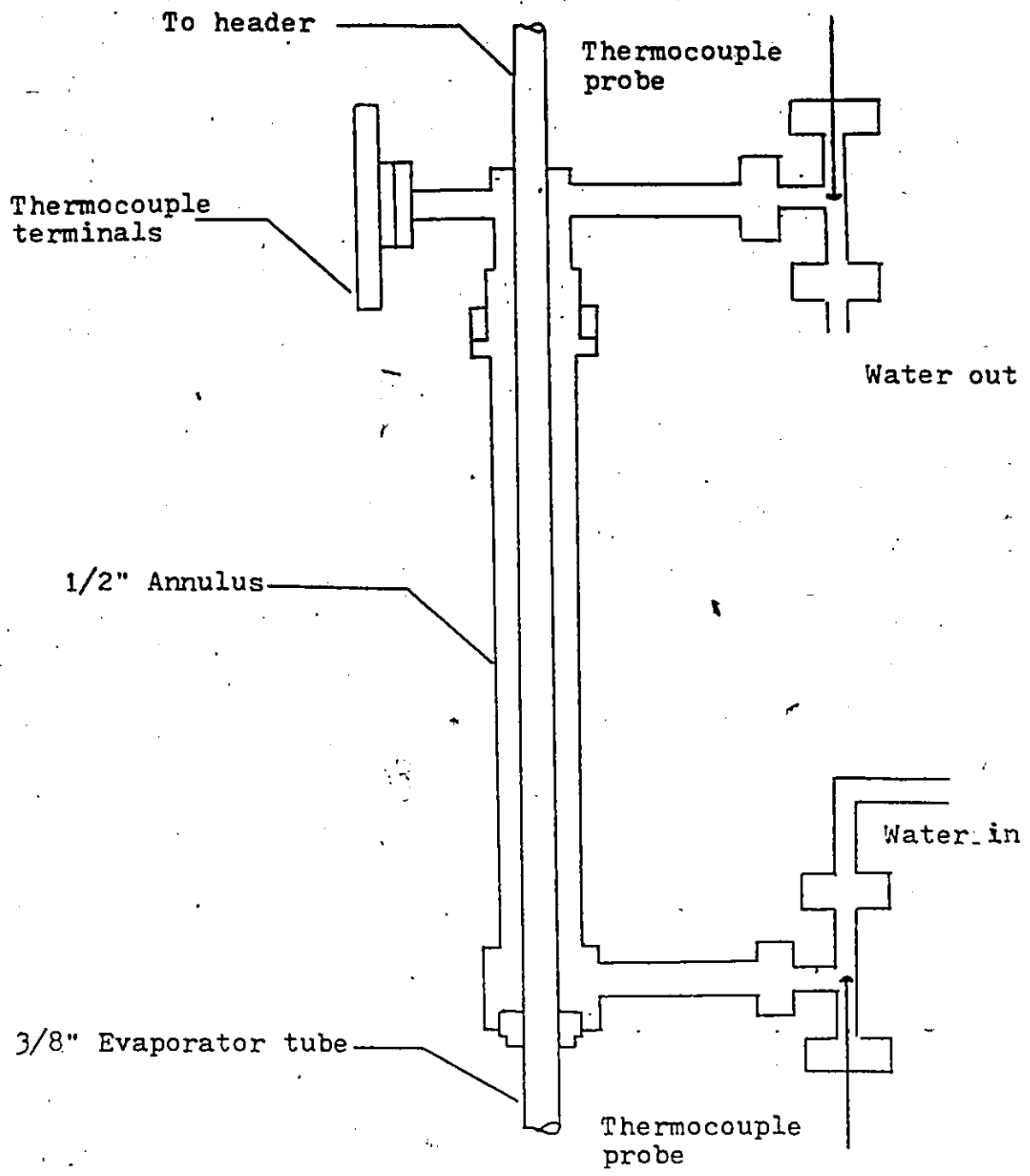


FIG. 8: Side view of the evaporator tube

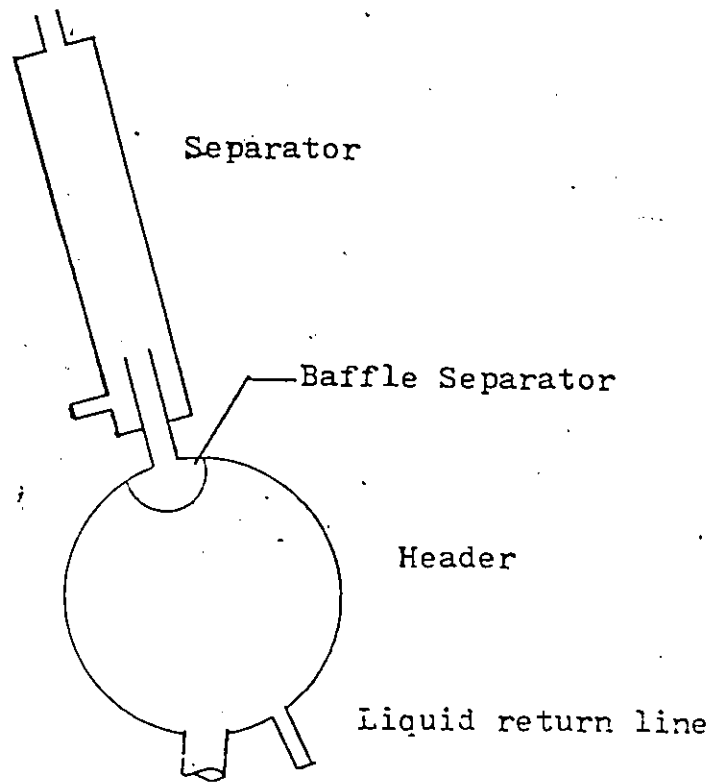
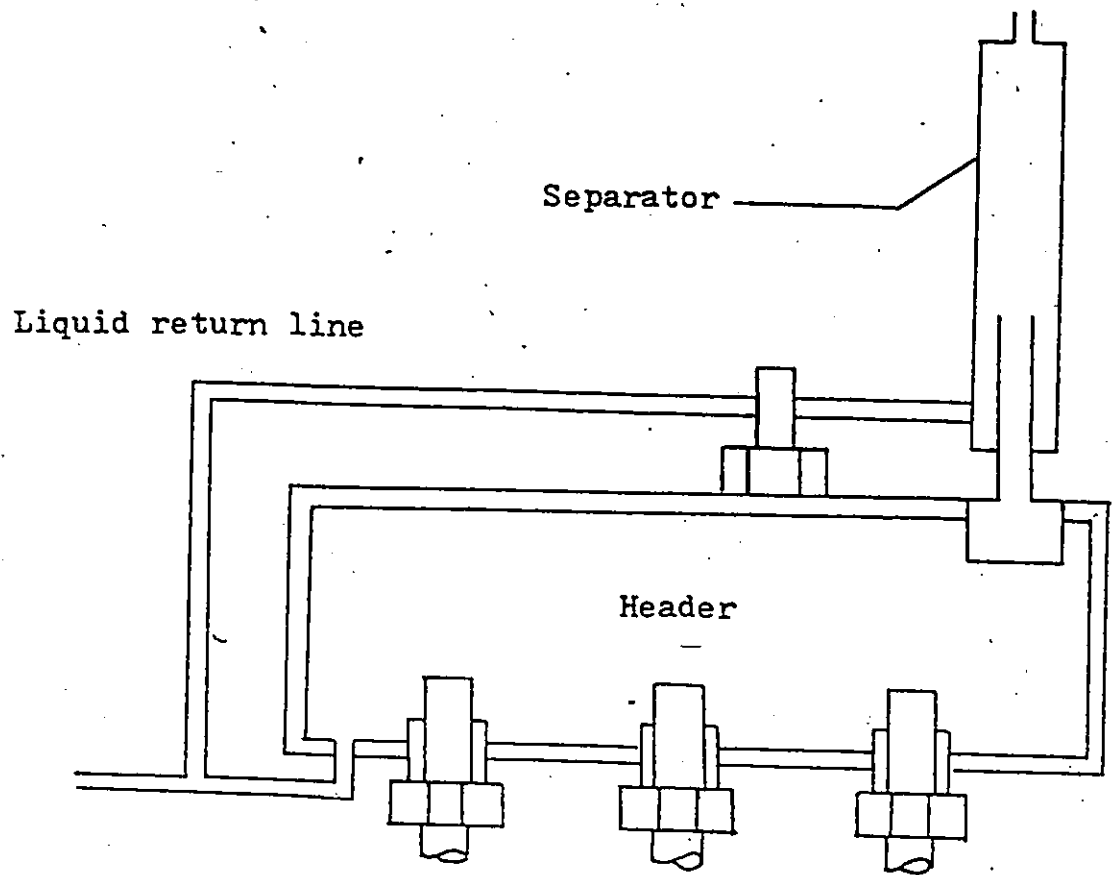


FIG. 9: Front and side view of the evaporator header and separator assembly

The 1/4" dia tube vapour header was slightly smaller in length. A baffle-separator, present in the vapour header, minimized any liquid carryover to the separator. Excess liquid in the vapour header was carried away by a liquid return line located in the bottom of the header. The working fluid temperature was recorded by means of a copper-constantan thermocouple in the vapour header. An additional thermocouple measured the tube wall temperature at the entrance to the liquid return line.

3.2.2 SEPARATOR:

As the name implies its purpose is to prevent any liquid carryover to the condenser. The separator, positioned over the evaporator header is 15.2 cm in length and 2.8 cm in diameter. The separator positioned over the condenser header, 1/4" dia tubes, was slightly larger in diameter. As shown in Fig. 9, the separator is mounted over the header offset by 45 deg. to the vertical, so that when the unit is tilted its function is not hampered and liquid could still be readily drained to the recirculation line.

3.3 CONDENSER LIQUID-HEADER:

As shown in Fig. 10, a condenser liquid header, 21.6 cm in length and 2.9 cm in diameter, was mounted below the condenser tubes. In addition to channelling the condensate from each condenser tube into the condensate return line, the condenser liquid header was utilised to

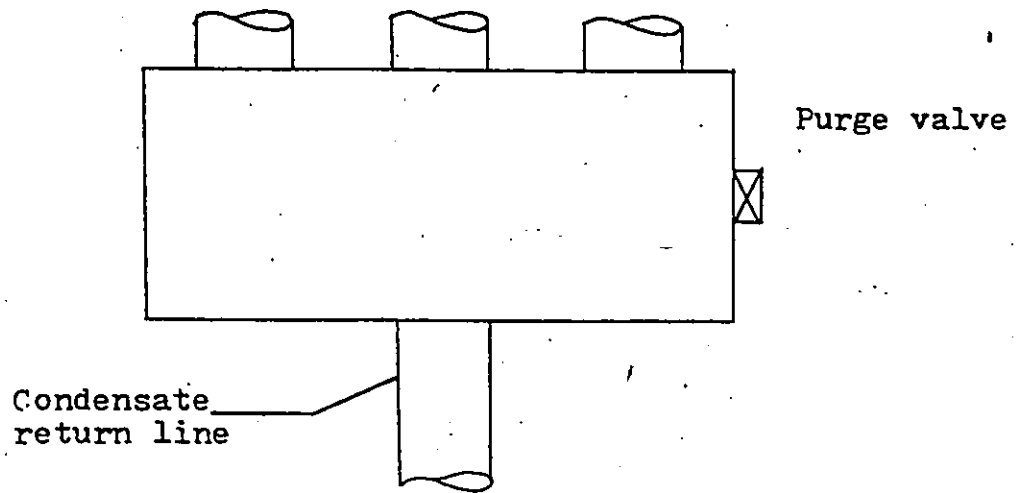


FIG. 10: Front view of the condenser liquid header

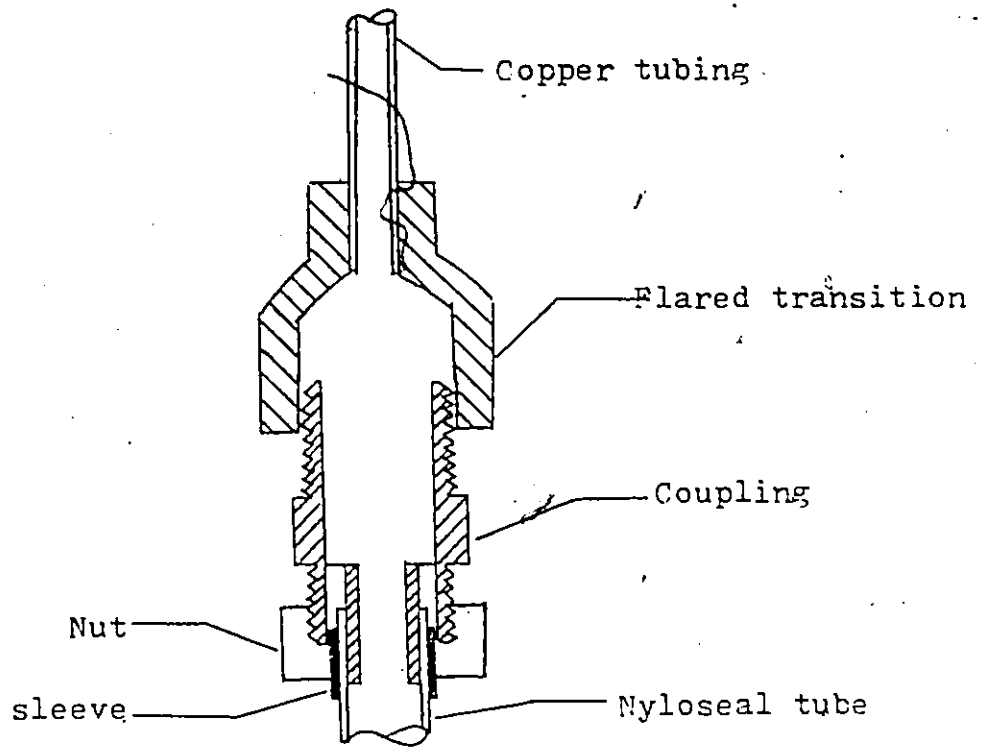


FIG. 11: Joint between flexible and copper tubing

purge noncondensables from the condenser tubes. It was kept cool by a moist cloth such that it was the coolest region in the entire assembly in order to maximize the concentration of noncondensables.

3.4 FLEXIBLE TUBING:

One of the important parameters in Sampath's work was to study the effect of relative elevation between the evaporator and the condenser on the loop performance. It was essential to use flexible tubing to achieve the aforementioned objective. Insulated, transparent teflon tubes, being inert to fluromethanes, were used by Sampath. The liquid level in different sections of the loop assembly could be easily observed through slits in the covering insulation.

When the present study was initiated in 1982 it was found that the teflon tubing had become porous to R-11. As a result its replacement became essential. It was decided not to continue with teflon tubing because of their cost and their non-standard sizes which caused considerable difficulty in joining them to the copper tubes. Based on a manufacturer's catalog (10) Polyflo (polyethylene) tubing was selected as the best alternative due to its low price and very high chemical resistance to Freons. Another great advantage of using Polyflo tubing was the availability of flareless male and female tube fittings so that they could be conveniently connected to copper tubes.

The use of polyflo tubing was catastrophic since the refrigerant was found to slowly diffuse through the tube walls. Since R-11 is widely used in industry as a cleaning agent, it permeates through

materials much more easily than other Freons. The misreporting on the part of the manufacturer resulted in a significant loss of time, effort and money. Another type of tubing which could use flareless fittings, Nyloseal, made of nylon-11, was tested in the laboratory. Its physical and chemical properties were found to be suitable for the test conditions. The results indicated the desirability of using this type of tubing, therefore, all the Polyflo tubing was replaced by Nyloseal flexible colorless tubing. Fig. 11 shows a typical joint between the flexible tubing and a copper tube.

3.5 FLOWMETER ASSEMBLY:

It was decided to build a new stand for the flowmeters and to redesign the entire plumbing network around the rotameters since the original assembly was highly susceptible to leaks due to several unnecessary fittings.

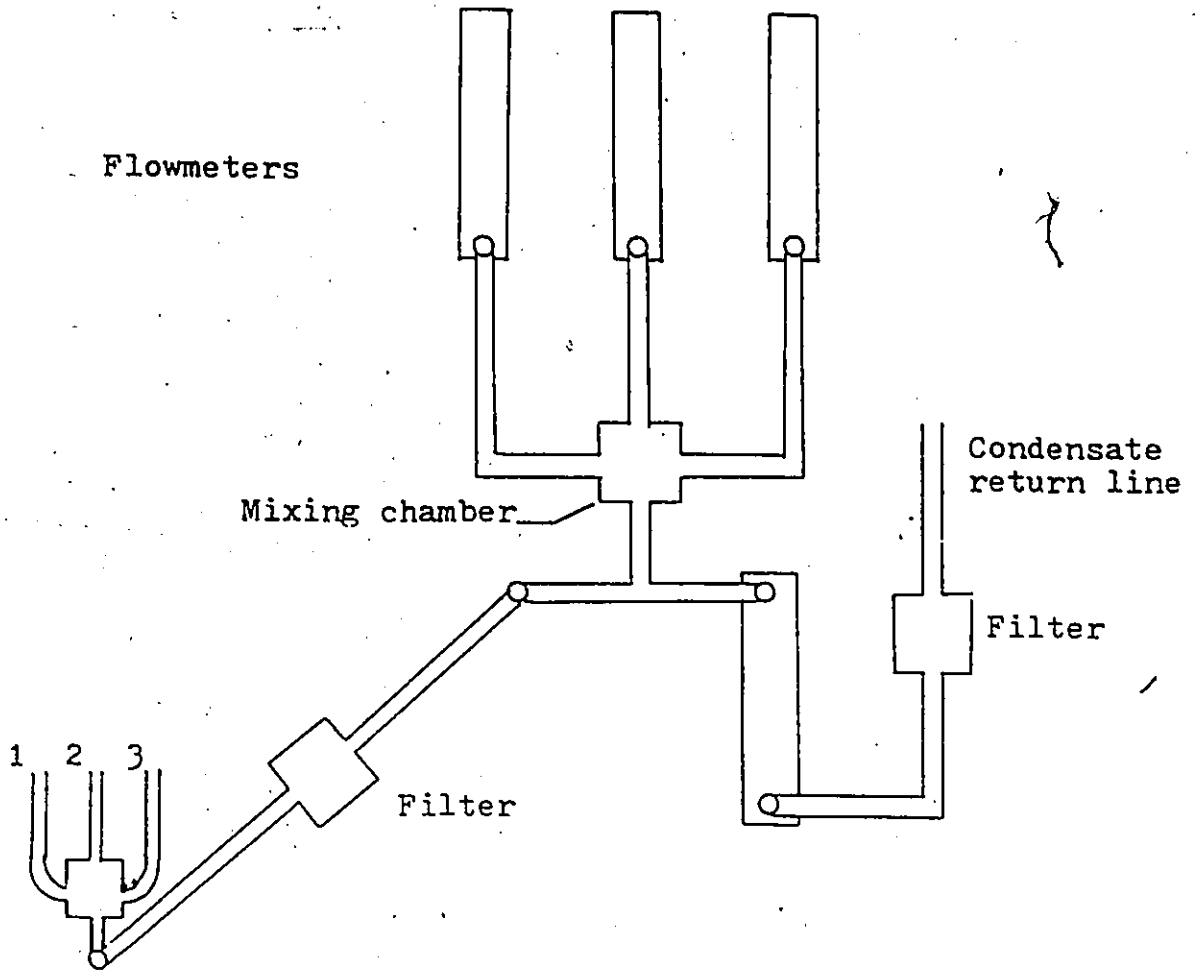
Three SK 1/8-20-G-7 rotameters with black glass floats having a range of 0-30 cubic centimeters of R-11 per minute, were used to measure the mass flowrate in each tube. The flowmeters have needle valves to regulate the flow if necessary. Another, SK 1/8-20-G-7 flowmeter with a stainless steel float, having a range of 0-75 cubic centimeters of R-11 per minute was used to measure the total condensate mass flowrate. The system originally had a rotameter to measure the total recirculation rate, however, this rotameter was inadvertently broken while installing it in position. Since the absence of this flowmeter was not crucial to the study, only four rotameters were used to monitor the

mass flowrates. All four flowmeters were calibrated prior to their use, see appendix F for a calibration curve.

Two filters were installed, one at the entrance to the condensate flowmeter and one at the junction of the evaporator and the condensate recirculation lines, to prevent any particles from blocking the flowmeters. The filter also acts as a drier and has the capability of removing any dissolved water in the refrigerant. It is also capable of removing any acids which may be formed in the system. After passing through the condensate flowmeter the working fluid mixes with the recirculation liquid from the evaporator and the condenser in a small mixing chamber before being supplied to each evaporator tube individually. Fig. 12 shows a schematic of the piping in this region. Flared fittings were used at the entrance and the exit of the flowmeters.

3.6 RESERVOIR:

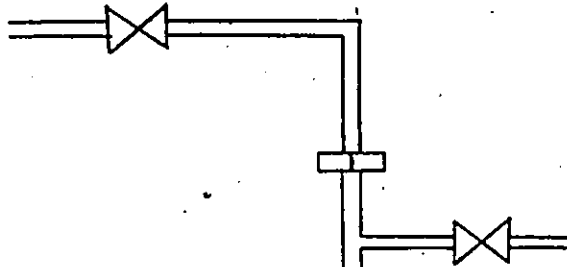
A glass reservoir 3.4 cm in diameter 30.5 cm in length, with a volume roughly twice the total volume of the evaporator and the condenser tubes was used for storing the refrigerant. By changing the elevation of the glass reservoir, under non-operating conditions, the percentage static charge in the evaporator could be varied between 0 to 100%. The reservoir could be isolated from the main loop assembly by shutting the refrigeration valves. Fig. 13 shows the reservoir assembly and Fig. 6 shows the position of the reservoir relative to the evaporator.



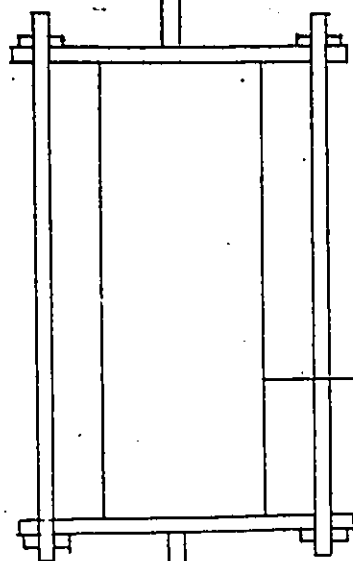
- 1 Condenser recirculation line
- 2 Reservoir line
- 3 Evaporator recirculation line

FIG. 12: Schematic of the plumbing arrangement to supply the flowmeters

To riser



Purge valve



Glass reservoir



To flowmeter assembly

FIG. 13: Reservoir

3.7 HEAT SOURCE AND SINK:

For most of the studies two commercially built constant temperature baths, using distilled water as the source and the sink fluids, were used. In order to investigate the effect of unequal heating of the evaporator tubes, two additional source fluid baths were used. Four flowmeters calibrated prior to testing measured the mass flowrate in each circuit.

3.8 DATA ACQUISITION SYSTEM:

A FLUKE 2240B datalogger was coupled to a TRS-80 Radio Shack Colour computer. A data acquisition program was written to monitor the temperatures at one minute intervals. The program evaluated the heat transfer rates and the loop conductance values based on the average and the current set of data. Five scans were made to establish a standard deviation datum. If the difference in the standard deviation of the loop conductance (based on the average heat transfer rate in the evaporator and the condenser and the average areas of these two units) between two successive scans was less than 3% of the current value of the standard deviation, further scanning was stopped, otherwise, it was continued until ten temperature scans were made. Appendix B gives a listing of the computer program used for data acquisition and evaluation, appendix C gives a sample output. In this output the numbers in parentheses indicate the standard deviations of the values indicated.

3.9 LEAKAGE TEST:

It is imperative that any two phase thermosiphon system be leak free, not only to minimize refrigerant loss, but to prevent air from flowing into the system and adversely affecting the performance of the condenser.

In order to check for leaks, after reassembly, the entire system was charged with nitrogen to a pressure of 40 psig. The leaks were initially detected using a soap solution. Those which went unnoticed by this method were detected by introducing refrigerant into the system and circulating hot water in the evaporator to vaporize the refrigerant. The system was then checked by a halogen electronic detector which is capable of detecting leaks of the order of 1/2 oz per year.

Considerable time was spent in making the system leak free since numerous leaks were encountered in the evaporator and the condenser units, and also near the flowmeter assembly. Depending on the nature of the leaks they were fixed by the use of silver solder, Loctite sealant or double strength epoxy sealant. At times, when it was difficult to ascertain the exact location of leaks, the component was dipped in a water bath to determine the precise location.

The use of flareless tube fittings for connecting the flexible tubing to copper tubes was reassuring since few leaks occurred in these connections. The system was considered suitable for testing when it could hold nitrogen at 40 psig without any noticeable change in the gage

reading for twenty four hours. Also, the system was evacuated to 74.4 cm of mercury, and it was found to hold the vacuum during twenty four hours.

CHAPTER IV

EXPERIMENTAL PROCEDURE

4.1 CHARGING PROCEDURE:

In order to charge the system, a container of refrigerant was connected to a small circulating pump which in turn was attached to the charging valve beneath the condensate flowmeter. The container was held at an elevation of 3 feet in order to avoid cavitation in the pump. The two valves which isolate the reservoir from the loop assembly were kept open. The purge valve immediately above the reservoir was kept closed during charging. The system was charged until the reservoir, positioned centrally with respect to the evaporator, was almost completely full.

Once the system was charged, hot and cold water were run through the evaporator and the condenser sides respectively to vaporize the refrigerant and concentrate the noncondensables on the condenser side and in the glass reservoir. Intermittently, the purge valves in the condenser liquid header and on top of the reservoir were opened to drive away the noncondensables. The condenser liquid header was kept cool by ice cubes or a moist cloth. The system was left running in this fashion for atleast twenty four hours before starting any tests. L

In order to further minimize the presence of noncondensables, for some tests a vacuum pump assembly was used to pull a vacuum on the system, overnight before introducing the charge. At other times, while charging the system the purge valve on top of the reservoir unit was connected to the vacuum pump via two liquid nitrogen traps and kept open for a few seconds to enable flashing of the refrigerant to drive away

the noncondensables. The liquid nitrogen traps prevented the refrigerant from entering the vacuum pump.

It is important to point out at this stage that the modifications made to the original charging procedure discussed in the first paragraph of this section did not show any signs of a substantial decrease in the noncondensables, and therefore they were not repeated.

4.2 TESTING PROCEDURE:

- i) Position the reservoir such that the evaporator static charge is atleast 10% more than the static charge value for which the evaporator performace is to be studied.
- ii) Make sure that the charging and purging valves on top of the reservoir are properly closed.
- iii) Place a moist cloth over the condenser liquid header.
- iv) Program the datalogger to scan all temperatures at one minute intervals.
- v) Set the constant temperature baths to the desired temperature and run hot and cold water through the evaporator and the condenser units. Leave the system running for atleast half an hour and make sure that the constant temperature baths have attained the desired temperature. In the meantime, intermittently purge noncondensables from the system using the valve in the condenser liquid header.
- vi) Turn off the source hot water and after approximately five minutes shut off the sink cold water , allow the system

to reach equilibrium and keep monitoring the temperature in the evaporator header continuously. When the temperature reaches 25C (in order to keep the loop slightly pressurized) move the reservoir such that the desired level of charge is present again in the evaporator tubes.

- vii) Isolate the reservoir from the loop assembly by shutting the two valves shown in Fig. 6.
- viii) Turn on the source and the sink and adjust the water mass flowrates to approximately 35 g/s .
- ix) Load the data acquisition program in the computer and use the RS-232 interface to couple the computer to the datalogger.
- x) Allow atleast twenty minutes to one half hour for the system to stabilize. Next, monitor the temperatures in the evaporator and the condenser header several times to observe whether they are steady. Once steady state conditions are achieved press RUN on the computer and input all the necessary data. The computer next displays a complete scan of all temperatures on the console and asks the question " Do you want to proceed ?". Typing in "YES" and hitting ENTER tells the computer to regard this scan as the first set of experimental data, pressing any other key then hitting ENTER tells the computer to disregard this scan, wait for another scan and repeat the aforementioned procedure.
- xi) After typing "YES" then pressing ENTER on the computer, note the level of the liquid in the evaporator recirculation

line, and record the refrigerant flowrates at the beginning of 2nd, 5th, & 8th minutes. Also, check the source and the sink flowrates during the test. Check the recirculation rate at the end of the test.

- xii) At the end of the test the highlights of the results are displayed on the console. Shut off the source fluid and allow the system to cool.
- xiii) Type the refrigerant flowrates into the computer then have the results printed on paper and/or cassette.
- xiv) After approximately fifteen minutes shut off the sink and allow the system to cool.
- xv) At five minute intervals keep checking the temperatures in the condenser and the evaporator header. When the evaporator header temperature is approximately 25C, again note the liquid level in the evaporator recirculation line. The test is now regarded as complete.

4.3 DETAILS OF TESTS:

The tests carried out in this study can be divided into three categories:

- a) To repeat some of the experimental test runs by Sampath(1) by choosing a typical set of conditions from the available data.
- b) To study the effect of unequal distribution of charge in each tube.

c) To study the effect of unequal heating of evaporator tubes.

4.3.1 TEST SEQUENCE I:

The tests described in this test sequence pertain to category (a).

Working Fluid	R-11
Evaporator inclination	0.0
Evaporator rotation	0.0
Condenser inclination	45.0
Condenser rotation	0.0
Evaporator diameter	1/4"
Condenser diameter	3/8"
Elevation	0.9 m
Source temperature	35.0 C
Sink temperature	25.0 C

The level of liquid in the evaporator recirculation tube under dynamic conditions was varied in this sequence from 10% to 78%.

4.3.2 TEST SEQUENCE II:

The tests in this sequence pertain to category (b). For these tests the evaporator static charge was varied from 20% to 90%. Two constant temperature baths were used as source and sink respectively.

Evaporator diameter 3/8"

Condenser diameter . 1/4"
 Condenser inclination 45.0
 Condenser rotation 0.0
 Elevation 0.9 m
 Mean temperature 30.0 C

With the above parameters held constant the evaporator geometry was varied as follows:

```
#####
Evaporator > Inclination Rotation
orientation > (Rot. L =0) (Incl. L =0)
                Degrees Degrees
-----
Tsource-Tsink 0.0 15 30 45 15 30 45
-----
40 C---20 C x x x x x x
35 C---25 C x x x x x
-----
```

4.3.3 TEST SEQUENCE III:

The tests described in this sequence pertain to category(c). The evaporator static charge was varied from 25% to 90% in these tests.

Working fluid R-11
 Evaporator diameter 3/8"
 Condenser diameter 1/4"
 Condenser rotation 0.0
 Condenser inclination 45.0
 Evaporator inclination 0.0

Evaporator rotation 0.0
 Elevation 0.9 m
 Sink temperature 20.0 C

With the above parameters held constant the source temperatures were varied as follows:

```
#####
```

Temp in tube#1(C)	Temp in tube#2(C)	Temp in tube#3(C)
42.0	40.0	38.0
43.0	40.0	37.0
44.0	40.0	36.0
42.0	40.0	40.0
42.0	42.0	40.0

```
#####
```

4.4 DATA ANALYSIS:

An examination of the evaporator tube wall temperatures and their standard deviations indicated the presence of two phase heat transfer, dryout and boiling suppression. A high standard deviation in a temperature reading was indicative of a transition in flow taking place at that particular location.

Generally at low evaporator charges considerable superheating in the evaporator was observed and hence the temperature recorded in the

evaporator header was no longer the saturation temperature. Use of this temperature in evaluating the average evaporator heat transfer coefficient resulted in an unrealistically high value. As the mass flow rates encountered in this study were small, the heat required to superheat the saturated vapour by as much as 3C was nearly 1% of the heat transfer taking place in that evaporator tube, and its magnitude was between 0-3 Watts. Since this superheat is readily lost in the interconnecting vapour header, the temperature recorded in the condenser header was the saturation temperature. Thus, the temperature in the evaporator header was estimated indirectly by using the condenser vapour header temperature and the pressure drop between the two headers.

4.5 EXPERIMENTAL UNCERTAINTY:

The uncertainties in the estimation of the heat transfer rate and the average evaporator heat transfer coefficient were of the order of $\pm 9.2\%$ and $\pm 9.4\%$ of their values respectively for a source-sink temperature difference of 20C and $\pm 16.7\%$ and $\pm 16.9\%$ for a source-sink temperature difference of 10C. Details of uncertainty analysis are shown in Appendix D.

The standard deviation in the loop conductance for $\Delta T=20C$ & 10C was always below 5% and 10% respectively of the value of the loop conductance. Also, the standard deviation in the heat input for $\Delta T=20C$ & 10C rarely exceeded 5% and 10% respectively of the value of the heat input.

CHAPTER V

RESULTS AND DISCUSSION

5.1 COMPARISON WITH EARLIER WORK:

Test sequence I was carried out to compare the loop conductance of the repaired loop with the previous results reported by Sampath(1). In these preliminary tests it was more convenient to measure the liquid level in the evaporator recirculation tube rather than the static charge.

Fig. 14 shows the results of these tests together with those of Sampath(1). The present set of results are plotted against the percentage of evaporator recirculation tube flooded with liquid, whereas Sampath's results are plotted against the static charge. The level of the liquid in the evaporator recirculation tube under operating conditions, which represents the head required to sustain a particular mass flow rate, is always less than the static charge. This comparison clearly shows that the present performance is roughly 50% of that reported by Sampath.

A careful analysis of the present set of results indicated that the new tube in the evaporator was performing very poorly. Its tube wall temperatures were approximately 1C higher than those of the other tubes. In addition, the heat transfer rates in this tube were found to be 15% to 66% of the heat transfer rates in each of the other two tubes, which were in close agreement with each other. Considerable time and effort was spent trying to unravel this mystery. At room temperature all of the evaporator tube wall temperatures agree very well with each other. It

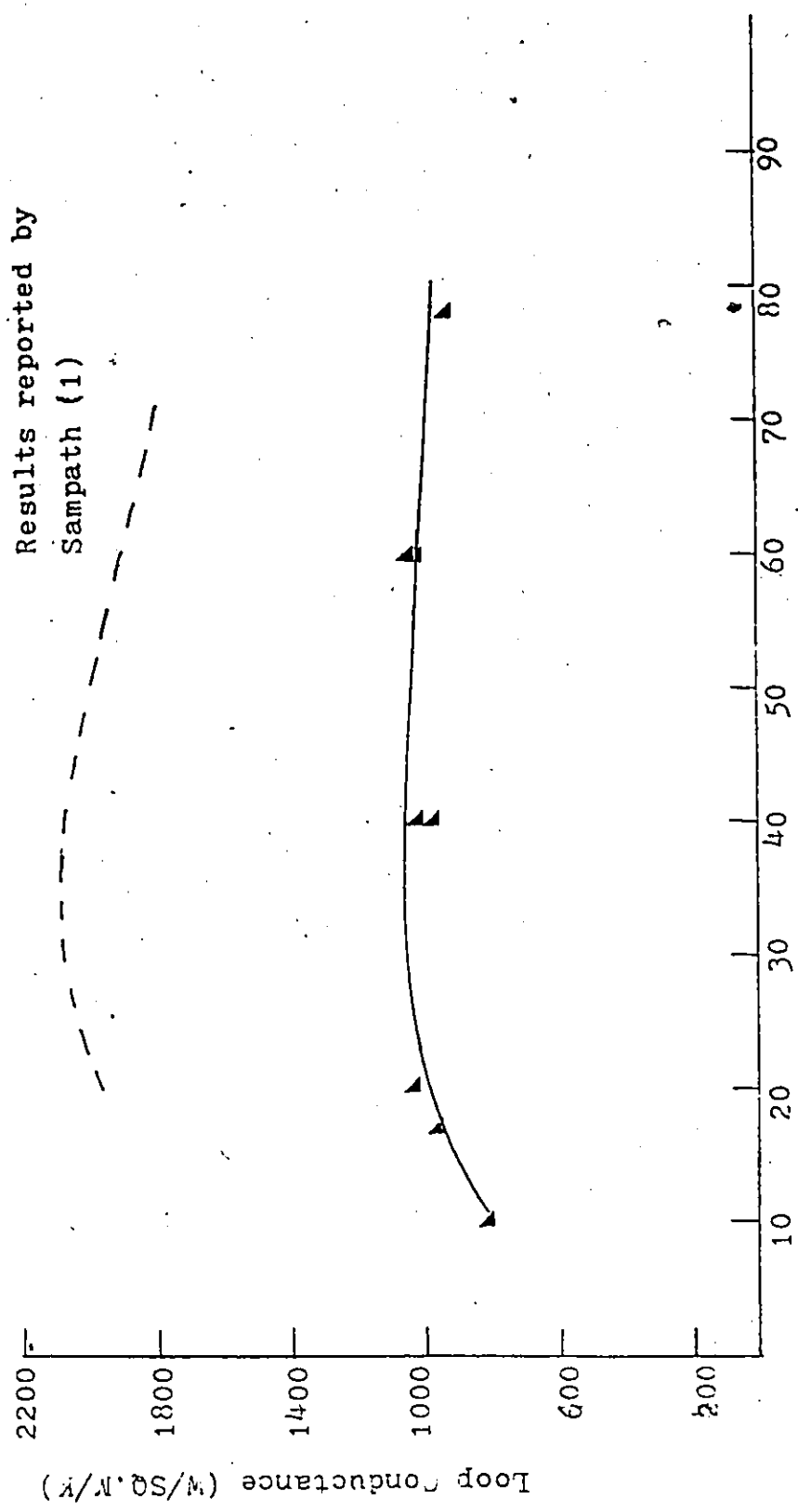


FIG. 14: Comparison of present performance data with that reported by Sampath (1). T(source)=35C, T(sink)=25C. Vertical evaporator. $D_e = 1/4"$, $D_c = 3/8"$.

was thus concluded that the temperature monitoring equipment was functioning properly. To check for the possibility of liquid backflow from the vapour header the evaporator tube bank was rotated and inclined slightly. No change in its behaviour was observed. Since at the time these tests were carried out these evaporator tubes were all being heated by a single source from a common header it was thought that perhaps a different flowrate of water was flowing in the annulus of the new tube. To check this the supply source header was reversed but no change was observed in the tube performance. No explanation for this behaviour was found so it was concluded that the surface finish on the new tube must have been substantially different from that of the older tubes thus causing radically different boiling characteristics. Because of this difference in performance between the old tubes and the new tube it was subsequently decided to carry out this investigation using the 3/8" diameter tube heat exchanger as the evaporator and the 1/4" diameter unit as the condenser.

The discrepancy between the present set of results and those reported by Sampath raises serious questions. Even if the new evaporator tube performed as well as the other two there would still be a significant difference between the present set of results and those reported by Sampath. The non-availability of outputs of Sampath's data makes it impossible to make a thorough comparison between the two sets of experimental data. In the following paragraphs it will be pointed out why I believe that Sampath's results are not reliable.

In the draft of his M.A.Sc Thesis entitled "Multiple tube two phase thermosyphon heat exchangers" (8), an examination of his

experimental data reveals very little scatter and exceptionally good agreement with the predictions of the computer simulation program. Although the computer simulation program was validated against Hwang's and Dicciccio's test loops Sampath's experimental data shows a much better correlation with the program. The absence of scatter in the data of an experimental study involving boiling and condensation is most unusual due to the stochastic nature of boiling, no matter how accurately experiments have been carried out.

Serious errors in Sampath's thesis draft have come to the author's notice. The information provided about the flowmeters is wrong. He reports that the floats in the three flowmeters which measure the mass flowrate to the evaporator are made of red sapphire. A visual observation proves his statement to be incorrect. A determination of the density of the floats revealed them to be made of black glass. His calibration was found to be grossly in error. The present calibration data was double checked by comparing the theoretical and experimental mass flowrates through the condensate flowmeter and they were found to be in good agreement.

Sampath has neither submitted nor defended his thesis.

All of these factors raise serious doubts about the validity of his experimental results.

5.2 THE BASE SYSTEM:

The performance of the evaporator with all three tubes charged

equally and subject to the same source fluid temperature, is shown in Figs. 15 & 16 for the loop operating at a mean temperature of 30C, with source and sink fluid temperature differences of 20C and 10C respectively. The plotted curves are the best least squares curve fit through the data to a second order polynomial (see appendix G for equations) . These curves provide a datum against which the results for the unequal heating and unequal charge distribution are compared. The data indicates an increase in the heat transfer rate with increasing static charge then a gradual decrease. This type of phenomenon occurs since at low charges considerable dryout occurs in the evaporator. At low static charges as many as the top three thermocouple readings in each tube showed the presence of dryout (high tube wall temperatures) indicating that approximately 60% of the tube area is subject to dryout. An increase in the charge results in a decrease in the area over which dryout occurs and an increase in the area for two phase flow, with its significantly larger heat transfer coefficients. At high evaporator static charges dryout is completely eliminated, however, boiling suppression (indicated by a high tube wall temperature) was observed in the bottom of the evaporator.

Figs. 17 & 18 are plots of the average evaporator heat transfer coefficient versus evaporator static charge for source to sink temperature differences of 20C and 10C respectively. The smaller heat transfer coefficients at lower static charges are due to dryout taking place over a large area. The solid curve in each figure represents the best least squares curve fit for a second order polynomial. In fig 17, with the exception of a single data point, all the data falls within an envelope of $\pm 10\%$ of the values for the plotted curve. Similarly, in

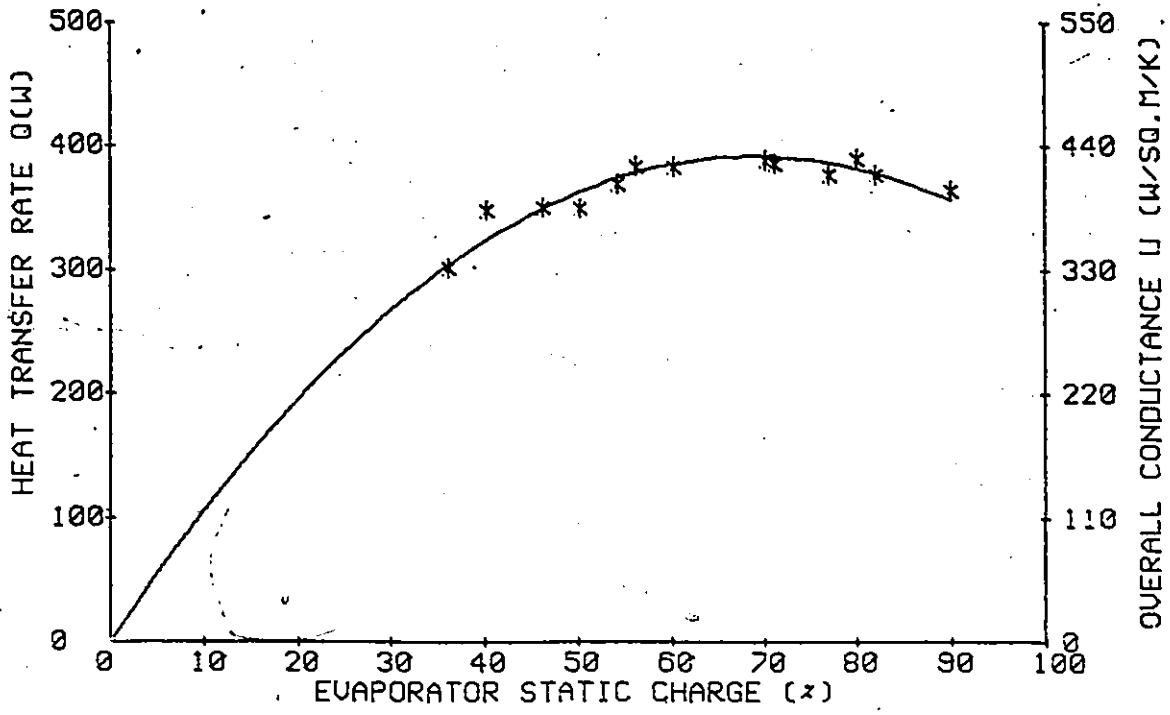


FIG. 15: Heat transfer rate and overall conductance vs static charge for $T(\text{source})= 40\text{C}$ and $T(\text{sink})= 20\text{C}$

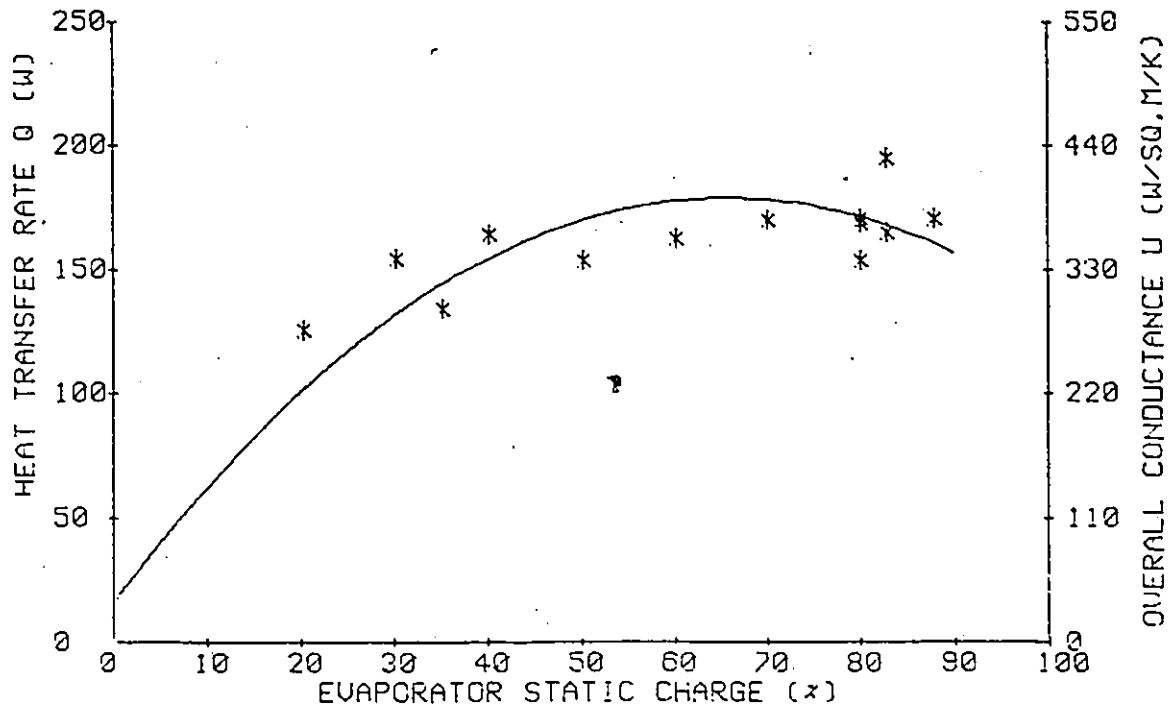


FIG. 16: Heat transfer rate and overall conductance vs static charge for $T(\text{source})= 35\text{C}$ and $T(\text{sink})= 25\text{C}$

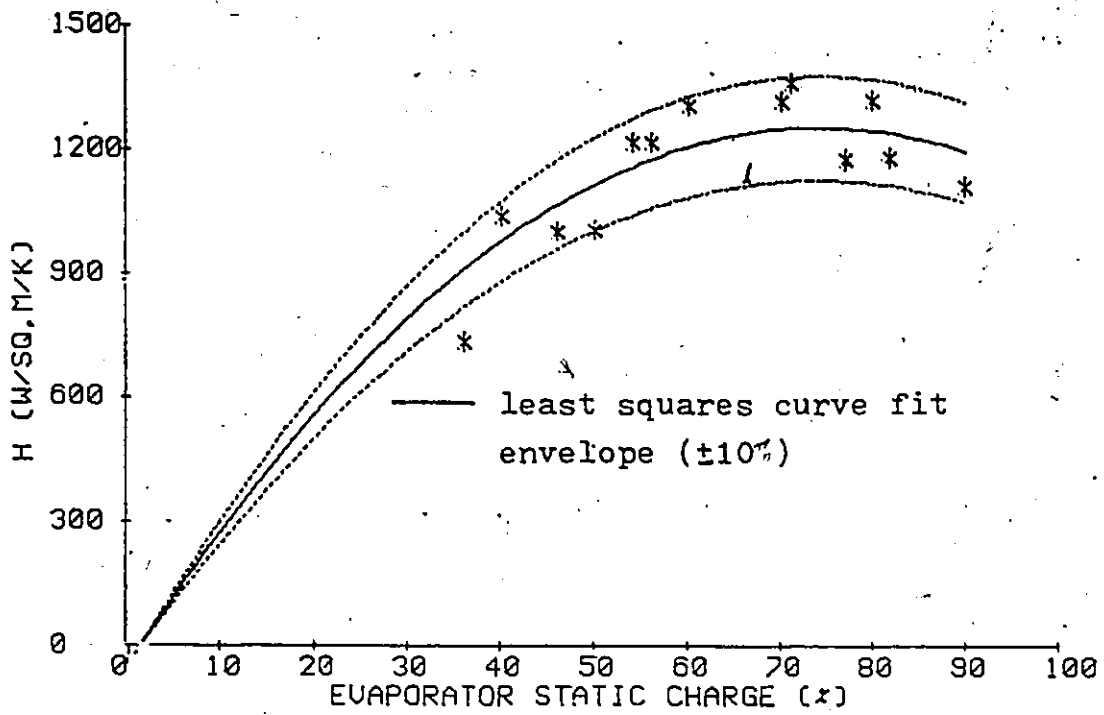


FIG. 17: Average evaporator heat transfer coefficient vs static charge for $T(\text{source}) = 40\text{C}$ and $T(\text{sink}) = 20\text{C}$

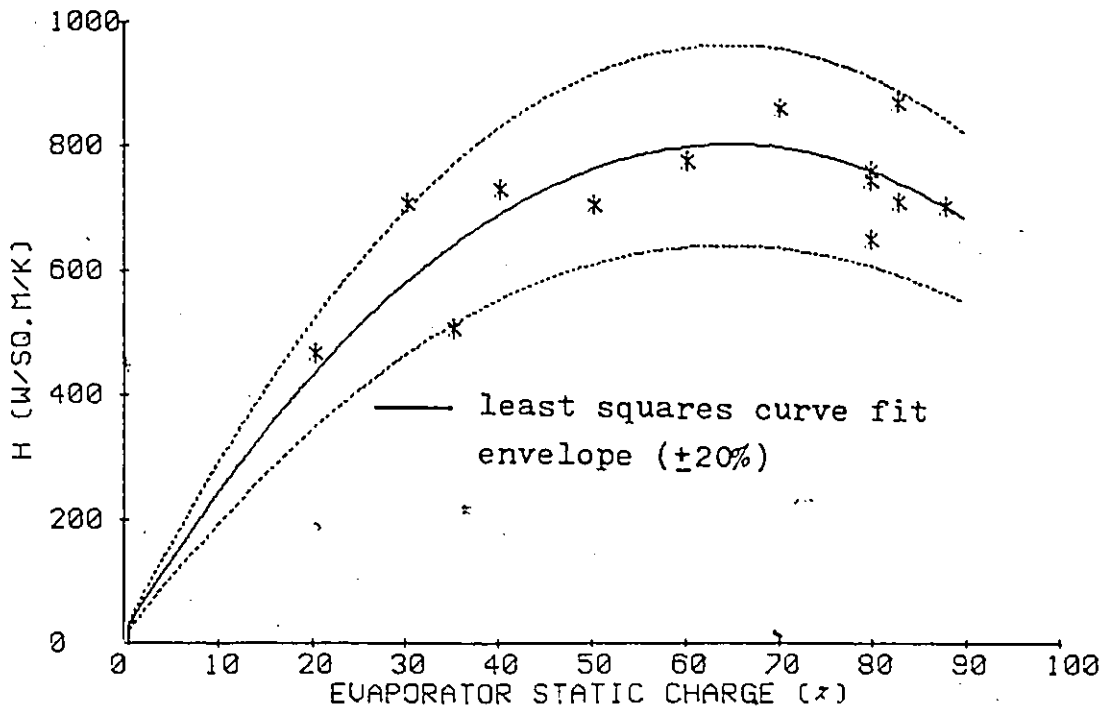


FIG. 18: Average evaporator heat transfer coefficient vs static charge for $T(\text{source}) = 35\text{C}$ and $T(\text{sink}) = 25\text{C}$

fig. 18 all but two of the data points lie within $\pm 20\%$ of the values for the plotted curve. The greater scatter in the data for a source-sink temperature difference of 10°C compared to that for a difference of 20°C is due a greater relative error in the estimation of the heat transfer rate and the average evaporator heat transfer coefficient.

The improved heat transfer performance with an increase in the temperature difference from 10°C to 20°C between the source and the sink fluids is due to an increased vigour of boiling resulting in higher flow rates in the evaporator tubes for the latter case.

Flow oscillations in the range of $\pm 5\%$ - 15% have been observed when operating with a temperature difference of 10°C between the source and the sink, whereas their range is between $\pm 2\%$ - 8% when operating with a temperature difference of 20°C . These flow oscillations suggest the presence of instabilities.

It was considered important to investigate the effect of subcooling on the performance of the evaporator. In these tests the liquid level in the evaporator recirculation tube was measured instead of the static charge. Table I gives the performance data for a source-sink temperature difference of 10°C .

An examination of the heat transfer rates and loop conductance in Table 1 indicates the performance to be independent of the degree of subcooling. This occurs due to the small flow rates in the evaporator tubes and the specific heat capacity of R11. The sensible heat required to bring the refrigerant to its saturation temperature is of the order of 5% of the heat transfer rate in the evaporator and therefore

TABLE 1. Performance data with different degrees of subcooling.
 T(source) = 35C, T(sink) = 25C. Vertical evaporator.

Serial #	%CHG	ΔT_{sub}	Q (W)	U _{ee} (W/SQ.M/K)
1	81	4.0	155.5	497.4
2	81	-0.4	157.3	503.9
3	80	4.6	164.6	534.2
4	50	5.3	181.5	601.3
5	50	1.9	187.8	640.6
6	40	4.1	187.7	656.3
7	39	0.4	184.1	634.0
8	38	3.4	189.6	659.5
9	30	0.8	175.2	600.8
10	30	3.7	180.4	618.7

subcooling does not have a significant affect on evaporator performance.

5.2.1 COMPARISON WITH THEORETICAL PREDICTIONS:

It is most appropriate at this stage to make a comparison between a typical set of experimental results and the predictions of the available theoretical correlations. This has been accomplished by using Ali's computer simulation program with corrections and modifications by Mathur (9).

In the earlier studies, the correlation used by Ali to model the heat transfer phenomenon in the two phase region was one proposed by Sachs and Long(11). Choice of this particular correlation was made since it provided very good agreement between simulated and experimental results of Hwang. Of those available, this particular correlation predicts the highest heat transfer coefficients for two phase flow. Use of this correlation overpredicted the current set of experimental results. It was replaced by one proposed by Davis and David(12). Use of this correlation, which yields the second highest heat transfer coefficients, resulted in a satisfactory agreement between the current experimental and simulated results.

The overall heat transfer rates and the average evaporator heat transfer coefficients obtained from the simulation program, as reported by Mathur(9), for a typical set of conditions are shown in Figs. 19 & 20 respectively alongwith experimental results. The figures indicate a good agreement between the experimental and the simulated results . It

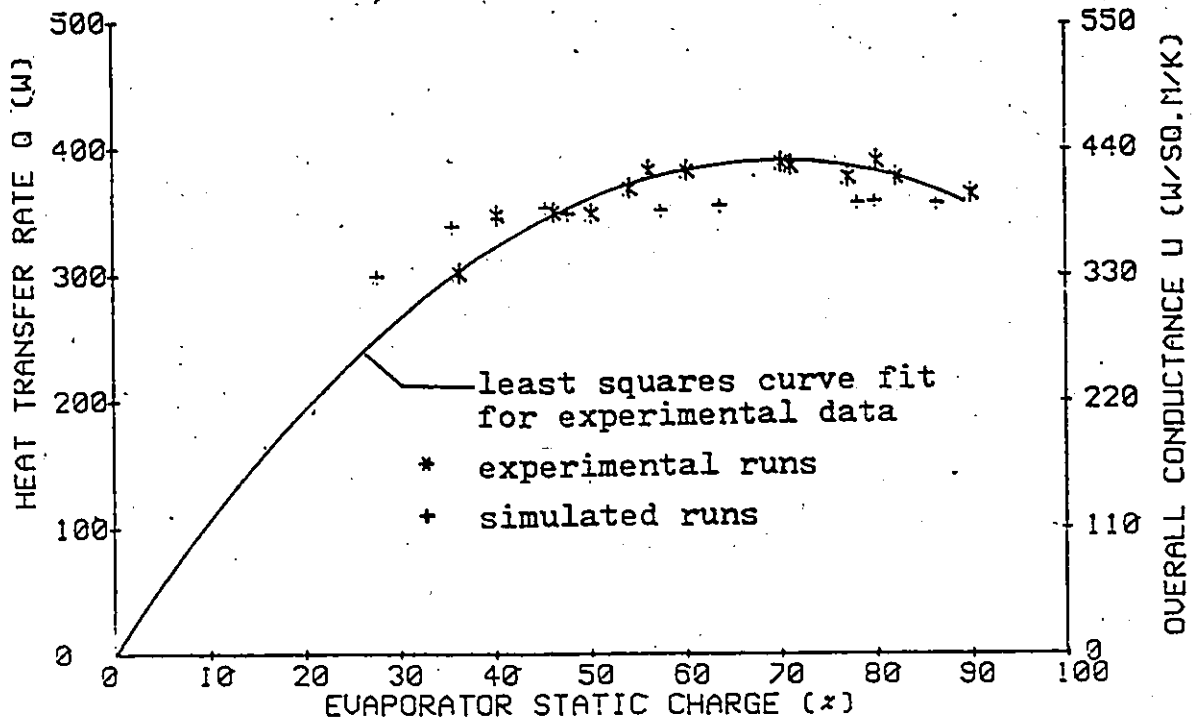


FIG. 19: Comparison of experimental and simulated results for $T(\text{source}) = 40\text{C}$ and $T(\text{sink}) = 20\text{C}$

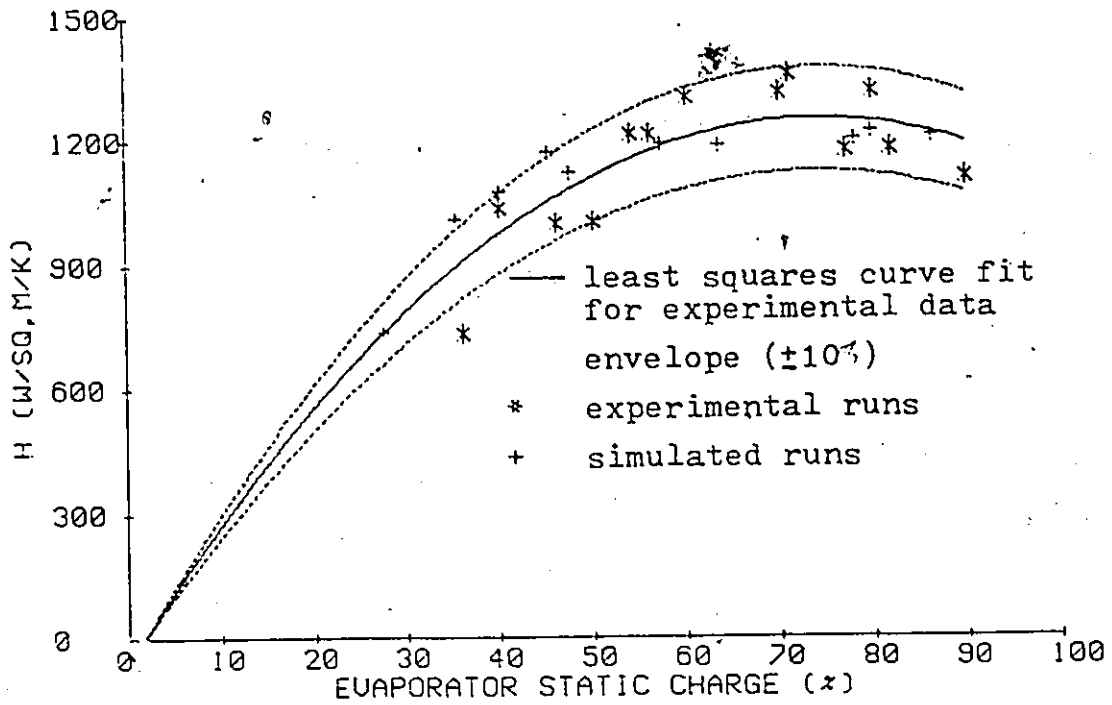


FIG. 20: Comparison of the average evaporator heat transfer coefficient between experimental and simulated results for $T(\text{source}) = 40\text{C}$ and $T(\text{sink}) = 20\text{C}$

is not appropriate here to give the mechanics of the computer simulation program. For an indepth study the reader is referred to reference (3). However, some of the correlations used in the computer program are given in appendix E.

5.3 EFFECT OF CHARGE DISTRIBUTION:

In order to determine the effect of charge distribution brought about by a rotation of the evaporator tubes in the vertical plane about a horizontal axis, it was first necessary to study the effect of inclining the tubes with the same charge in each tube. Figs. 21 & 22 show the heat transfer rates and the overall conductance values as a function of charge for three angles of inclination for the 40C/20C and 35C/25C tests respectively. Figs. 23 & 24 are plots of the average evaporator heat transfer coefficient as a function of static charge for the aforementioned conditions respectively. The results indicate that for inclination angles greater than or equal to 30 deg. the performance is lower at smaller charges and higher at larger charges. This difference occurs as a result of two factors; a shift in the dynamic operating condition and dryout in the tubes. A shift in the dynamic operating condition is due to the fact that the actual charge in the evaporator under operating conditions for an inclined/rotated evaporator is smaller than that for a vertical evaporator under identical operating conditions. The reason being the increased flooding of the recirculation tube for an inclined/rotated evaporator in order to sustain a particular mass flow rate than for a vertical evaporator. An examination of the tube wall temperatures for inclined tubes

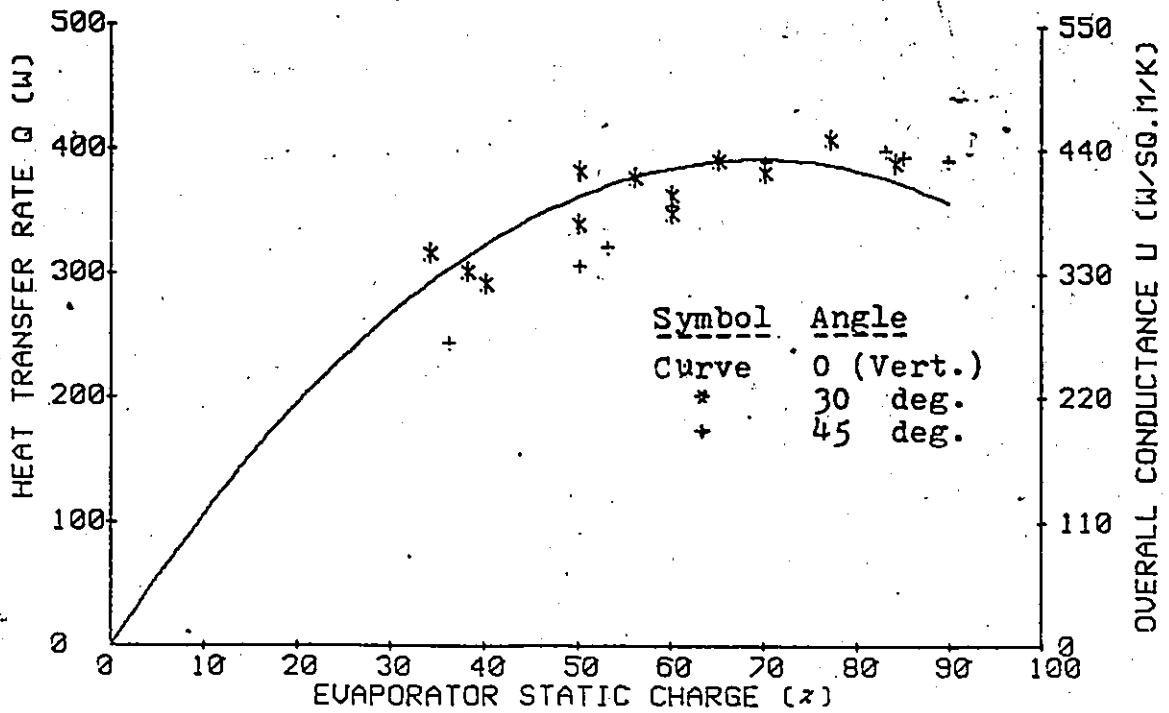


FIG. 21: Heat transfer rate and overall conductance vs static charge for $T(\text{source})=40\text{C}$ and $T(\text{sink})=20\text{C}$ with the evaporator tube bank inclined 0, 30 and 45 deg.

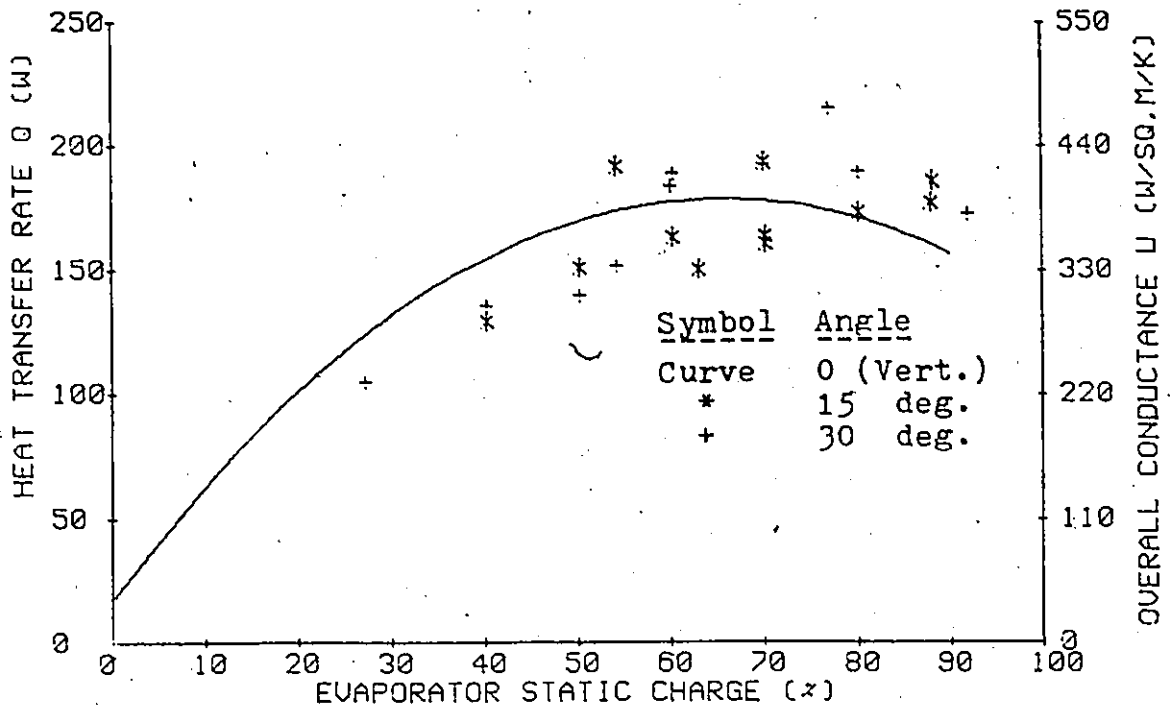


FIG. 22: Heat transfer rate and overall conductance vs static charge for $T(\text{source})=35\text{C}$ and $T(\text{sink})=25\text{C}$ with the evaporator tube bank inclined 0, 15 and 30 deg.

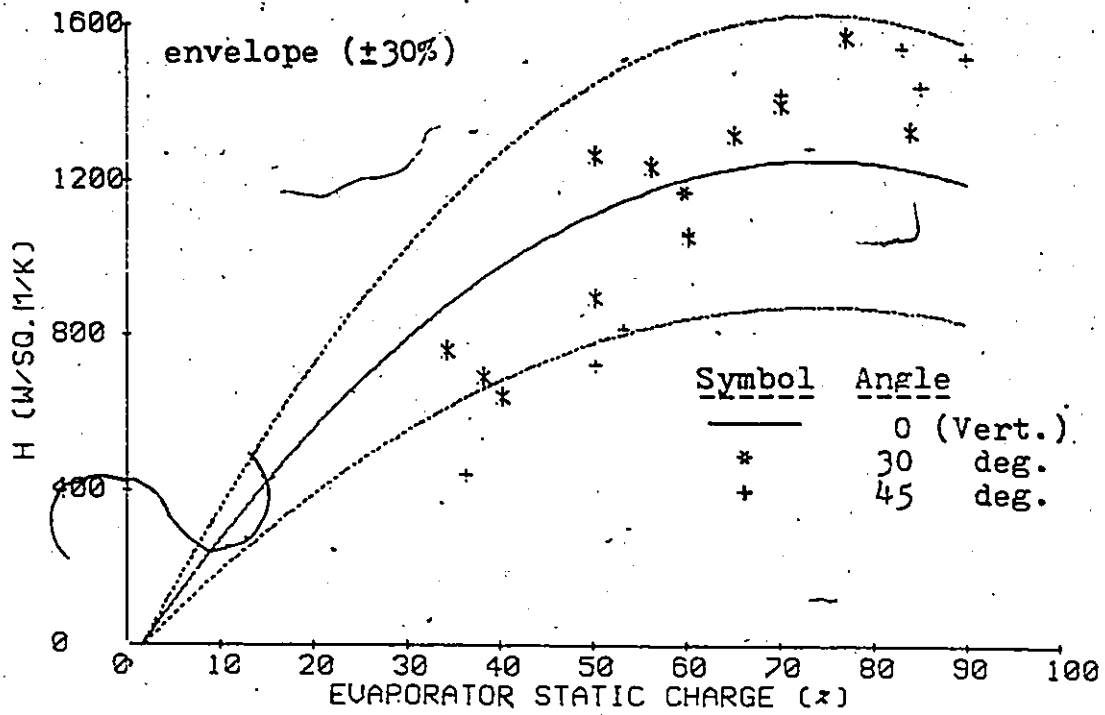


FIG. 23: Average evaporator heat transfer coefficient vs static charge for $T(\text{source}) = 40\text{C}$ and $T(\text{sink}) = 20\text{C}$ with the evaporator tube bank inclined 0, 30 and 45 deg.

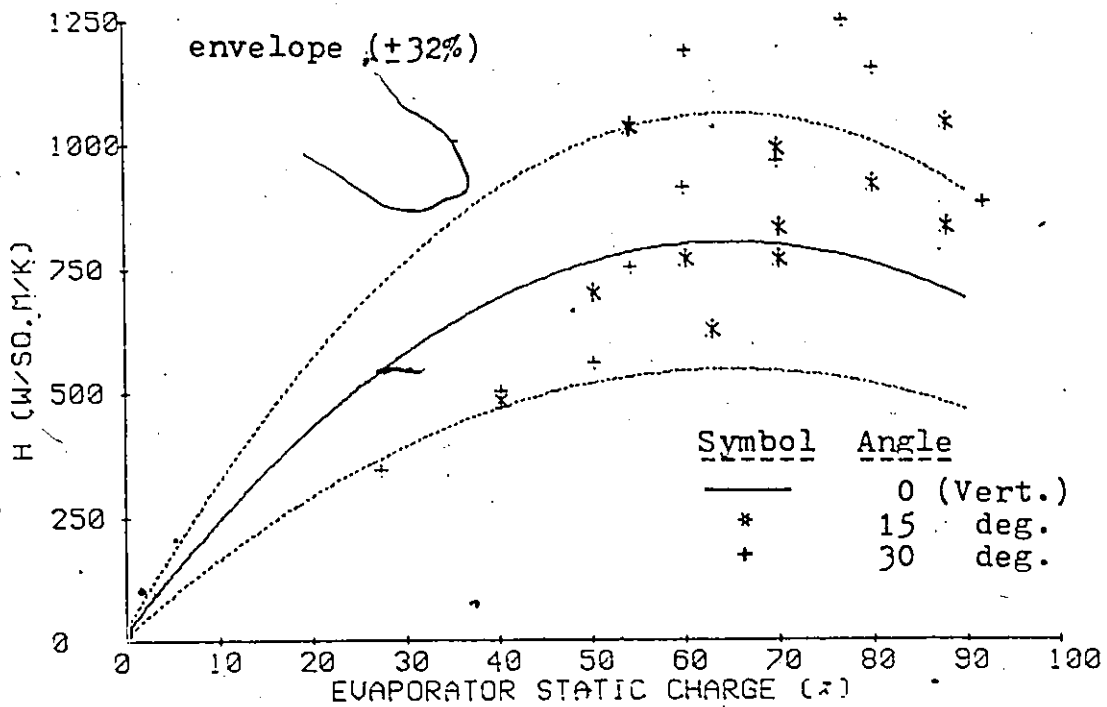


FIG. 24: Average evaporator heat transfer coefficient vs static charge for $T(\text{source}) = 35\text{C}$ and $T(\text{sink}) = 25\text{C}$ with the evaporator tube bank inclined 0, 15 and 30 deg.

indicated greater susceptibility to dryout than for vertical tubes under identical operating conditions. This is probably due to the location of the thermocouple junctions. They are located on the uppermost part of the tube when inclined and hence would be most subject to the formation of a thin vapour blanket in their immediate vicinity. This vapour film increases the resistance to heat flow and consequently there is an increase in the tube wall temperatures, and consequently low average evaporator heat transfer coefficients at low static charges.

As shown in Fig. 23, for an inclination angle of 30 deg. for a static charge of 50% the substantial difference in the heat transfer coefficient values is due to a difference of 1C in the saturation temperature.

In Fig. 24 the significant difference in the two values of the average evaporator heat transfer coefficient for 60% static charge for an inclination angle of 30 degrees is solely due to the difference in the extent of boiling suppression and dryout in the two cases. The cumulative heat transfer rates for the two cases agreed very well. The substantial difference in the heat transfer coefficient values for a static charge of 70% for an inclination angle of 15 deg. is due to a difference of 30W in the evaporator heat transfer rate. For a static charge of 88% for an inclination angle of 15 deg. the heat transfer coefficient values differ because of differences of approximately 9W in the heat transfer rates and 0.7C in the average evaporator wall temperatures.

Figs. 25 & 26 show the heat flow rates and the overall conductance values as a function of average static charge for three

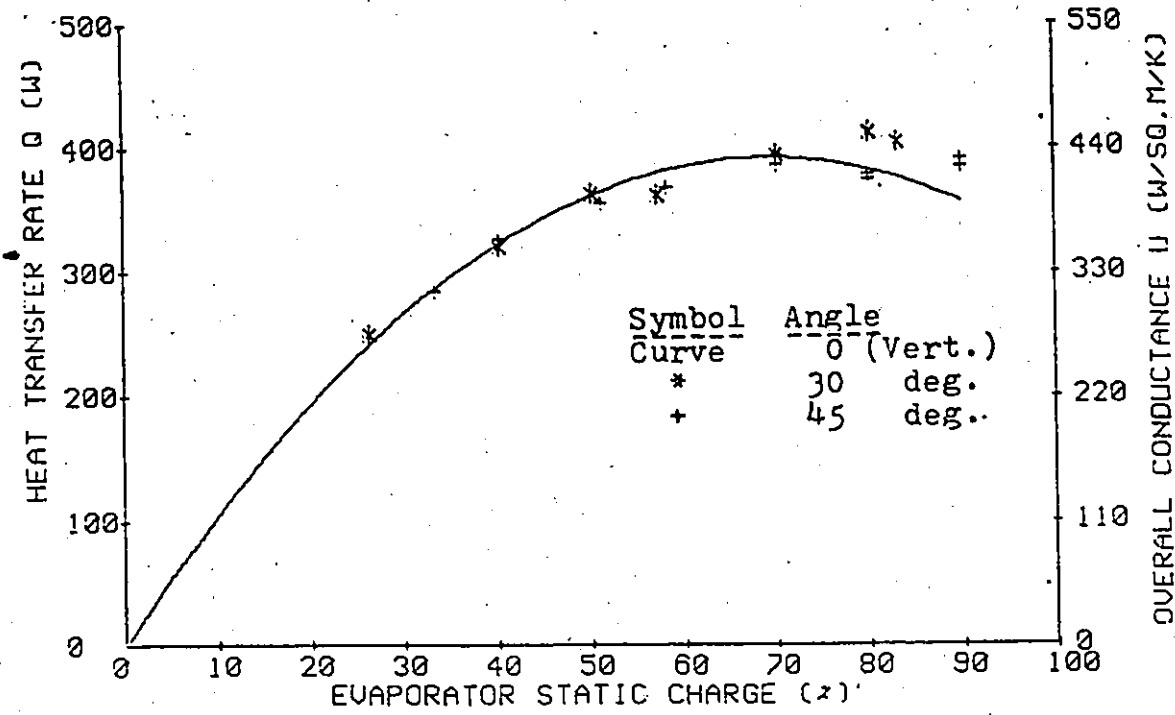


FIG. 25: Heat transfer rate and overall conductance vs static charge for T(source)= 40C and T(sink)= 20C with the evaporator tube bank rotated 0, 30 and 45 deg.

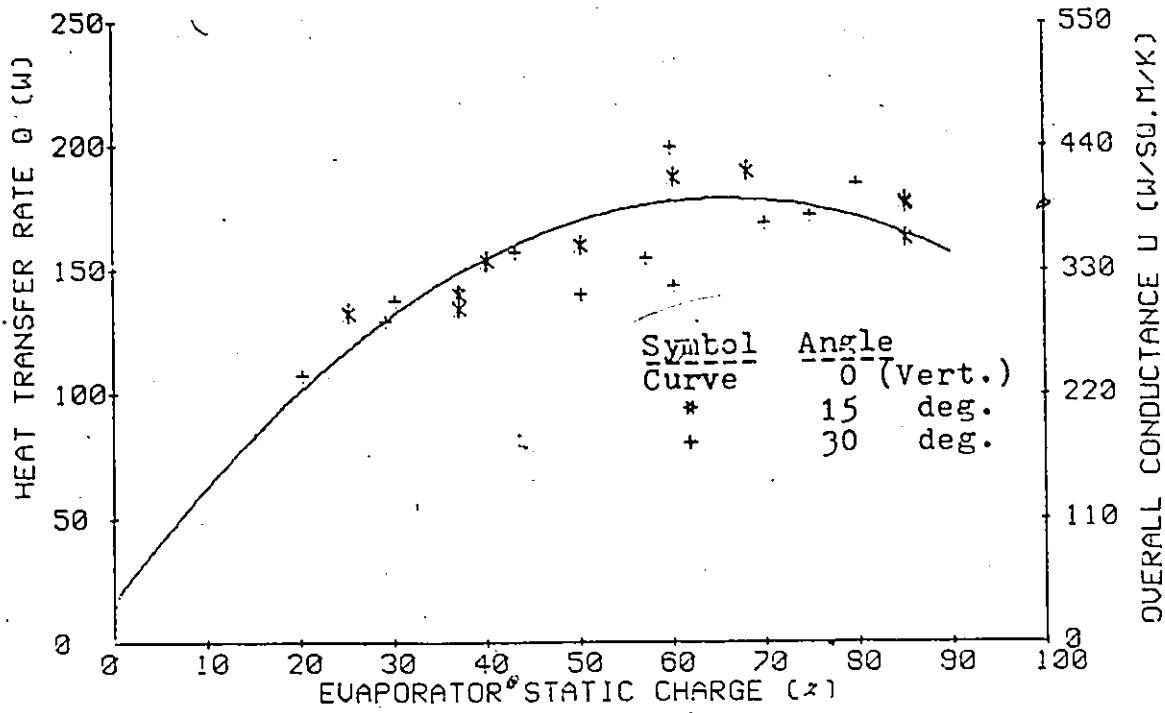


FIG. 26: Heat transfer rate and overall conductance vs static charge for T(source)= 35C and T(sink)= 25C with the evaporator tube bank rotated 0, 15 and 30 deg.

different rotation angles for the 40C/20C and 35C/25C tests respectively. It is apparent from a comparison of Figs. 21 & 25 and of Figs. 22 & 26 that charge variations of 3%, and 13% between adjacent tubes, which occur at rotation angles of 15 and 45 deg. respectively have a negligible affect on the performance of the system for mean static charges between 20 and 90%.

Figs. 27 & 28 are plots of the average evaporator heat transfer coefficient vs. evaporator static charge for the 40C/20C and 35C/25C tests respectively.

The heat transfer rates for rotated and vertical evaporators agree well for a 40C/20C tests, as shown in Fig. 25. However, an examination of Fig. 27 indicates greater scatter in the data. The enhanced scatter in the data is probably due to the indirect estimation of the saturation temperature using the condenser vapour header temperature and the pressure drop between the two headers, this was necessary due to considerable superheating in the evaporator at low charges.

As shown in Fig. 27 a difference of 12.3% in the heat transfer coefficient values at a static charge of 70%, for a rotation angle of 45 deg, results because of boiling suppression at the bottommost thermocouple in the lowest elevation tube and the presence of dryout at the topmost thermocouple in the highest elevation tube for one of the runs. However, the heat transfer rates for these two cases agreed very well with each other.

In Fig. 28 small heat transfer coefficient values for a

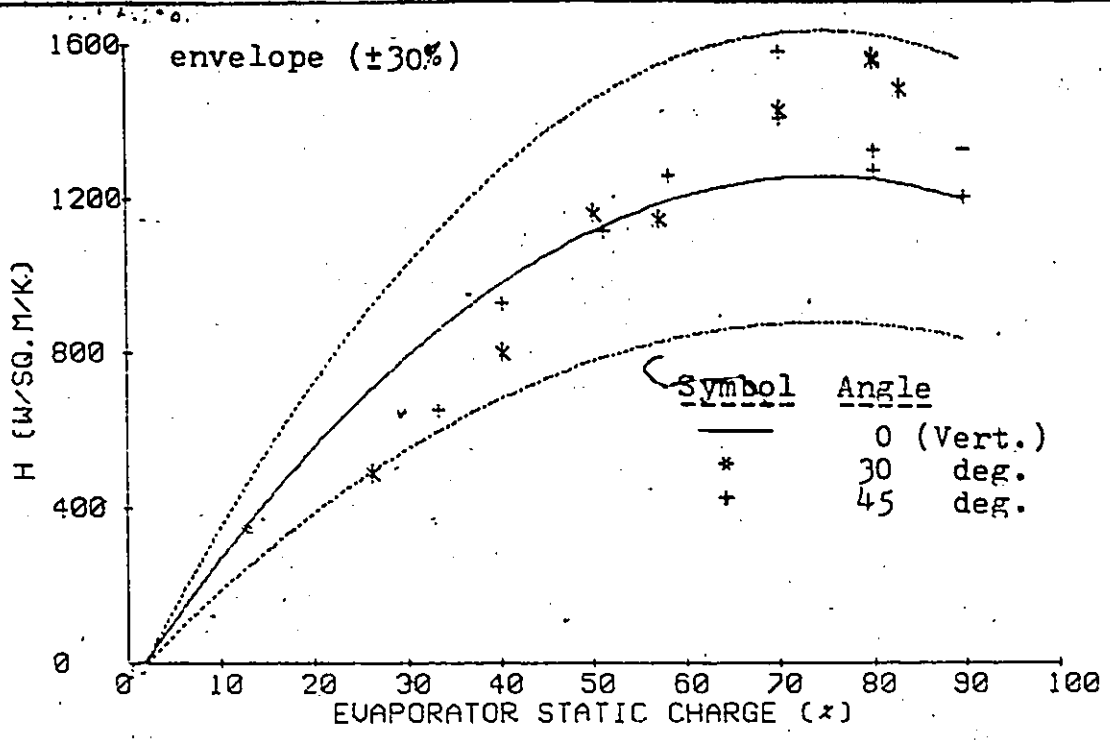


FIG. 27: Average evaporator heat transfer coefficient vs static charge for $T(\text{source})=40\text{C}$, $T(\text{sink})=20\text{C}$ with the evaporator tube bank rotated 0, 30 and 45 deg.

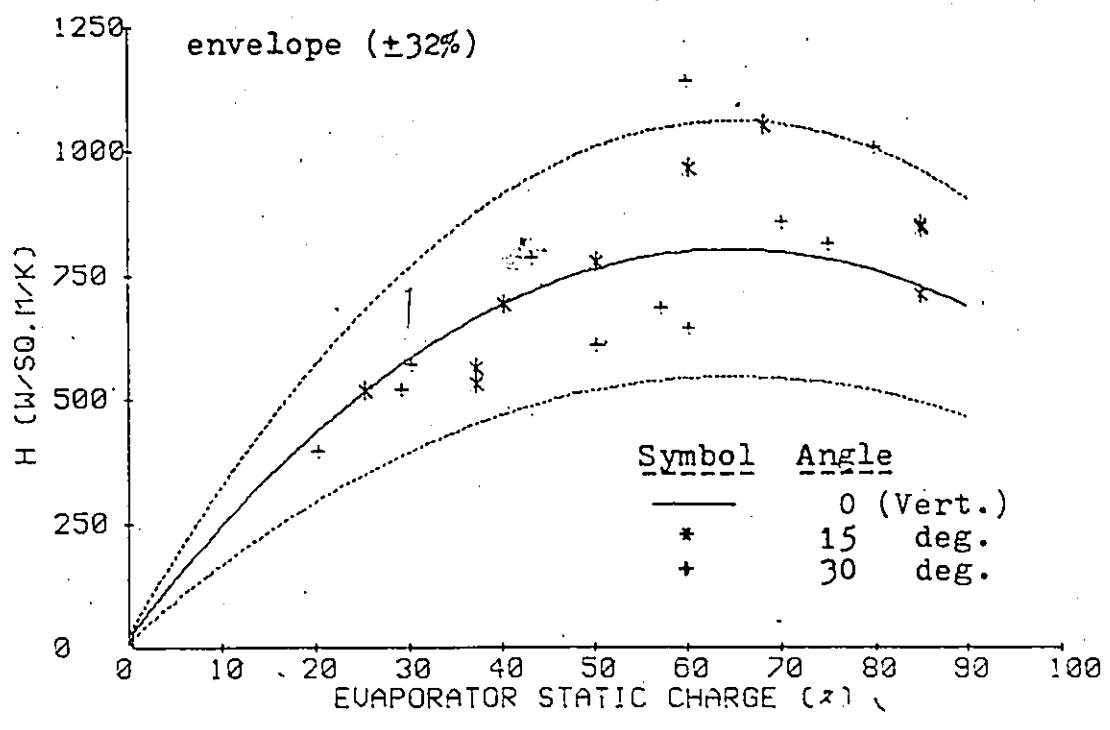


Fig. 28: Average evaporator heat transfer coefficient vs static charge for $T(\text{source})=35\text{C}$, $T(\text{sink})=25\text{C}$ with the evaporator tube bank rotated 0, 15 and 30 deg.

rotation angle of 30 degrees between 50% to 60% static charge are due to dryout in the top region of the evaporator. There is significant variation in the heat transfer coefficient values for a static charge of 60%. The saturation temperatures for the two runs differ by 1.3C, although the average evaporator tube wall temperatures are almost identical in the two runs. The higher heat transfer coefficient value for a rotation angle of 30 degrees for a static charge of 80% is due to improved heat transfer in the highest elevation tube.

In Fig. 28 the significant difference in the heat transfer coefficient values at 60% static charge for a rotation angle of 15 deg and the vertical case is due to an increase of nearly 0.5C in the saturation temperature for the rotated evaporator, although the average evaporator tube wall temperatures are identical. For the 85% static charge the lower heat transfer value results because of negligible heat transfer in the lowest elevation tube, its wall temperatures at different locations indicate pool boiling rather than flow boiling.

5.4 EFFECT OF UNEQUAL HEATING:

As mentioned previously, one of the objectives of this experimental work was to study the effect of unequal heating of evaporator tubes interconnecting common vapour and liquid headers. Such a situation would arise when the source fluid passes through adjacent banks of evaporator tubes subjecting them to a decreased energy input due to a decreased source fluid temperatures. Several tests were run with different source fluid temperature differences between adjacent

tubes with the average source fluid temperature maintained at 40C. Temperature differences of 2C, 3C and 4C, which are typical of temperature drops which might occur between adjacent tubes for air flowing past evaporator tube banks, were investigated.

Due to the nonavailability of flowmeters in the initial stages of experimentation the source water flow rates could not always be set at the same value. It was found that an increase in the source water flow rate results in higher heat transfer rates in the evaporator for a given set of conditions. The performance of the evaporator was found to increase by 6% when the average source water flow rate was increased from 33.6 gm/s to 77.7 gm/s. In this test the average source fluid temperature was 40C, with a temperature difference of 2C between adjacent evaporator tubes, and the sink temperature was 20C.

Tables 2 (a & b), 3 and 4 give the performance data for the unequal heating tests with temperature differences between adjacent tubes of 2, 3, and 4C respectively. In each of these tables the numbers in parentheses indicate the source fluid temperature. The heat transfer rate in each tube is identified by $Q(T)$; the ratio of the tube heat transfer rate to the average heat transfer for all three tubes by $R(T)$; the average heat transfer rate per tube by Q_A ; and the ratio of the average heat transfer rate to the corresponding value with equal heating at the average source fluid temperature (40C) by Q_A/Q_{AE} . The heat transfer rate with equal heating which appears in the rightmost column of each Table was scaled to have the same source fluid mass flow rate as the average mass flow rates for the unequally heated tubes in order to have a realistic comparison.

TABLE 2a. Performance data for adjacent tube temperature difference of 2C for T(source)avg=40C and T(sink)=20C. Q (Watts). m(wtr) gm/s. R(T)=Q(T)/QA.

#####									
m(wtr)=89.4 m(wtr)=78.1 m(wtr)=65.7									
RUN#	%CHG	Q(42)	R(42)	Q(40)	R(40)	Q(38)	R(38)	QA	QA/QAE
1	90	225.0	1.71	156.9	1.19	13.8	0.10	131.9	1.04
2	80	187.5	1.38	147.1	1.08	73.4	0.54	136.0	0.99
3	67	224.5	1.55	124.2	0.86	85.3	0.59	144.7	1.04
4	67	229.2	1.63	138.9	0.98	55.0	0.39	141.0	1.01
5	56	224.5	1.60	147.1	1.05	50.5	0.35	140.7	1.08
6	53	194.6	1.45	124.2	0.93	82.6	0.62	133.8	1.01
7	50	179.6	1.36	127.5	0.97	88.1	0.67	131.7	1.02
8	31	165.1	1.46	121.4	1.07	53.5	0.47	113.3	1.16
AVERAGES			1.52		1.02		0.46		1.04

TABLE 2b. Performance data for adjacent tube temperature difference of 2C for T(source)avg=40C and T(sink)=20C. Q (Watts). m(wtr) gm/s. R(T)=Q(T)/QA

#####									
m(wtr)=33.7 m(wtr)=33.6 m(wtr)=33.4									
RUN#	%CHG	Q(42)	R(42)	Q(40)	R(40)	Q(38)	R(38)	QA	QA/QAE
9	86	169.3	1.30	135.1	1.04	85.3	0.66	129.9	1.04
10	75	191.7	1.41	140.7	1.04	73.9	0.55	135.4	1.03
11	65	163.7	1.25	147.7	1.13	81.1	0.62	130.8	0.99
12	48	159.0	1.25	136.5	1.07	85.8	0.68	127.1	1.06
13	30	127.0	1.24	113.9	1.11	67.1	0.65	102.7	1.14
AVERAGES			1.29		1.08		0.63		1.05

TABLE 3. Performance data for adjacent tube temperature difference of 3C for T(source) avg=40C and T(sink)=20C.
Q (Watts). m(wtr) gm/s. R(T)=Q(T)/QA

#####									
m(wtr)=76.8 m(wtr)=35.8 m(wtr)=26.0									
RUN#	%CHG	Q(43)	R(43)	Q(40)	R(40)	Q(37)	R(37)	QA	QA/QAE
14	90	257.2	1.88	104.9	0.76	49.0	0.36	137.0	1.12
15	81	268.0	2.00	114.9	0.86	18.1	0.14	133.7	1.02
16	80	289.4	2.30	66.6	0.53	21.8	0.17	125.9	0.95
17	80	233.1	1.73	99.3	0.74	70.8	0.53	134.4	1.02
18	70	187.0	1.38	143.9	1.06	76.2	0.56	135.7	1.01
19	60	193.4	1.48	151.3	1.16	46.8	0.36	130.5	0.98
20	50	253.3	1.87	128.8	0.95	23.3	0.17	135.1	1.09
21	45	216.7	1.51	136.0	0.95	77.3	0.54	143.3	1.21
22	45	186.5	1.52	118.4	0.97	62.1	0.51	122.3	1.03
23	25	151.1	1.50	94.4	0.93	57.7	0.57	101.1	1.26
AVERAGES			1.72		0.89		0.39		1.07

TABLE 4. Performance data for adjacent tube temperature difference of 4C for T(source) avg=40C and T(sink)=20C.
Q (Watts). m(wtr) gm/s. R(T)=Q(T)/QA

#####									
m(wtr)=33.7 m(wtr)=33.6 m(wtr)=33.4									
RUN#	%CHG	Q(44)	R(44)	Q(40)	R(40)	Q(36)	R(36)	QA	QA/QAE
24	87	261.0	1.90	138.9	1.01	* 12.0	0.09	137.3	1.11
25	80	258.7	1.91	138.3	1.02	* 9.6	0.07	135.5	1.05
26	68	261.0	1.95	140.7	1.05	0.0	0.00	133.9	1.01
27	57	211.6	1.68	147.7	1.18	* 17.6	0.14	125.6	0.98
28	52	183.4	1.41	165.3	1.28	40.2	0.31	129.6	1.04
29	30	171.7	1.65	140.7	1.35	0.0	0.00	104.1	1.16
AVERAGES			1.75		1.15		0.10		1.06

NOTE: m(wtr) for * runs was 22.9 gm/s.

Fig. 29 shows the heat transfer rate and the overall conductance values as a function of evaporator static charge for these three cases as well as the curve for the equal heating case. Fig. 30 is a plot of the average evaporator heat transfer coefficient versus evaporator static charge for these cases and the curve for the equal heating case. The broken curves on this figure define a $\pm 10\%$ band about the curve for the equal heating case within which all of the equal heating data lies, with the exception of one point. The curve for the equal heating case was obtained for water flow rate of 24.8 gm/s.

A number of observations can be made from the results shown in Tables 2-4 and Figs. 29 & 30:

1. In all three cases the heat flow rate, on average, is slightly better (4%-7%) than for the equal heating case.
2. The average evaporator heat transfer coefficient remains unaffected by unequal heating, nearly 80% of the data points lie within 10% of the curve for the equal heating case.
3. Unequal heating causes a dramatic shift in the heat flow rate between the three tubes, a shift far greater than would be expected on the basis of predictions using the results for equal heating with the same 20C temperature difference. The tube subject to the highest temperature source fluid transferred, on average, 23%-54% more heat than would be expected if all the tubes were subjected to the same elevated temperature with the same temperature difference. On the other hand, the tubes subjected to the lowest temperature difference operated at a level 27%-87% below that if all tubes were subjected to the same reduced temperature with the same temperature difference.

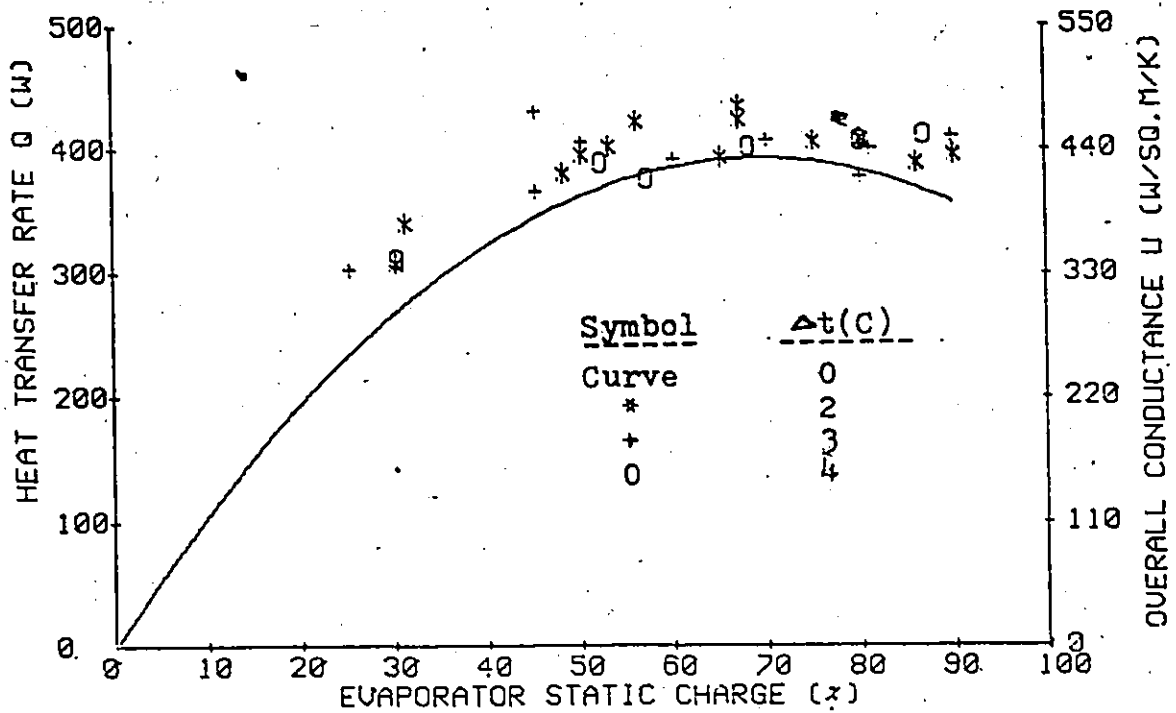


FIG. 29: Heat transfer rate and overall conductance for $T(\text{source})$ average = 40C, $T(\text{sink}) = 20\text{C}$ with source fluid temperature differences, Δt , of 0, 2, 3, and 4C

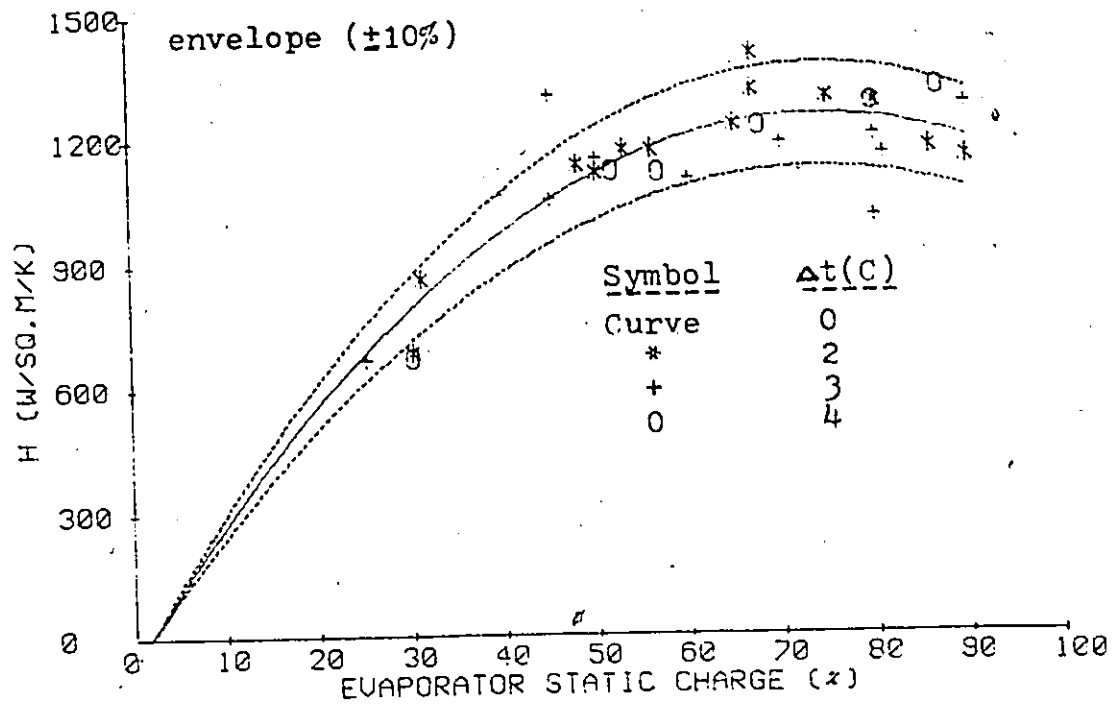


FIG. 30: Average evaporator heat transfer coefficient vs static charge for $T(\text{source})$ average = 40C, $T(\text{sink}) = 20\text{C}$ with source fluid temperature differences, Δt , of 0, 2, 3, and 4C

4. Based on all the data presented in Tables 2-4 the heat flow rate $Q(40)$ is, on average, 9% better than the average heat flow rate for equally heated tubes at the same temperature.

5. Substantially different heat flow rate distributions can and do occur for very similar charges for the same temperature distributions. These shifts can also result in substantial changes in the average heat flow rate. Note, for example, runs 3 & 4; 15, 16, & 17; and 21 & 22. The differences in these data give a measure of the variation which may be expected in the results for any given test.

6. For static charges between 40% and 90% the system performance appears to be essentially independent of the static charge. If any trend exists it has been masked by fluctuations in the data.

One can get some idea about the stochastic nature of boiling by studying the performance data for runs 21 & 22. Fig. 29 indicates a difference of approximately 63 Watts in the heat transfer rate for these two runs. This substantial difference in the heat transfer rate is due to different flow regimes encountered which resulted in a different proportion of dryout in each case. In run 22 dryout manifests itself at four thermocouple locations, whereas in run 21 dryout was observed only at the topmost thermocouple in the tube subjected to the highest source fluid temperature.

From above it can be surmised that more than one stable operating condition is possible for a given set of conditions. In many cases the system behaves such that the cumulative heat transfer remains approximately the same, although the distribution of heat transfer rates in adjacent tubes for two identical runs may be substantially different.

Figs. 31, 32 & 33 give the average heat transfer coefficients for individual tubes for various temperature difference conditions between adjacent tubes. Where appropriate, the data points are joined by a curve, otherwise, due to scatter in the data the upper and lower bounds of the region where the data falls are indicated. The width of the bands where the data lies is indicative of the region where the heat transfer coefficients for any particular condition may be expected to fall. At low evaporator charges the improved heat transfer coefficients in the 40 C tube, as shown in Figs. 31, 32 & 33 when compared to those of the tube subjected to a higher source fluid temperature are due to dryout in the higher temperature tube. The smaller heat transfer coefficients in the 43 C tube, as shown in Fig. 32 at 60% and 70% static charges are due to the presence of both dryout and boiling suppression, observed at the topmost and bottom thermocouples respectively.

These results prompted the author to investigate the behaviour of the system if two tubes are subjected to the same source fluid temperature and the third tube subjected to a source fluid temperature either 2C above or below that of the other two tubes; such a situation would arise if a non-uniform temperature air stream approaches the face of an evaporator coil. The results obtained in these tests are shown in Tables 5&6.

The results shown in Tables 5&6 indicate that :

1. The total heat flow rate is approximately 5% higher than would be expected based on the individual performances for equally heated tubes.
2. The heat flow rate of identically heated tubes in Table 5

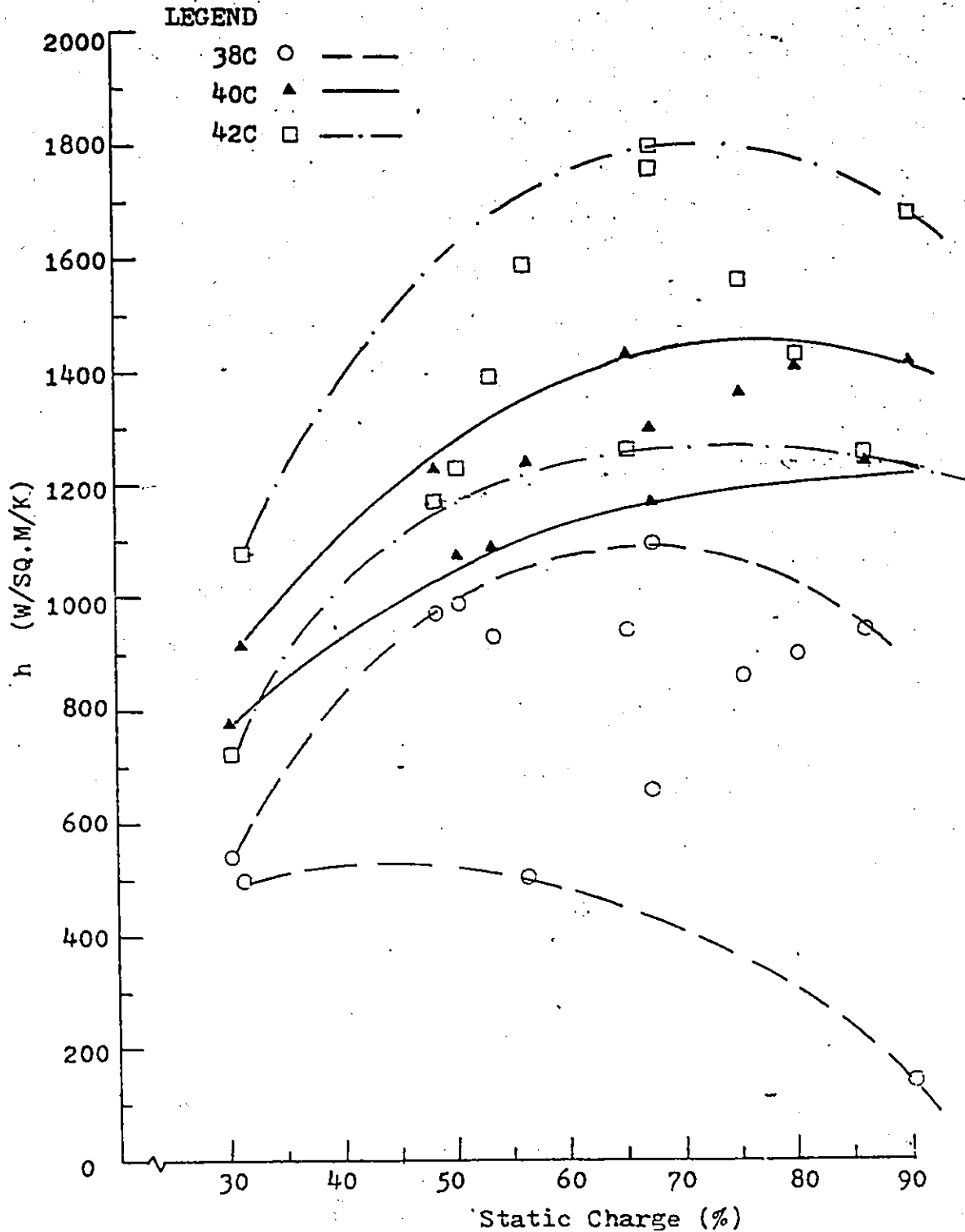


FIG. 31: Heat transfer coefficients in individual tubes vs static charge for $\Delta t = 20$.
 $T(\text{source})$ average = 40C , $T(\text{sink}) = 20\text{C}$.

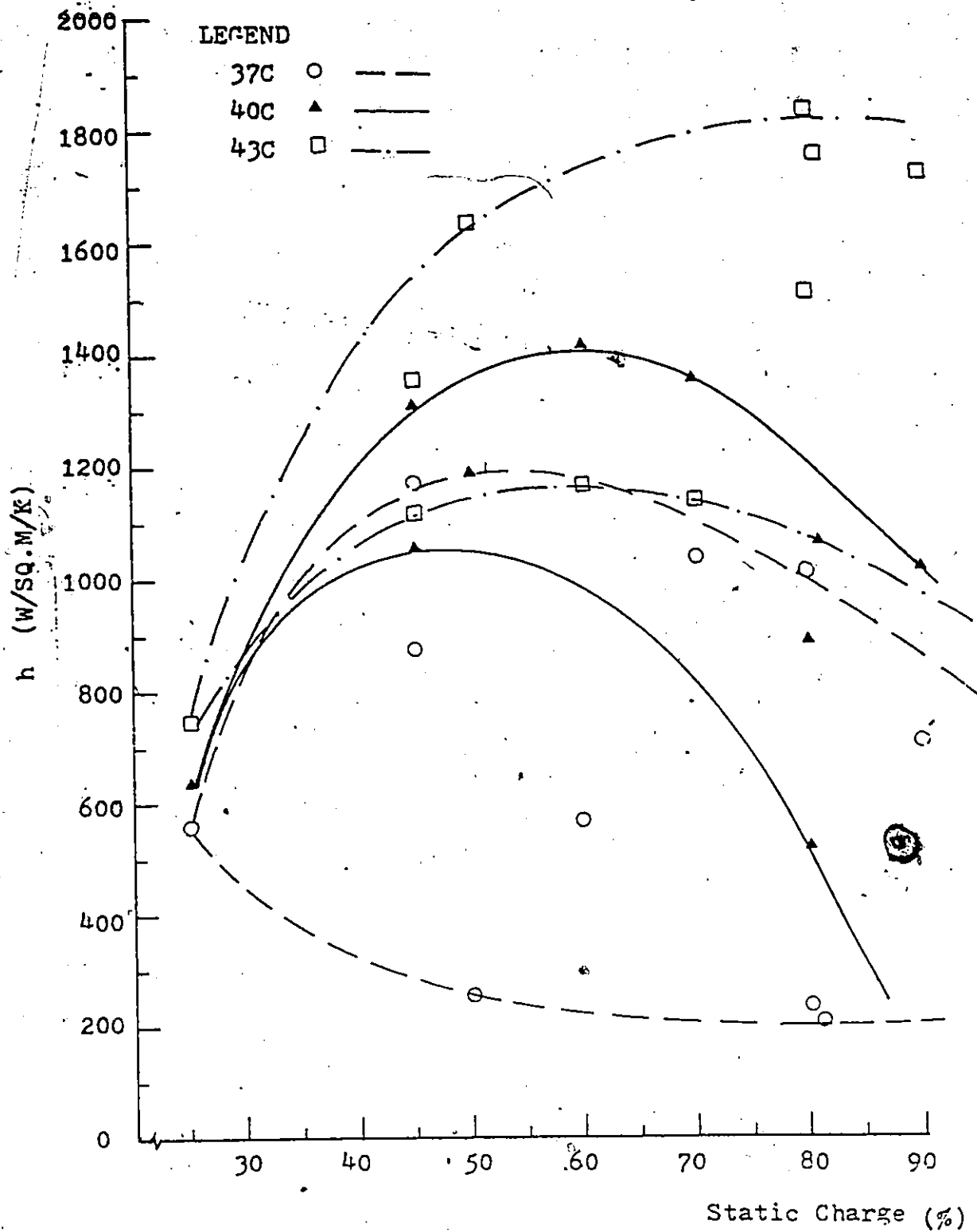


FIG. 32: Heat transfer coefficients in individual tubes vs static charge for $\Delta t = 3C$.
 $T(\text{source}) \text{ average} = 40C$, $T(\text{sink}) = 20C$.

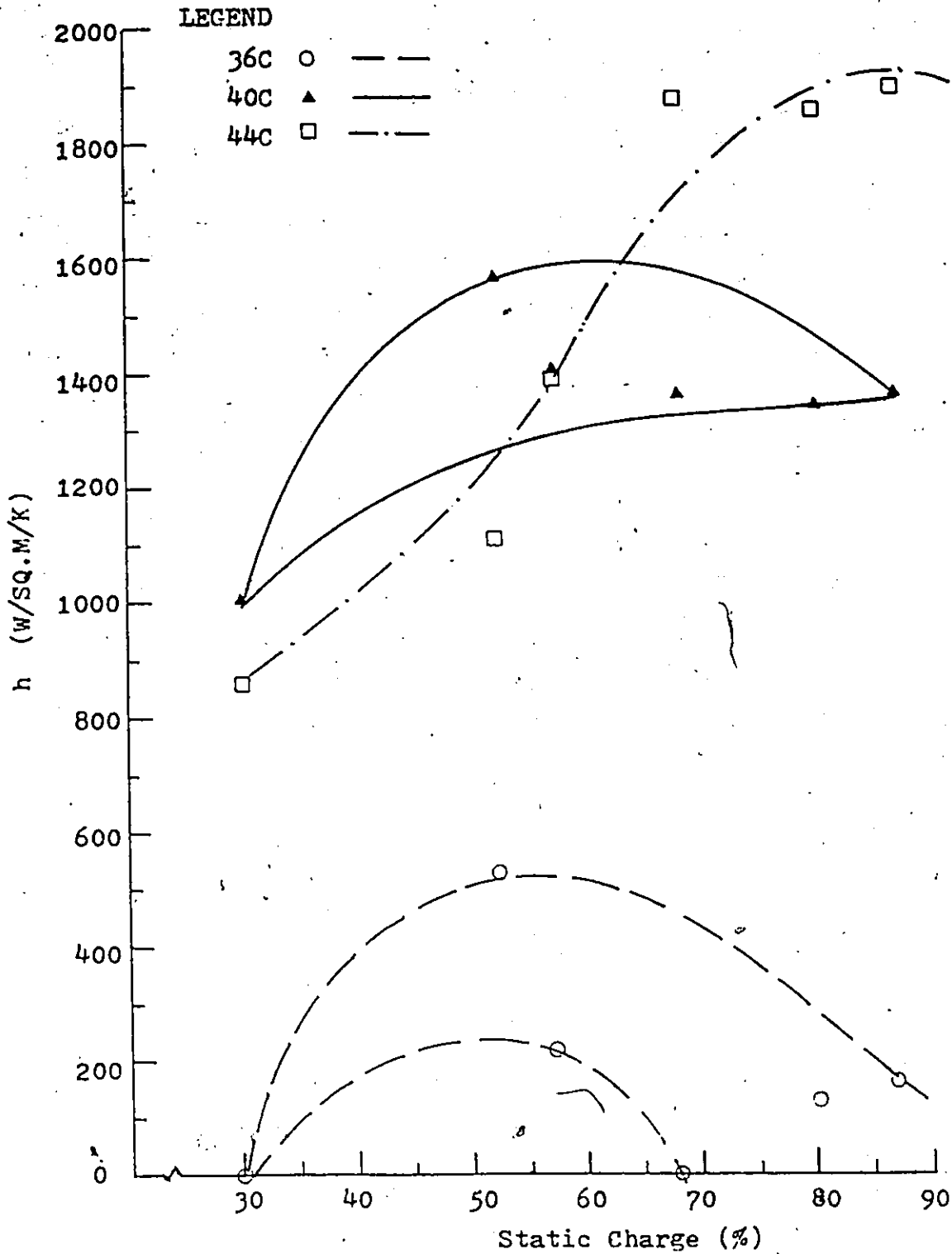


FIG. 33: Heat transfer coefficients in individual tubes vs static charge for $\Delta t = 4C$.
 $T(\text{source})$ average = $40C$, $T(\text{sink}) = 20C$.

TABLE 5. Performance data for source fluid temperatures of 42C, 42C and 40C. T(sink)=20C. Q(watts). m(wtr) gm/s. R(T)=Q(T)/QA

#####									
m(wtr)=35.1 m(wtr)=35.8 m(wtr)=33.6									
RUN#	%CHG	Q(42)	R(42)	Q(42)	R(42)	Q(40)	R(40)	QA	QA/QAE
*m(wtr)=33.6 *m(wtr)=33.7 *m(wtr)=33.4									
30	86	158.0	1.11	170.5	1.20	98.5	0.69	142.3	1.06
31 *	80	161.8	1.12	153.8	1.06	118.9	0.82	144.8	1.05
32	78	165.3	1.16	161.1	1.13	102.0	0.71	142.8	1.03
33	65	170.5	1.15	163.4	1.10	112.5	0.75	148.8	1.06
34 *	63	159.0	1.10	153.8	1.07	118.9	0.83	143.9	1.03
35 *	60	160.8	1.18	160.8	1.18	88.4	0.64	136.7	0.98
36 *	52	146.9	1.09	138.0	1.02	119.6	0.89	134.8	1.02
37	50	161.7	1.16	153.6	1.11	102.0	0.73	139.1	1.06
38 *	48	147.7	1.07	164.6	1.19	102.7	0.74	138.3	1.08
39	35	139.6	1.18	132.4	1.11	84.4	0.71	118.8	1.11
AVERAGES			1.13		1.12		0.75		1.05

NOTE: QAE is for a source-sink temperature difference of 21.3C.

TABLE 6. Performance data for source fluid temperatures of 42C, 40C and 40C. T(sink)=20C. Q(watts). m(wtr) gm/s. R(T)=Q(T)/QA

#####									
m(wtr)=33.6 m(wtr)=33.7 m(wtr)=33.4									
RUN#	%CHG	Q(42)	R(42)	Q(40)	R(40)	Q(40)	R(40)	QA	QA/QAE
*m(wtr)=35.1 *m(wtr)=35.8 *m(wtr)=26.0									
40 *	88	183.7	1.43	92.9	0.73	107.8	0.84	128.1	1.01
41	85	178.9	1.32	118.9	0.87	109.9	0.81	135.9	1.04
42	75	167.4	1.24	121.3	0.90	116.1	0.86	134.9	1.00
43	73	172.3	1.25	114.6	0.83	125.9	0.92	137.6	1.01
44 *	70	173.1	1.29	126.6	0.94	104.0	0.77	134.6	0.99
45 *	70	176.4	1.28	124.9	0.91	112.6	0.81	138.0	1.01
46	63	181.5	1.29	132.6	0.94	107.7	0.77	140.6	1.03
47 *	50	182.2	1.40	115.4	0.88	93.6	0.72	130.4	1.03
48	40	153.2	1.19	125.4	0.97	108.8	0.84	129.1	1.15
49 *	30	125.7	1.21	111.6	1.07	75.0	0.72	104.1	1.12
AVERAGES			1.29		0.90		0.81		1.04

NOTE: QAE is for a source-sink temperature difference of 20.7C.

differed by up to 11% and in Table 6 by upto 20%, except for the lowest charge where the difference is 39%.

3. There is no significant variation of heat flow rate with charge except for charges less than 40% where the performance drops off.

Figs. 34 & 35 are plots of heat transfer coefficients in individual tubes versus evaporator static charge.

An examination of run 35 in Table 5 indicates that the proportion of heat transfer taking place in the 40C tube is smallest when compared to other runs in the same Table. The small heat transfer rate in the 40C tube is due to the presence of both boiling suppression and dryout, indicated by high tube wall temperatures. This heat transfer rate results in a lower value of the heat transfer coefficient for a static charge of 60%, as shown in Fig. 34.

For a static charge of 52%, Fig. 34 shows lower heat transfer coefficients in the 42C tube compared to the 40C tube. The decreased heat transfer coefficients in the 42C tubes are due to dryout occurring in the top regions of this tube.

The significant difference shown in Fig. 35 for the heat transfer coefficients in the 40C tubes for a static charge of 30% is due to dryout occurring over 40% of the area in one tube and over 60% in the other tube.

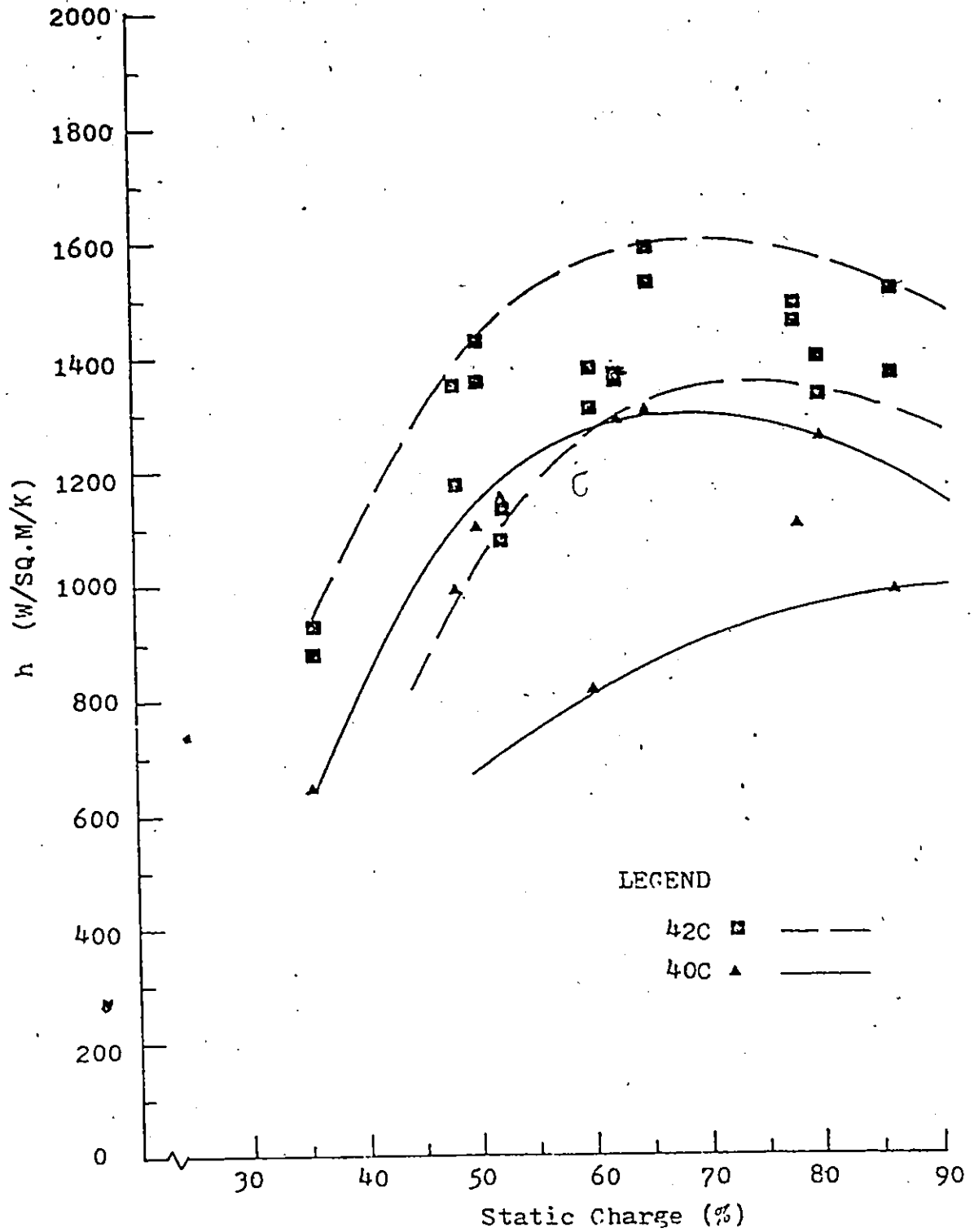


FIG. 34: Heat transfer coefficients in individual tubes vs static charge for a 42C-42C-40C source temperature configuration. $T(\text{sink}) = 20\text{C}$.

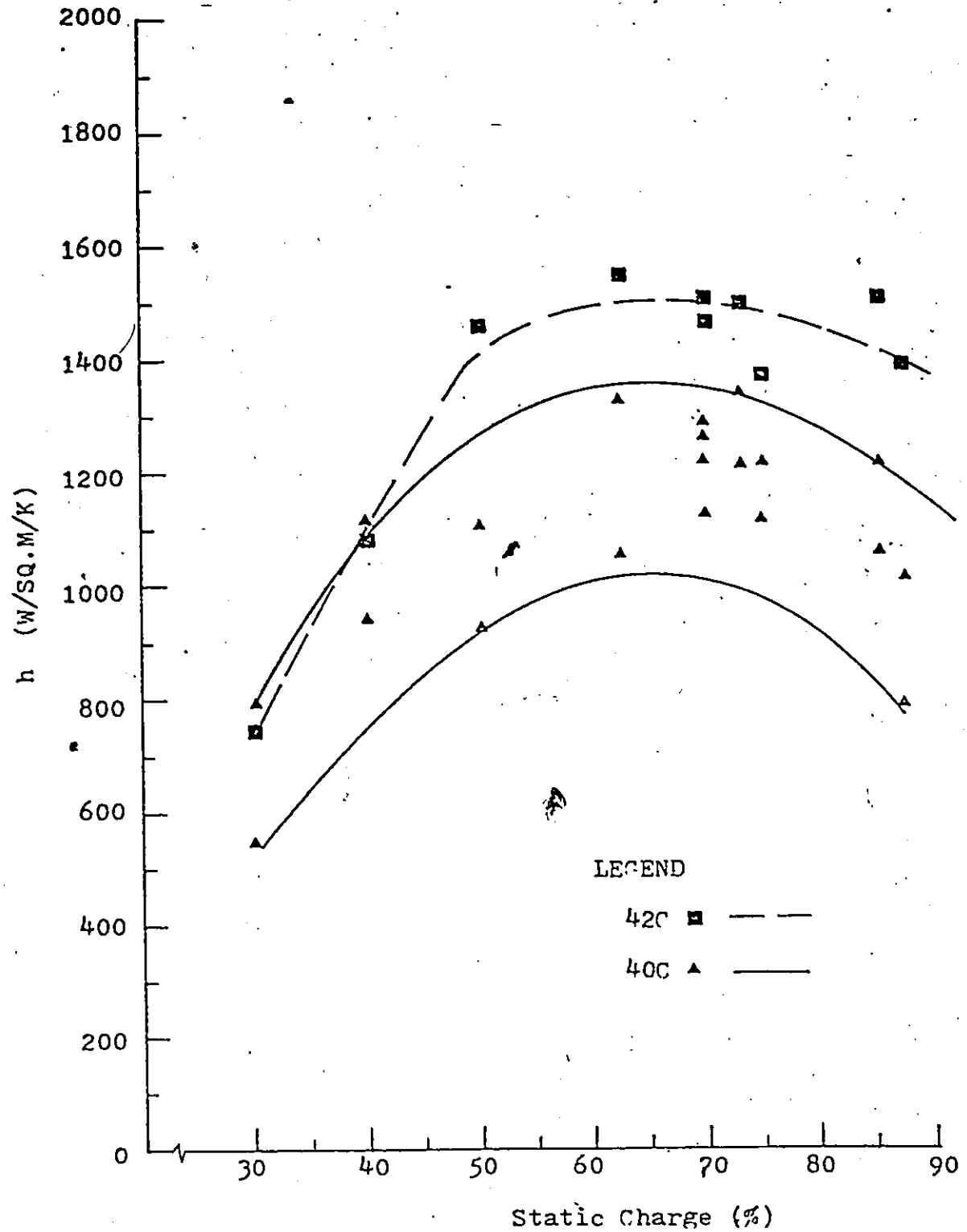


FIG. 35: Heat transfer coefficients in individual tubes vs static charge for a 42C-40C-40C source temperature configuration. $T(\text{sink}) = 20\text{C}$.

CHAPTER VI

CONCLUSIONS

The following conclusions can be drawn about the operation of the system:

GENERAL:

- i) The performance of the system was found to be substantially lower than that reported by Sampath(1).
- ii) Between static charges of 40%-90% the system performance appears to be independent of static charge.
- iii) Inclining the tubes from the vertical shifts the performance curve to the right.

UNEQUAL CHARGE DISTRIBUTION:

- i) Charge variations between adjacent tubes of 3% to 13% have a negligible affect on the heat transfer rate and average evaporator heat transfer coefficient for the system for source to sink temperature differences of 20C and 10C.
- ii) For a majority of static charges the average evaporator heat transfer coefficient was found to lie within $\pm 30\%$ and $\pm 32\%$ of the curve for a vertical evaporator for the 40C/20C tests and the 35C/25C tests

respectively.

UNEQUAL HEATING:

- i) Temperature differences between the three evaporator tubes of as much as 40% of the average source to evaporator saturation temperature difference slightly increased the heat transfer rate (4%-7%) in the evaporator compared with their expected performance with all tubes equally heated.
- ii) The average evaporator heat transfer coefficient in these tests were unaffected by unequal heating. Nearly 80% of the data falls within $\pm 10\%$ of the curve for the equal heating case.
- iii) The tubes subjected to the highest source fluid temperatures transferred, on average, 23%-54% more heat than would be expected for equal heating.
- iv) The heat flow rate in the tube subjected to the average source fluid temperature of 40C was 9% better than the average heat flow rate for equally heated tubes.
- v) The tube subjected to the lowest source fluid temperature transferred, on average, 27%-87% less heat than that for equal heating.
- vi) Substantially different heat flow rate distributions were found to occur for similar charges for the same temperature distributions.

RECOMMENDATIONS:

The following recommendations are made on the basis of this study:

- i) It is important to either replace the rightmost 1/4" tube or identify the reasons for its malfunctioning and rectify its performance. After accomplishing this the effect of rotation and nonuniform heating of the evaporator should be studied with the 1/4" tubes as the evaporator.
- ii) A greater understanding of the types and causes of instabilities encountered in such systems is essential and therefore an exhaustive experimental study on a test rig with adequate instrumentation to record the fluctuations in the mass flowrate, temperature and pressure should be carried out.
- iii) It would be worth while to use another refrigerant and study the effect of the parameters varied in this study.

REFERENCES

1. Sampath, S., McDonald, T.W., Ali, A.F.M., " The unidirectional coil loop thermosyphon heat exchanger ", ASHRAE transactions 1978, vol 84, part II, paper no 2491, RP-188, p. 27.
2. Sampath, S., McDonald, T.W., " The bidirectional coil loop thermosyphon heat exchanger ", ASHRAE transactions 1980, vol 86, part II, paper no 2588, RP-188, p. 37.
3. Ali, A.F.M., " Two phase thermosyphon loops: Development of a computer simulation program ", Doctoral thesis, Department of Mechanical Engineering, University of Windsor (1977).
4. McDonald, T.W., " Development of performance characteristics for two phase thermosyphon loops ", Final report on ASHRAE RP-140 December, 1975.
5. Hwang, K.S., Diccio, R., McDonald, T.W. " Thermosyphon loop performance characteristics, Part I ", ASHRAE transactions 1977, vol 83, part II, paper no 2467, RP-140, p. 250.
6. Hwang, K.S. " Two phase thermosyphon loops, Part I ", Master's thesis, Department of Mechanical Engineering, University of Windsor (1976).
7. McDonald, T.W., " Recirculation thermosiphon loops with multiple tube evaporators and condensers ", Final Report on ASHRAE RP.188 January, 1979.
8. Sampath, S., " Multiple tube two phase thermosyphon heat exchanger ", Thesis draft submitted to the Department of Mechanical Engineering, University of Windsor.
9. Mathur, G.D. Personal communication to obtain simulated results.
10. Imperial Eastman Catalog No 114-C: Imperial Fluid Transmission Components (1981), Imperial Gould Inc., Fluid Components Division, p. 44.
11. Sachs, P., Long, A.K., " A correlation for heat transfer in stratified two phase flow with vaporization ", Int. Journal of Heat and Mass Transfer v.2 222 (1961).
12. Davis, E.J., David, M.M., " Heat transfer to high quality steam water mixtures flowing in a horizontal rectangular duct ", Canadian journal of Chemical Engineering 99 (June, 1961).
13. Kline, S.J., McClintock, F.A. " Describing uncertainties in single sample experiments ", Mechanical Engineering, p. 3, January 1953.

APPENDIX A

Table A-1 Experimental data for T(source)=40C, T(sink)=20C. Vertical evaporator.

```
#####
Serial #   Charge(%)   Q(Watts)   H(Watts/sq.m K)
#####
```

Serial #	Charge(%)	Q(Watts)	H(Watts/sq.m K)
1	90	366.0	1117.2
2	82	378.5	1184.7
3	80	391.1	1321.7
4	77	378.5	1179.7
5	71	387.1	1364.9
6	70	389.6	1316.7
7	60	382.6	1305.2
8	56	382.6	1216.7
9	54	368.9	1216.8
10	50	349.6	1007.0
11	46	350.0	1002.8
12	40	348.0	1040.4
13	36	302.4	736.4

Table A-2 Experimental data for T(source)=40C, T(sink)=20C. Evaporator tubes inclined at 30 deg.

```
#####
Serial #   Charge(%)   Q(Watts)   H(Watts/sq.m K)
#####
```

Serial #	Charge(%)	Q(Watts)	H(Watts/sq.m K)
1	84	389.4	1328.4
2	77	407.9	1574.0
3	70	382.2	1396.6
4	65	392.3	1319.8
5	60	349.5	1057.8
6	60	364.4	1170.6
7	56	377.9	1239.2
8	50	383.7	1267.5
9	50	340.1	896.5
10	40	292.1	640.4
11	38	301.8	692.6
12	34	316.3	763.3

Table A-3 Experimental data for T(source)=40C, T(sink)=20C, Evaporator tubes inclined at 45 deg.

Serial #	Charge(%)	Q(Watts)	H(Watts/sq.m K)
1	90	392.0	1523.3
2	85	394.0	1444.7
3	83	399.2	1546.1
4	70	390.6	1427.3
5	60	356.0	1063.0
6	53	321.5	819.9
7	50	306.9	726.5
8	36	244.7	440.9

Table A-4 Experimental data for T(source)=40C, T(sink)=20C. Evaporator tubes rotated at 30 deg.

Serial #	Charge(%)	Q(Watts)	H(Watts/sq.m K)
1	83	404.4	1480.3
2	80	412.7	1554.6
3	80	411.3	1562.7
4	70	394.0	1425.8
5	57	362.9	1144.1
6	50	364.7	1162.9
7	40	321.5	802.2
8	26	251.2	490.7

Table A-5 Experimental data for T(source)=40C, T(sink)=
20C. Evaporator tubes rotated at 45 deg.

Serial #	Charge(%)	Q(Watts)	H(Watts/sq.m K)
1	90	392.0	1326.8
2	90	385.7	1207.4
3	80	375.4	1270.6
4	80	379.1	1321.6
5	70	394.0	1578.7
6	70	387.1	1405.4
7	58	369.8	1259.6
8	51	356.7	1119.7
9	40	327.7	931.7
10	33	285.2	654.6

Table A-6 Experimental data for T(source)=35C, T(sink)=
25C. Vertical evaporator.

Serial #	Charge(%)	Q(Watts)	H(Watts/sq.m K)
1	88	170.9	705.2
2	83	195.3	874.1
3	83	165.4	713.3
4	80	169.0	749.4
5	80	171.1	764.7
6	80	154.1	652.9
7	70	170.4	864.9
8	60	162.8	779.9
9	50	153.8	709.0
10	40	164.4	733.5
11	35	134.6	508.6
12	30	154.5	710.8
13	20	125.7	468.8

Table A-7 Experimental data for T(source)=35C, T(sink)=25C. Evaporator tubes inclined at 15 deg.

Serial #	Charge(%)	Q(Watts)	H(Watts/sq.m K)
1	88	186.7	1043.9
2	88	178.0	834.8
3	80	174.2	920.6
4	70	161.8	771.6
5	70	164.9	831.4
6	70	194.3	991.0
7	63	151.1	626.8
8	60	163.8	769.8
9	54	192.2	1035.3
10	50	151.4	700.9
11	40	129.6	485.8

Table A-8 Experimental data for T(source)=35C, T(sink)=25C. Evaporator tubes inclined at 30 deg.

Serial #	Charge(%)	Q(Watts)	H(Watts/sq.m K)
1	92	173.3	886.1
2	80	190.5	1153.5
3	77	216.0	1264.6
4	70	193.6	967.2
5	60	184.6	914.0
6	60	189.8	1187.9
7	54	152.4	754.8
8	50	140.0	561.9
9	40	135.8	504.0
10	27	105.4	346.2

Table A-9 Experimental data for T(source)=35C, T(sink)=25C. Evaporator tubes rotated at 15 deg.

Serial #	Charge (%)	Q (Watts)	H (Watts/sq.m K)
1	85	163.3	714.1
2	85	178.6	855.5
3	85	177.3	849.4
4	68	190.5	1054.9
5	60	187.7	968.6
6	50	160.2	780.8
7	40	153.8	691.7
8	37	134.8	531.4
9	37	140.0	563.9
10	25	133.1	517.2

Table A-10 Experimental data for T(source)=35C, T(sink)=25C. Evaporator tubes rotated at 30 deg.

Serial #	Charge (%)	Q (Watts)	H (Watts/sq.m K)
1	80	185.6	1009.9
2	75	172.7	816.5
3	70	169.8	862.2
4	60	144.0	645.0
5	60	199.6	1145.3
6	57	155.5	686.9
7	50	140.0	612.1
8	43	157.6	789.3
9	30	137.8	569.5
10	29	129.6	521.2
11	20	107.8	396.7

Table A-11 Average evaporator heat transfer coefficient and heat transfer coefficients in individual tubes for T(source) average = 40C, T(sink) = 20C with a temperature difference of 2C between adjacent tubes. h, H (Watts/sq.m K).

Serial #	Chg(%)	h(42)	h(40)	h(38)	H
1	86	1263.3	1257.8	945.8	1174.7
2	75	1556.6	1364.1	860.3	1301.0
3	65	1260.2	1433.9	942.0	1230.3
4	48	1168.9	1234.8	971.0	1138.3
5	30	717.8	778.1	537.7	687.1

Table A-12 Average evaporator heat transfer coefficient and heat transfer coefficients in individual tubes for T(source) average = 40C, T(sink) = 20C with a temperature difference of 2C between adjacent tubes. h, H (Watts/sq.m K).

Serial #	Chg(%)	h(42)	h(40)	h(38)	H
1	90	1676.7	1422.2	141.7	1154.6
2	80	1429.7	1411.1	896.8	1284.3
3	67	1796.6	1171.2	1095.1	1404.3
4	67	1763.6	1298.4	656.8	1318.7
5	56	1589.5	1238.2	505.9	1172.7
6	53	1390.4	1088.3	934.6	1172.8
7	50	1232.8	1074.2	992.1	1119.1
8	31	1078.0	917.8	499.1	866.1

Table A-13 Average evaporator heat transfer coefficient and heat transfer coefficients in individual tubes for T(source) average = 40C, T(sink) = 20C with a temperature difference of 3C between adjacent tubes. h, H (Watts/sq.m K).

Serial #	Chg(%)	h(43)	h(40)	h(37)	H
1	90	1733.5	1018.5	703.4	1279.7
2	81	1757.7	1071.4	212.0	1161.2
3	80	1843.1	530.5	236.7	1009.1
4	80	1514.4	895.1	1020.5	1205.5
5	70	1140.9	1354.7	1043.0	1186.5
6	60	1169.7	1422.7	568.0	1106.1
7	50	1638.8	1195.6	262.4	1152.8
8	45	1361.3	1315.7	1174.1	1308.7
9	45	1123.7	1063.6	881.4	1055.7
10	25	748.4	636.5	560.9	668.9

Table A-14 Average evaporator heat transfer coefficient and heat transfer coefficients in individual tubes for T(source) average = 40C, T(sink) = 20C with a temperature difference of 4C between adjacent tubes. h, H (Watts/sq.m K).

Serial #	Chg(%)	h(44)	h(40)	h(36)	H
1	87	1902.6	1376.8	163.3	1323.2
2	80	1859.1	1347.2	129.3	1283.6
3	68	1877.3	1366.1	0.0	1227.7
4	57	1393.5	1405.0	221.6	1120.9
5	52	1110.4	1573.6	528.1	1123.2
6	30	859.8	1006.5	0.0	672.8

Table A-15 Average evaporator heat transfer coefficient and heat transfer coefficients in individual tubes for a source temperature configuration of 40C-40C-42C and T(sink)=20C. h, H (Watts/sq.m K).

Serial #	Chg(%)	h(42)	h(40)	h(40)	H
1	88	1392.7	789.4	1017.5	1081.8
2	85	1508.9	1220.4	1059.1	1274.2
3	75	1326.4	1220.9	1115.3	1228.7
4	73	1499.8	1208.3	1346.3	1361.8
5	70	1463.9	1282.9	1125.8	1304.3
6	70	1510.9	1263.0	1216.1	1343.2
7	63	1507.1	1330.5	1051.5	1307.2
8	50	1464.5	1103.8	926.5	1185.9
9	40	1084.2	1117.4	942.3	1049.9
10	30	745.9	792.1	545.5	698.7

Table A-15 Average evaporator heat transfer coefficient and heat transfer coefficients in individual tubes for a source temperature configuration of 40C-42C-42C and T(sink)=20C. h, H (Watts/sq.m K).

Serial #	Chg(%)	h(42)	h(42)	h(40)	H
1	86	1374.2	1524.0	992.3	1310.4
2	80	1398.4	1331.8	1266.9	1337.0
3	78	1494.8	1463.2	1105.3	1368.3
4	65	1593.5	1533.8	1307.1	1490.4
5	63	1372.3	1366.5	1290.2	1347.2
6	60	1307.6	1378.1	819.5	1179.4
7	52	1145.4	1080.6	1156.3	1125.5
8	50	1426.8	1361.8	1101.7	1309.1
9	48	1184.8	1349.0	993.4	1186.1
10	35	927.4	883.2	642.3	825.0

APPENDIX B DATA ACQUISITION PROGRAM

```

10 CLEAR 200, &H6F00
20 INPUT "PM"; PM
30 INPUT "PX"; PX
40 INPUT "ELEV"; EL
50 INPUT "CHARGE"; CG
60 INPUT "COND TILT"; IN
70 INPUT "COND ROTATION"; SX
80 INPUT "EVAP ROTATION"; SY
90 INPUT "EVAP TILT"; TI
100 INPUT "TEST"; TE
110 INPUT "DATE"; DS
120 INPUT "REFRIGERANT"; FS
130 DIM T(47), TT(47), TA(47), VT(47), TS(47), GA(PX), HA(PX), PA(PX), RR(10), M*(10), Ls
    (10), P*(10); IR=1
140 INPUT "HOT WATER FLW, COLD WATER FLW"; MR, MI, ML, CF
150 CP=.1858; XV=0.; YV=0.; ZV=0.; N=1; FOR I=0 TO 47: TS(I)=0.; VT(I)=C.; NEXT I; A=.07
311: C=.02773; B=.04538; HF=MR+MI+ML
160 FOR I=&H7FAE TO &H7FFF: READ X: POKE I, X: NEXT I
170 DATA 142, 134, 0, 182, 255, 34, 71, 37, 250, 189, 127
180 DATA 236, 182, 255, 34, 71, 37, 241, 127, 127
190 DATA 255, 134, 8, 193, 127, 254, 189, 127, 245
200 DATA 120, 127, 255, 246, 255, 34, 195, 1, 250
210 DATA 127, 255, 86, 86, 247, 127, 255, 122, 127
220 DATA 254, 38, 232, 231, 128, 193, 20, 39, 5
230 DATA 189, 127, 245, 32, 198, 57, 204, 0, 128
240 DATA 131, 0, 1, 39, 251, 57, 204, 1, 164, 131
250 DATA 0, 1, 38, 251, 57, 0, 10
260 DEFUSR0=&H7FAE
270 CS="AB": F=VARPTR(CS)
280 Y=USR0(0) "LOOK AT FLUKE"
290 I=&H6F00
300 Y=PEEK(I)
310 IF Y=89 THEN 350 "Y"
320 IF Y=25 THEN 420 "A"
330 IF Y=20 THEN 470 "DC"
340 I=I+1: GO TO 300
350 POKE K, I: POKE K+2, INT(I/256)
360 POKE K+3, I-INT(I/256)*256
370 DD=VAL(MID$(CS, 2, 3))
380 HH=VAL(MID$(CS, 5, 2))
390 MM=VAL(MID$(CS, 9, 2))
400 SS=VAL(MID$(CS, 12, 2))
410 I=I+24: GO TO 300
420 POKE K, I: POKE K+2, INT(I/256): POKE K+3, I-INT(I/256)*256
430 CH=VAL(MID$(CS, 2, 3))
440 T(CH)=VAL(MID$(CS, 7, 5))
450 IF MID$(CS, 15, 2)="BT" THEN T(CH)=T(13)
460 I=I+12: GO TO 300
470 "FOUND END OF DATA"
480 CLS
490 PRINT USING "####"; N, HH, MM, SS
500 FOR I=0 TO 47: PRINT USING "#####.##"; T(I); NEXT I
510 IF N=1 THEN S=0
520 PRINT: INPUT "DO YOU WANT TO PROCEED?"; S

```

```

530 IF A1="YES" THEN 600 ELSE 280
540 FOR I=0 TO 47
550 IF ABS(T(I)-TT(I))>=.10*TT(I) THEN 570
560 GOTO 590
570 PRINT "UNSTEADY CONDITIONS AT THERMOCOUPLE #" I
580 PRINT "SCAN NUMBER" N:PRINT "CURRENT TEMP" T(I):PRINT "TEMP IN FIRST SCAN" TT(I)
590 NEXT I
600 RS=0.:ST=0.:FOR I=1 TO 15
610 RS=RS+T(I-1):ST=ST+T(I+14):NEXT I
620 AH=(T(39)+T(40)+T(41))/3.
630 BH=(T(36)+T(37)+T(38))/3.
640 WL=T(30)-T(33):WM=T(31)-T(34):WR=T(32)-T(35)
650 CW=AH-BH
660 QC=CF*CP*CW:QL=CP*WL*ML:QM=CP*WM*MI:QR=CP*WR*MR:QE=QL+QM+QR
670 LE=-ST/15+PS/15
680 HA(N)=QE/(P*LE):PA(N)=QC/(C*LE):GA(N)=(QE+QC)/(A*LE)
690 FOR I=0 TO 47:TS(I)=TS(I)+T(I):TA(I)=TS(I)/N.
700 NEXT I
710 CS=0.:DS=0.:FOR I =0 TO 14
720 CS=CS+TA(I):DS=DS+TA(I+15):NEXT I
730 AT=DS/15.:RA=CS/15.
740 AA=(TA(39)+TA(40)+TA(41))/3.:BA=(TA(36)+TA(37)+TA(38))/3.:WA=TA(30)-TA(33):W
E=TA(31)-TA(34):WC=TA(32)-TA(35):DA=(TA(30)+TA(31)+TA(32))/3
750 EA=AA-BA
760 NAQC=CF*CP*EA:QA=CP*WA*ML:QB=CP*WE*MI:QD=CP*WC*MR:MAQE=QA+QB+QD
770 ZC=-AT+RA
780 UE=MA/(B*ZD):UC=NA/(C*ZD):UA=(MA+NA)/(A*ZD)
790 ES=MA/(A/2*ZD):FS=NA/(A/2*ZD)
800 GE=(MA+NA)/(2*B*ZD):IA=(MA+NA)/(2*C*ZD)
810 IF N <> 1 THEN VP=AV
820 VA=0.:VE=0.:VC=0.:FOR I =1 TO N
830 VA=(GA(I)-UA)^2+VA
840 VE=(HA(I)-UE)^2+VE
850 VC=(PA(I)-UC)^2+VC
860 NEXT I
870 AV=SQR(VA/N):EV=SQR(VE/N):CV=SQR(VC/N)
880 IF N <= PM THEN 980
890 FOR I=0 TO 47
900 VT(I)=(VT(I)*(N-PM-1)+(T(I)+TA(I))^2)/(N-PM):NEXT I
910 VA=(XA*(N-PM-1)+(GA-QL)^2)/(N-PM)
920 XB=(XB*(N-PM-1)+(QB-QM)^2)/(N-PM)
930 XD=(XD*(N-PM-1)+(QD-QR)^2)/(N-PM)
940 XV=(XV*(N-PM-1)+(QE-MAQE)^2)/(N-PM)
950 YV=(YV*(N-PM-1)+(QC-NAQC)^2)/(N-PM)
960 ZV=(ZV*(N-PM-1)+.5*(QE+QC)-.5*(MAQE+NAQC))^2)/(N-PM)
970 IF ABS(AV-VP) < (.03*AV) OR N=PX THEN 1010
980 IF N=1 THEN 990 ELSE 1000
990 FOR I=0 TO 47:TT(I)=T(I):NEXT I
1000 N=N+1:GOTO 280 "FOR ANOTHER SCAN"
1010 IF ABS(AV-VP) < (.03*AV) THEN PRINT "VARIANCE DOES NOT FALL WITHIN LIMIT"
1020 PRINT "N=" N:"AQIN=" MAQE:"AQOUT=" NAQC:"UEE=" UE:"UAE=" GS:"UAA=" UA
1030 PRINT "HWIN=" DA:"HWOUT=" CA:"CUIN=" BA:"CWOUT=" AW
1040 INPUT "WHAT NEXT?(1-RERUN,2-PRINT RESULTS ON CASSETTE,3-STOP):"UN
1050 ON UN GOTO 1050,1060,2350
1060 INPUT "NUMBER OF FLOWMETER READINGS:"JA
1070 FOR I=1 TO JA
1080 INPUT "RIGHT FLOWMETER READING:"R#(I)
1090 INPUT "MIDDLE FLOWMETER READING:"M#(I)
1100 INPUT "LEFT FLOWMETER READING:"L#(I)
1110 INPUT "BOTTOM FLOWMETER READING:"B#(I)
1120 NEXT I

```

```

1130 FOR I=0 TO 47:VT(I)=SQR(VT(I)):NEXT I:XA=SQR(XA):YO=SQR(YO):XB=SQR(XB):XD=S
QR(XD):XV=SQR(XV)
1140 INPUT "DO YOU WANT TO RECORD RESULTS ON TAPE":Y$
1150 IF Y$="YES" THEN 1160 ELSE 1520
1160 PRINT "POSITION TAPE --PRESS PLAY AND RECORD":INPUT "READY, ENTER FILE NAME":
R$
1170 OPEN "O".#-1,R$
1180 PRINT #-1,TE
1190 PRINT #-1,D$
1200 PRINT #-1,TI
1210 PRINT #-1,SI
1220 PRINT #-1,SY
1230 PRINT #-1,IN
1240 PRINT #-1,EL
1250 PRINT #-1,F$
1260 PRINT #-1,CG
1270 PRINT #-1,ML,MI,MR
1280 PRINT #-1,CF
1290 PRINT #-1,N
1300 PRINT #-1,BA
1310 PRINT #-1,AA
1320 PRINT #-1,DA
1330 PRINT #-1,AT
1340 PRINT #-1,RA
1350 PRINT #-1,QA,QB,QC,QD,XA,XB,XD,XV
1360 PRINT #-1,NA,YV
1370 PRINT #-1,UE,EV
1380 PRINT #-1,ES
1390 PRINT #-1,UC,CV
1400 PRINT #-1,FS
1410 PRINT #-1,UA,AV
1420 PRINT #-1,GS
1430 PRINT #-1,IA
1440 FOR I=0 TO 47:PRINT #-1,I,TA(I),VT(I):NEXT I
1450 PRINT #-1,PM
1460 PRINT #-1,PX
1470 PRINT #-1,JA
1480 FOR I=1 TO JA
1490 PRINT #-1,L$(I),M$(I),RR$(I),B$(I)
1500 NEXT I
1510 CLOSE #-1
1520 INPUT "DO YOU WANT A PRINT OUT":Y$
1530 IF Y$="YES" THEN 1540 ELSE 2310
1540 SOUND 100,100
1550 INPUT "HAVE YOU CONNECTED THE PRINTER TO THE COMPUTER ":Y$
1560 IF Y$="YES" THEN 1570 ELSE 1540
1570 PRINT #-2,"DATE:"D$,TAB(50)"TEST#:"TE
1580 PRINT #-2,"EVAP TILT ANGLE( DEG):"TAB(40)TI
1590 PRINT #-2,"EVAP ROTATION ANGLE( DEG):"TAB(40)SY
1600 PRINT #-2,"COND TILT ANGLE( DEG):"TAB(40)IN
1610 PRINT #-2,"COND ROTATION ANGLE( DEG):"TAB(40)SI
1620 PRINT #-2,"COND ELEV(M):"TAB(40)EL
1630 PRINT #-2,"WORKING FLUID:"TAB(40)F$
1640 PRINT #-2,"EVAP CHARGE(G):"TAB(40)CG
1650 PRINT #-2,"HOT WATER FLOW IN LEFT TUBE (GM/SEC):"TAB(40)ML
1660 PRINT #-2,"HOT WATER FLOW IN MIDDLE TUBE (GM/SEC):"TAB(40)MI
1670 PRINT #-2,"HOT WATER FLOW IN RIGHT TUBE (GM/SEC):"TAB(40)MR
1680 PRINT #-2,"COLD WATER FLOW(GM/SEC):"TAB(40)CF
1690 PRINT #-2,"AVG HOT WATER INLET TEMP(C):"TAB(41):PRINT #-2,USING"###,##":DA
1700 PRINT #-2,"AVG COLD WATER INLET TEMP(C):"TAB(41):PRINT #-2,USING"###,##":DB
1710 PRINT #-2,"AVG COLD WATER OUTLET TEMP(C):"TAB(41):PRINT #-2,USING"###,##":

```

```

1720 PRINT #2, "COND. WATER TEMP RISE(C):"TAB(41);PRINT #2,USING"###.##";AA-BA
1730 PRINT #2, "AVG. EVAP. WALL TEMP(C):"TAB(41);PRINT #2,USING"###.##";RA
1740 PRINT #2, "AVG COND. WALL TEMP:"TAB(41);PRINT #2,USING"###.##";AT
1750 PRINT #2, "ENERGY IN LEFT TUBE(W):"TAB(40);PRINT #2,USING"###.##";QA;PRI
NT #2,TAB(60)"(1);PRINT #2,USING"###.##";XA;PRINT #2,")";
1760 PRINT #2, "ENERGY IN MIDDLE TUBE(W):"TAB(40);PRINT #2,USING"###.##";QB;P
RINT #2,TAB(60)"(2);PRINT #2,USING"###.##";XB;PRINT #2,")";
1770 PRINT #2, "ENERGY IN RIGHT TUBE(W):"TAB(40);PRINT #2,USING"###.##";QD;PRI
NT #2,TAB(60)"(3);PRINT #2,USING"###.##";XD;PRINT #2,")";
1780 PRINT #2, "ENERGY IN(W):"TAB(40);PRINT #2,USING"###.##";MA;PRINT #2,TAB
(60)"(4);PRINT #2,USING"###.##";XV;PRINT #2,")";
1790 PRINT #2, "ENERGY OUT(W):"TAB(40);PRINT #2,USING"###.##";NA;PRINT #2,TA
B(60)"(5);PRINT #2,USING"###.##";YV;PRINT #2,")";
1800 PRINT #2, "EVAP EFFECTIVENESS:"TAB(41);PRINT #2,USING"###.##";MA/(CP*(ML+(
2*(TA(10)+TA(11)+TA(12)+TA(13)+TA(14))-TA(42))+MI*(.2*(TA(5)+TA(6)+TA(7)+TA(8)+
TA(9))-TA(42))+MR*(.2*(TA(8)+TA(1)+TA(3)+TA(4))-TA(42))))
1810 PRINT #2, "UEE"TAB(39);PRINT #2,USING"###.##";UE;PRINT #2,TAB(60)"(6);
PRINT #2,USING"###.##";EV;PRINT #2,")";
1820 PRINT #2, "UEA"TAB(39);PRINT #2,USING"###.##";ES
1830 PRINT #2, "UCC"TAB(39);PRINT #2,USING"###.##";JC;PRINT #2,TAB(60)"(7);
PRINT #2,USING"###.##";CV;PRINT #2,")";
1840 PRINT #2, "UCA"TAB(39);PRINT #2,USING"###.##";FS
1850 PRINT #2, "UAA"TAB(39);PRINT #2,USING"###.##";UA;PRINT #2,TAB(60)"(8);
PRINT #2,USING"###.##";AV;PRINT #2,")";
1860 PRINT #2, "UAE"TAB(39);PRINT #2,USING"###.##";GS
1870 PRINT #2, "UAC"TAB(39);PRINT #2,USING"###.##";IA
1880 PRINT #2, "*****"
1890 PRINT #2, "CONDENSER SIDE TEMPERATURES:"
1900 PRINT #2, "*****"
1910 PRINT #2,PRINT #2,TAB(5)"VAPOUR HEADER TEMP:";TAB(60);PRINT #2,USING"###.##";TA(43);PRINT #2,")";PRINT #2,USING"###.##";VT(43);PRINT #2,")";PRINT #2,")";
1920 PRINT #2,TAB(5)"WATER OUTLET TEMPS:";TAB(30);PRINT #2,USING"###.##";TA(41);PRINT #2,")";PRINT #2,USING"###.##";VT(41);PRINT #2,")";TAB(45);PRINT #2,USING"###.##";TA(40);PRINT #2,")";PRINT #2,USING"###.##";VT(40);PRINT #2,")";TAB(40);
1930 PRINT #2,USING"###.##";TA(39);PRINT #2,")";PRINT #2,USING"###.##";VT(39);PRINT #2,")";PRINT #2,")";
1940 PRINT #2,TAB(5)"COND WALL TEMPS:"
1950 FOR I=1 TO 5
1960 PRINT #2,TAB(30);PRINT #2,USING"###.##";TA(I+14);PRINT #2,")";PRINT #2,USING"###.##";VT(I+14);PRINT #2,")";TAB(45);PRINT #2,USING"###.##";TA(I+19);PRINT #2,")";PRINT #2,USING"###.##";VT(I+19);PRINT #2,")";TAB(60);
1970 PRINT #2,USING"###.##";TA(I+24);PRINT #2,")";PRINT #2,USING"###.##";VT(I+24);PRINT #2,")";
1980 NEXT I
1990 PRINT #2,PRINT #2,TAB(5)"WATER INLET TEMPS:";TAB(30);PRINT #2,USING"###.##";TA(38);PRINT #2,")";PRINT #2,USING"###.##";VT(38);PRINT #2,")";TAB(45);PRINT #2,USING"###.##";TA(37);PRINT #2,")";PRINT #2,USING"###.##";VT(37);PRINT #2,USING"###.##";VT(36);PRINT #2,")";
2010 PRINT #2, "*****"
2020 PRINT #2, "EVAPORATOR SIDE TEMPERATURES:"
2030 PRINT #2, "*****"
2040 PRINT #2,PRINT #2,TAB(5)"VAPOUR HEADER TEMP:";TAB(60);PRINT #2,USING"###.##";TA(40);PRINT #2,")";PRINT #2,USING"###.##";VT(40);PRINT #2,")";PRINT #2,")";

```



```

2050 PRINT #2,TAB(5)"WATER OUTLET TEMPS:";TAB(30);:PRINT #2,USING"##.##";TA(33)
);:PRINT #2,"(::PRINT #2,USING"##.##";VT(33);:PRINT #2,"";TAB(45);:PRINT #-
2,USING"##.##";TA(34);:PRINT #2,"(::PRINT #2,USING"##.##";VT(34);
2060 PRINT #2,"";TAB(60);:PRINT #2,USING"##.##";TA(35);:PRINT #2,"(::PRINT
#2,USING"##.##";VT(35);:PRINT #2,"";:PRINT #2
2070 PRINT #2,TAB(5)"EVAP WALL TEMPS:"
2080 FOR I=0 TO 4
2090 PRINT #2,TAB(30);:PRINT #2,USING"##.##";TA(I+10);:PRINT #2,"(::PRINT #-
2,USING"##.##";VT(I+10);:PRINT #2,"";TAB(45);:PRINT #2,USING"##.##";TA(I+5);
PRINT #2,"(::PRINT #2,USING"##.##";VT(I+5);:PRINT #2,"";TAB(60);
2100 PRINT #2,USING"##.##";TA(I+0);:PRINT #2,"(::PRINT #2,USING"##.##";VT(I+
0);:PRINT #2,""
2110 NEXT I
2120 PRINT #2:PRINT #2,TAB(5)"WATER INLET TEMPS:";TAB(30);:PRINT #2,USING"##.
##";TA(30);:PRINT #2,"(::PRINT #2,USING"##.##";VT(30);:PRINT #2,"";TAB(45);
:PRINT #2,USING"##.##";TA(31);:PRINT #2,"(::PRINT #2,USING"##.##";VT(31);
2130 PRINT #2,"";TAB(60);:PRINT #2,USING"##.##";TA(32);:PRINT #2,"(::PRINT
#2,USING"##.##";VT(32);:PRINT #2,""
2140 PRINT #2,"*****"
2150 PRINT #2,"SUBCOOLED LIQUID LINE TEMPS:";TAB(30);:PRINT #2,USING"##.##";TA
(44);:PRINT #2,"(::PRINT #2,USING"##.##";VT(44);:PRINT #2,"";TAB(45);:PRINT
#2,USING"##.##";TA(45);:PRINT #2,"(::PRINT #2,USING"##.##";VT(45);:PRINT #-
2,"";TAB(60);
2160 PRINT #2,USING"##.##";TA(46);:PRINT #2,"(::PRINT #2,USING"##.##";VT(46)
;:PRINT #2,""
2170 PRINT #2,"*****"
2180 PRINT #2,"FLOWMETER READINGS:"
2190 PRINT #2,"*****"
2200 PRINT #2,TAB(10)"LEFT";TAB(30)"MIDDLE";TAB(50)"RIGHT";TAB(70)"BOTTOM"
2210 PRINT #2,TAB(10)"****";TAB(30)"****";TAB(50)"****";TAB(70)"****"
2220 FOR I=1 TO JA
2230 PRINT #2,TAB(10)RIGHT$(L$(I),7);TAB(30)RIGHT$(M$(I),7);TAB(50)RIGHT$(RR$(I
),7);TAB(70)RIGHT$(P$(I),7)
2240 NEXT I
2250 PRINT #2,"*****"
2260 PRINT #2,"SATURATION TEMP (C):"TAB(39);:PRINT #2,USING"##.##";TA(47);:PRI
NT #2,TAB(60)"(::PRINT #2,USING"##.##";VT(47);:PRINT #2,""
2270 PRINT #2,"NO OF SCANS:"TAB(40)N
2280 PRINT #2,"MAX NO OF SCANS:"TAB(40)PX
2290 PRINT #2,"MIN NO OF SCANS:"TAB(40)PM
2300 PRINT #2,"*****"
2310 INPUT "DO YOU WANT TO REPEAT THE PRINTING PROCEDURE";Q$
2320 IF Q$="YES" THEN 1140 ELSE 2330
2330 GO TO 2350
2350 PRINT "END OF TEST";STOP

```

APPENDIX C SAMPLE OUTPUT

DATE: MAY 22 TEST # 293

EVAP TILT ANGLE(DEG): 0.0
 EVAP ROTATION ANGLE(DEG): 0.0
 COND TILT ANGLE(DEG): 45.0
 COND ROTATION ANGLE(DEG): 0.0
 COND ELEV(M): 0.9
 WORKING FLUID: R11
 EVAP CHARGE(%): 87.0
 HOT WATER FLOW IN LEFT TUBE(GM/S): 33.7
 HOT WATER FLOW IN MIDDLE TUBE(GM/S): 33.6
 HOT WATER FLOW IN RIGHT TUBE(GM/S): 33.4
 COLD WATER FLOW(GM/S): 63.2
 AVG HOT WATER INLET TEMP(C): 39.93
 AVG COLD WATER INLET TEMP(C): 19.95
 AVG COLD WATER OUTLET TEMP(C): 21.31
 COLD WATER TEMP RISE(C): 1.36
 AVG EVAP WALL TEMP(C): 37.59
 AVG COND WALL TEMP(C): 24.01
 ENERGY IN LEFT TUBE(W): 169.31 (6.55)
 ENERGY IN MIDDLE TUBE(W): 135.05 (7.39)
 ENERGY IN RIGHT TUBE(W): 85.30 (1.84)
 ENERGY IN(W): 389.67 (10.74)
 ENERGY OUT(W): 360.75 (3.50)
 EVAP EFFECTIVENESS: 0.13
 UEE: 632.18 (23.18)
 UEA: 784.80
 UCC: 957.78 (23.74)
 UCA: 726.56
 UAA: 755.68 (20.26)
 UAE: 608.72
 UAC: 996.17

 CONDENSER SIDE TEMPERATURES:

VAPOUR HEADER TEMP: 29.95(.09)

WATER OUTLET TEMPS: 21.35(.23) 21.25(.23) 21.32(.26)

COND WALL TEMPS:

24.80(.22)	24.58(.19)	23.40(.23)
24.85(.20)	24.56(.23)	23.22(.22)
24.66(.26)	24.65(.26)	23.57(.26)
24.90(.21)	24.56(.20)	23.24(.26)
23.23(.23)	23.22(.28)	22.63(.28)

WATER INLET TEMPS: 19.94(.28) 19.97(.25) 19.93(.26)

 EVAPORATOR SIDE TEMPERATURES:

VAPOUR HEADER TEMP: 30.23(.09)

WATER OUTLET TEMPS: 40.70(.05) 39.04(.05) 37.23(.01)

EVAP WALL TEMPS:

38.10(.25)	37.28(.07)	35.33(.11)
39.08(.07)	36.59(.09)	35.83(.11)
38.62(.11)	36.74(.05)	35.76(.08)
39.34(.08)	37.33(.04)	36.00(.05)
41.58(.05)	39.95(.05)	37.73(.04)

WATER INLET TEMPS: 41.90(.00) 40.00(.00) 37.90(.00)

 SUBCOOLED LIQ LINE TEMPS: 25.17(.08) 25.37(.04) 25.07(.04)

 FLOWMETER READINGS:

LEFT	MIDDLE	RIGHT	BOTTOM
175	175	135-170	175

 SATURATION TEMP(C): 30.25(.08)
 # OF SCANS: 10
 MAX # OF SCANS: 10
 MIN # OF SCANS: 5

APPENDIX D UNCERTAINTY ANALYSIS

The uncertainties in the loop conductance, heat transfer rate and the average evaporator heat transfer coefficient are estimated in this appendix.

If ϕ is a function of independent variables x_1, x_2, \dots, x_n then

$$\phi = \phi(x_1, x_2, x_3, \dots, x_n)$$

Let w be the uncertainty in the result and let $w_1, w_2, w_3, \dots, w_n$ be the uncertainties in the independent variables then according to Kline and McClintock (13):

$$w_\phi = \sqrt{\left(\frac{\partial \phi}{\partial x_1} w_1\right)^2 + \left(\frac{\partial \phi}{\partial x_2} w_2\right)^2 + \dots + \left(\frac{\partial \phi}{\partial x_n} w_n\right)^2}$$

Similarly, the equation for estimating the loop conductance is given by

$$U_{ee} = \frac{m c_p \Delta T_1}{\Pi D L \Delta T_2}$$

where ΔT_1 is the temperature change in the source fluid and ΔT_2 is the temperature difference between the evaporator and the condenser walls.

The expression for the uncertainty in the loop conductance divided by the value of the loop conductance in simplified form may be written as

$$\frac{w_u}{U_{ee}} = \sqrt{\left(\frac{w_m}{m}\right)^2 + \left(\frac{w_{\Delta T_1}}{\Delta T_1}\right)^2 + \left(\frac{w_D}{D}\right)^2 + \left(\frac{w_L}{L}\right)^2 + \left(\frac{w_{\Delta T_2}}{\Delta T_2}\right)^2}$$

The uncertainty in the measurement of the mass flow rate of the source fluid was of the order of 4% of its value, the accuracy of measurement of the data logger was found to be 0.10

from the manufacturers catalog. The manufacturing tolerances were estimated to be 0.005" for the diameter and 0.0052' for the length (ref.4). Thus

$$w_m = 2.675 \text{ gm/s}$$

$$w_D = 0.005"$$

$$w_L = 0.0052'$$

$$w_{\Delta T_1} = \sum_{i=1}^6 (w_T/3)^2 = 6(1/3)^2(0.1)^2 = 0.08165$$

$$w_{\Delta T_2} = \sum_{i=1}^{30} (w_T/15)^2 = 30(0.1)^2/225 = 0.0365$$

For a temperature difference of 20C between the source and the sink fluids (test # 175):

$$\Delta T_1 = 0.97C$$

$$\Delta T_2 = 13.75C$$

$$m = 74.3 \text{ gm/s}$$

thus, $w_u/U_{ee} = 9.3\%$

Similarly, the uncertainty in the heat transfer rate in the evaporator is given by

$$w_Q/Q = \sqrt{(w_m/m)^2 + (w_{\Delta T_1}/\Delta T_1)^2}$$

$$w_Q/Q = 9.2\%$$

The uncertainty in the estimation of the average evaporator heat transfer coefficient is given by

$$(w_h/h) = \sqrt{(w_m/m)^2 + (w_{\Delta T_1}/\Delta T_1)^2 + (w_D/D)^2 + (w_L/L)^2 + (w_{\Delta T_3}/\Delta T_3)^2}$$

where ΔT_3 is the temperature difference between the evaporator wall and the saturation temperature in the evaporator.

$$\Delta T_3 = 9.05C$$

$$w_{\Delta T_3} = 0.1033$$

thus, $w_h/h = 9.4\%$

For a source-sink fluid temperature difference of 10C, for a static charge of 30% (test # 137) the uncertainty of estimation is found to be

$$w_u/U_{ee} = 16.8\%$$

$$w_Q/Q = 16.7\%$$

$$w_h/h = 16.9\%$$

APPENDIX E

EQUATIONS USED IN THE SIMULATION PROGRAM

(See page 101 for nomenclature)

Heat transfer coefficient calculations

Single phase forced convection (point value)

For laminar flow

$$h_a = 1.24(kF_1/D)(Re Pr D/z)^{1/3}(\mu/\mu_w)^{0.14} \quad (E1)$$

For turbulent flow

$$h_a = 0.027(kF_2/D)(Re)^{0.8} Pr^n (\mu/\mu_w)^{0.14} \quad (E2)$$

where

n = 0.4 for heating, n = 0.3 for cooling

Two phase forced convection (point value)

$$hD/k_L = 0.033(DG_t/\mu_{2p})(c_L \mu_L/k_L)^{0.4} \quad (E3)$$

Entrance effect factors

$$F_1 = 1 + 5 \exp(-z/10D) \quad (E4)$$

$$F_2 = 1 + 7 D/z \quad (E5)$$

$$F_3 = 0.344 Re^{-0.078} (D/z)^{1.93/Re^{0.3}} \quad (E6)$$

$$F_4 = 1 + 3.5 \exp(-z/10D) \quad (E7)$$

Boiling

$$q = \mu \sqrt{\lambda} \left\{ \frac{g(\rho_L - \rho_g)}{\sigma} \right\}^{1/2} \left\{ \frac{C_L(T_w - T_s)}{\lambda(CSF)Pr^{1.2}} \right\}^r \quad (E8)$$

where

$$r = 1.8, \quad CSF = 0.01$$

$$h_b = q/(T_w - T_s) \quad (E9)$$

Combined boiling and two phase convection

$$h_{fb} = (h_f^2 + h_p^2)^{1/2} \quad (E10)$$

Combined boiling and two phase forced convection with dryout

Criterion for transition to dryout:

$$x > x_c \quad (E11)$$

where

$$x_c = \left\{ \frac{We \sigma \rho_g}{C_L \mu_L (Re_L / (1-x))^{0.125}} \right\}^{0.5} \quad (1/3) \quad (E12)$$

and

$$We = 3.07 \times 10^{-8} Re_g (C_L \lambda / q)^{0.06} (\rho_L / \rho_g) \quad (E13)$$

$$h_{bfd} = C_1 h_d + C_2 h_{fb} \quad (E14)$$

where

$$C_2 = (1-x)^a / (1-x_c)^a \quad (E15)$$

and

$$C_1 = 1 - C_2 \quad (E16)$$

and $h_d = h_a$ for complete dryout at $T = T_s$

Subcooled boiling

If $T < T_s$ and if $q > q_{IB}$, then

$$h_{fb} = (h_f + h_b)^{1/p} \quad (E17)$$

where

$$p = 2 - (T_s - T_x) / (T_s - T_x)_{IB} \quad (E18)$$

for turbulent flow,

$$q_{IB} = \frac{k_L \lambda}{8 \sigma T_s (v_g - v_L)} \left\{ \frac{D^{0.2} \nu_L^{0.8} q}{0.023 Pr_L^{0.4} k_L \nu_L^{0.8}} - (T_s - T) \right\}^2 \quad (E19)$$

for laminar flow,

$$q_{IB} = \frac{k_L \lambda}{8 \sigma T_s (v_g - v_L)} \left\{ \frac{(D \nu_L z)^{0.33} q}{1.86 \nu_L^{0.33} Pr_L^{0.33} k_L} - (T_s - T) \right\}^2 \quad (E20)$$

Condensation

For an inclined tube

$$h_c = B \left(\frac{k_L^3 \rho_L^2 \lambda}{\mu_L D (T_s - T_w)} \right)^{1/4} \quad (E21)$$

where B is a function of tube diameter and angle

For a vertical tube

$$h_c = k_L / \delta$$

where

$$\delta = (3 \mu_L \Gamma / \rho_L^2)^{1/3} \quad (E22)$$

Pressure drop calculations

Friction factor

for laminar flow

$$f = 64 / Re \quad (E23)$$

for turbulent flow

$$f = 0.316 Re^{-0.25} \quad (E24)$$

Frictional pressure drop

For single phase flow

$$\Delta P_a = f (z/D) (\rho V^2 / 2) \quad (E25)$$

For two phase flow

$$\Delta P_f = \frac{P}{\Delta L} \phi^2 \quad (E26)$$

For liquid phase laminar and vapour phase laminar

$$\phi = (1 + X^{-0.7})^{1.43} \quad (E27)$$

$$X = (1-x/x) \left(\frac{\rho_g}{\rho_L} \right) \left(\frac{\mu_L}{\mu_g} \right)^{0.5} \quad (E28)$$

For liquid phase laminar and vapour phase turbulent

$$\phi = (1 + X^{-0.56})^{1.80} \quad (E29)$$

$$X = 18.65 \text{Re}_g^{-0.4} (1-x/x)^{0.5} \left(\frac{\rho_g}{\rho_L} \right)^{0.5} \left(\frac{\mu_L}{\mu_g} \right)^{0.5} \quad (E30)$$

For liquid phase turbulent and vapour phase laminar

$$\phi = (1 + X^{-0.56})^{1.80} \quad (E31)$$

where

$$X = 0.054 \text{Re}_L^{0.4} \left((1-x/x) \left(\frac{\rho_g}{\rho_L} \right) \left(\frac{\mu_L}{\mu_g} \right) \right)^{0.5} \quad (E32)$$

For liquid phase turbulent and vapour phase turbulent

$$\phi = (1 + X^{-0.49})^{2.05} \quad (E33)$$

$$X = \left(\frac{\mu_L}{\mu_g} \right)^{0.1} \left(\frac{\rho_g}{\rho_L} \right)^{0.5} (1-x/x)^{0.9} \quad (E34)$$

Acceleration pressure drop

For separated flow

$$\Delta P = \frac{G_t^2 \Delta x}{\rho_g a} (2x + \Delta x) - \frac{G_t^2 \Delta x}{\rho_L (1-a)} (2-2x-\Delta x) \quad (E35)$$

For homogenous flow.

$$\Delta P = \left(\frac{G^2}{\rho_L} \right) \left((1-x)^2 + x \left(\frac{\rho_L}{\rho_g} \right) - 1 \right) \quad (E36)$$

Hydrostatic pressure drop

$$\Delta P = \rho g z \quad (E37)$$

Liquid fraction calculation

$$R = (1 + x^{-0.42})^{-2.38} \quad (E38)$$

NOMENCLATURE FOR APPENDIX E

c	Specific heat, J/kgK
CSF	Surface liquid combination constant in Rohsenow's boiling equation
D	Tube diameter, m
F ₁	Entrance effect factor for laminar flow in the evaporator
F ₂	Entrance effect factor for turbulent flow in the evaporator
F ₃	Entrance effect factor for turbulent flow in the condenser
F ₄	Entrance effect factor for laminar flow in the condenser
f	Fanning friction factor
G	Mass flow rate at a point per unit of flow cross sectional area, kg/sq.m/s
g	Acceleration due to gravity, m/s/s
h	Heat transfer coefficient, W/sq.m/K
k	Thermal conductivity, W/mK
p	Pressure, N/sq.m
p	exponent used to combine boiling heat transfer coefficient with single phase convection
Pr	Prandtl number
q	Heat flux, W/sq.m
R	Liquid fraction
r	Exponent used in Rohsenow's boiling equation
Re	Reynolds number

Re _g	Superficial vapour Reynolds number defined as $Gx/D/\mu_g$
Re _l	Superficial liquid Reynolds number defined as $G(1-x)D/\mu_l$
T	Temperature (with no subscript, bulk fluid temperature K)
V	Velocity, m/s.
v	specific volume, cubic meters/kg
We	Weber number
x	Quality
x _c	Quality at which partial dryout starts to occur
Z	Distance along the evaporator or condenser from its entrance
λ	Latent heat of vaporization, J/kg
μ	Dynamic viscosity, kg/m-s
σ	Surface tension
α	Void fraction
ρ	Fluid density, kg/cubic meters
δ	Liquid film thickness, m
Γ	Condensate mass flow rate per unit perimeter, kg/m-s
ν	Kinematic viscosity, square meters/s
X	Lochart-Martinelli parameter

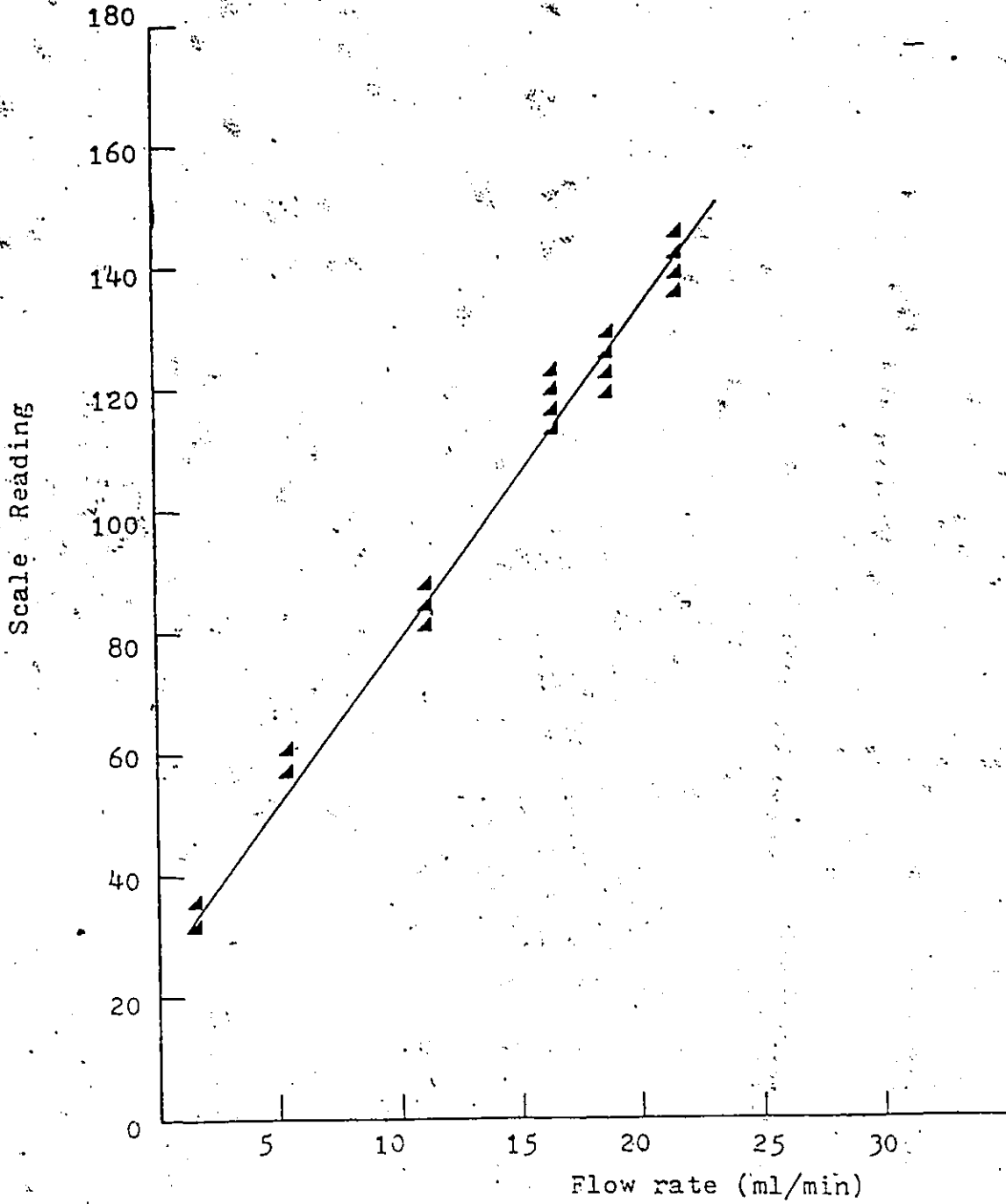
Subscripts

a	Single-phase liquid
b	Nucleate pool boiling
c	Condensation
d	Single-phase vapour
f	Two phase flow
g	Saturated vapour state
IB	Incipient boiling
L	Liquid

s Saturation
t Total
w Wall]

APPENDIX F

Calibration curve for R11 using a black glass float.



APPENDIX G

Least squares polynomial equations

The best least squares curve fit through the experimental to a second order polynomial for the heat transfer rate and the average evaporator heat transfer coefficient are as follows:

$$\underline{T(\text{source})=35\text{C}, T(\text{sink})=25\text{C}}$$

$$Q = 18.33 + 4.91 \cdot \text{charge} - 0.04(\text{charge})^2$$

$$H = 29.33 + 23.97 \cdot \text{charge} - 0.18(\text{charge})^2$$

$$\underline{T(\text{source})=40\text{C}, T(\text{sink})=20\text{C}}$$

$$Q = 3.93 + 11.23 \cdot \text{charge} - 0.08(\text{charge})^2$$

$$H = -46.45 + 35.03 \cdot \text{charge} - 0.24(\text{charge})^2$$

VITA AUCTORIS

- 1958 Born in Karachi, Pakistan on December 2.
- 1974 Completed the Cambridge Overseas School Certificate examination from St. Patrick's High School, Karachi, Pakistan.
- 1976 Completed the General Certificate of Education 'Advanced Level' examination of the University of London from Karachi Grammar School, Karachi, Pakistan.
- 1981 Completed the Bachelor of Science degree in Mechanical Engineering from Bogazici University, Istanbul, Turkey.
- 1983 Currently a candidate for the degree of Master of Applied Science.